Structural Characterization of Ligand-Binding Domain of Guanylyl Cyclase C

A Doctoral Thesis

Submitted to the Graduate School of Science, Osaka University

by

Makoto Hasegawa

1999

Acknowledgment

The studies in this thesis for the degree of Doctor of Science were carried out under the direction of Professor Yasutsugu Shimonishi, Institute for Protein Research, Osaka University. The author would like to express his sincerest gratitude to Professor Yasutsugu Shimonishi for thoughtful guidance, essential criticism and sincere encouragement.

The author wishes to express his thanks to Professor Toshiya Hirayama and Dr. Akihiro Wada (Institute of Tropical Medicine, Nagasaki University) for helpful discussion and collaboration for many years. The author greatly appreciate helpful advice and association from Professor Naoyuki Taniguchi and Dr. Jun-ichi Fujii (Osaka University Medical School) on the protein expression and recombinant DNA techniques. The author wishes to express his gratitude to Professor Saburo Aimoto and the members of Research Center for Structural Biology, Institute for Protein Research, for their kind help in peptide synthesis. The author is also thankful to the staffs of Radioisotope Center, Osaka University.

The author would like to express his thanks to the members of Professor Shimonishi's laboratory: Drs. Hiroshi Ozaki and Toshifumi Takao for their valuable comments and discussion. Dr. Yuji Hidaka for his fruitful suggestion and discussion as well as his sincere encouragement in the author's studies across the board. Dr. Takashi Sato (present: Faculty of Agriculture, Saga University) for valuable suggestion on the molecular structure of the synthetic STa analogs. Mr. Kazuya Matsumoto, Ms. Yuki Kawano, Mr. Toshifumi Sanni, and Ms. Yoshiko Matsumoto for their cooperation and exciting discussion, and the author is grateful to all the members of Professor Shimonishi's laboratory.

Makoto Hasegawa

February, 1999

Abbreviations

Three-letter and one-letter symbols for amino acids are according to JCBN Recommendations [Eur. J. Biochem., 138, 9-37 (1984)]. m/z denotes the quantity formed by dividing the mass number of an ion (m) by the number of charges carried by the ion (z). Other abbreviations are as follows : ANB-STp(4-17) ; N-5-azido-2-nitrobenzoyl-STp(4-17), Aph ; *p*-amino-L-phenylalanine, BB-STp(4-17) ; *p*-benzoylbenzoyl-STp(4-17), B_{max} ; maximum ligand-binding capacity, cGMP ; cyclic 3',5'-guanosine monophosphate, Con A ; concanavaline A, DSS ; disuccinimidyl suberate, ECD ; the extracellular domain of GC-C, ECD6H ; the extracellular domain with the C-terminal His_6 tag, *E. coli* ; *Escherichia coli*, ED_{50} ; median effective dose, egt ; ecdysteroid UDP-glycosyltransferase, GC ; guanylyl cyclase, His_6 ; a hexa-histidine, HPLC ; high performance liquid chromatography; IC_{50} ; median concentration of inhibition, ^{125}I-STp(4-17) ; a radioactive STp(4-17) with iodine-125 at Tyr^4, K_D ; dissociation constant, MALDI ; matrix-assisted laser desorption/ionization, Pap ; *p*-azido-L-phenylalanine, PBS(-) ; phosphate buffer saline without Mg^{2+} and Ca^{2+}, PCR ; polymerase chain reaction, PNGase F ; peptide-N-glycosidase F, SDS-PAGE ; sodium dodesyl sulfate polyacrylamide gel electrophoresis, Sf ; *Spodoptera frugiperda*, STa ; heat-stable enterotoxin, STp ; a heat-stable enterotoxin produced by porcine strain of enterotoxigenic *Escherichia coli*, STp(4-17) ; STp with the amino acid sequence from position 4 to 17, TOF ; time-of-flight, UV ; ultraviolet, λ ; wavelength.

Contents

Acknowledgments

Abbreviations

General Introduction ····· 1

Chapter 1. Expression and characterization of guanylyl cyclase C from baculovirus and Sf21 insect cells

1.1 Introduction ····· 6

1.2 Results

1.2.1 Expression of recombinant GC-C ····· 7

1.2.2 Expression of ECD ····· 9

1.2.3 The binding of recombinant GC-C and ECD to STa ····· 11

1.2.4 Guanylyl cyclase catalytic activity of recombinant GC-C ····· 14

1.2.5 Oligomerization of ECD ····· 15

1.3 Discussion

1.3.1 Establishment of over-expression system of GC-C ····· 17

1.3.2 Multiple ligand-binding affinity and oligomerization of ECD ····· 19

1.4 Materials and Methods

1.4.1 Materials ····· 20

1.4.2 Constructions of transfer vectors carrying cDNA's coding for porcine GC-C and ECD ····· 20

1.4.3 Preparation of recombinant proteins ····· 22

1.4.4 Preparation of membranes ····· 23

1.4.5 Purification of ECD6H ····· 23

1.4.6 Western blot analysis ····· 24

1.4.7 Analysis of N-terminal amino acid sequence ····· 24

1.4.8 Photoaffinity-labeling of recombinant proteins and binding assay to STa ·24
1.4.9 cGMP assay ·····25
1.4.10 Chemical cross-linking of ECD6H ·····25

Chapter 2. Development of photoaffinity-labeling with identification of the receptor-binding site in a ligand of guanylyl cyclase C

2.1 Introduction ·····26
2.2 Results and Discussion
2.2.1 Design of the photo-affinity labeling STa analogs ·····27
2.2.2 Synthesis of photoreactive STp analogs ·····28
2.2.3 Photoaffinity labeling of photo-reactive STp analogs to STp receptor on rat intestinal membranes ·····32
2.2.4 Binding affinity of STp analogs ·····34
2.3 Materials and Methods
2.3.1 Peptide synthesis ·····37
2.3.2 High-performance liquid chromatography (HPLC) ·····38
2.3.3 Circular Dichroism (CD) ·····38
2.3.4 Membrane preparation ·····38
2.3.5 Photoaffinity and cross-linking with ^{125}I-[Pap]STp analogs ·····39
2.3.6 Receptor binding assay ·····39
2.3.7 Enzyme-Linked Immunosorbent Assay (ELISA) ·····39

Chapter 3. Identification of photoaffinity labeling of the specific site on the extracellular domain of guanylyl cyclase C involved in ligand binding

3.1 Introduction ·····41
3.2 Results
3.2.1 Synthesis of biotinyl$(NH(CH_2)_4CO)_2$[Gly^4,Pap^{11}]STp(4-17) ·····43
3.2.2 Binding affinity of biotinyl$(NH(CH_2)_4CO)_2$[Gly^4,Pap^{11}]STp(4-17) toECD6H ·····47

3.2.3 Photoaffinity labeling of ECD6H with biotinyl($NH(CH_2)_4CO)_2$-[Gly^4,Pap^{11}]STp(4-17) and isolation of a labeled fragment(s) ·····48
3.2.5 Site-directed mutational analysis of the ligand-binding site ·····53
3.3 Discussion ·····55
3.4 Materials and Methods
3.4.1 Materials ·····61
3.4.2 Synthesis of biotinyl($NH(CH_2)_4CO)_2$[Gly^4,Pap^{11}]STp(4-17) ·····61
3.4.3 Photoaffinity-labeling of ECD6H with biotinyl($NH(CH_2)_4CO)_2$-[Gly^4,Pap^{11}]STp(4-17) ·····62
3.4.4 Digestion of photoaffinity-labeled ECD ·····63
3.4.5 Isolation of photoaffinity-labeled peptides ·····63
3.4.6 Site-directed mutagenesis of GC-C ·····63
3.4.7 Assay of cGMP production of GC-C mutant proteins ·····65

Chapter 4. The relevance of N-glycosylation to the binding of ligands to guanylyl cyclase C

4.1 Introduction ·····66
4.2 Results
4.2.1 Deglycosylation of recombinant ECD ·····68
4.2.2 Preparation of mutant proteins of ECD ·····70
4.2.3 Binding characteristics of mutant proteins of ECD to STa ·····71
4.2.4 Estimation of the stability of ECD and its mutant proteins to denaturant ··75
4.2.5 Characterization of mutant proteins of GC-C expressed in 293T cells ····75
4.3 Discussion ·····79
4.4 Materials and Methods
4.4.1 Materials ·····82
4.4.2 Constructions of expression vectors carrying cDNA of GC-C, ECD, and their mutant proteins. ·····83
4.4.3 Expression of recombinant GC-C and its mutant proteins in Sf21 insect cells or 293T mammalian cells ·····84
4.4.4 Purification of ECD6H and its mutant proteins ·····85

4.4.5 Deglycosylation of ECD6H ····85
4.4.6 Photoaffinity-labeling of recombinant GC-C, ECD, and their mutant proteins ····86
4.4.7 STa-binding assay of ECD and its mutant proteins ····86
4.4.8 Urea-induced inactivation of ECD6H and its mutant proteins ····86
4.4.6 cGMP assay ····87

Summary ····88

Publications ····90

References ····93

General Introduction

Most signal transduction to the inside of a cell from the outside is triggered by the highly specific binding of chemical substances, such as hormones, drugs, odorants, etc., to intrinsic receptor proteins. The second messenger hypothesis (Sutherland & Rall, 1960) suggests that a variety of receptor proteins generate a common cytoplasmic signaling substance, namely, a second messenger. After the discovery of cyclic 3',5'-guanosine monophosphate (cGMP) as a second messenger in cytoplasmic signal transduction (Ashman *et al.*, 1963), numerous research groups began investigating the biological role of cGMP-generating enzymes, guanylyl cyclases. In mammals, two α (α1, α2) and two β (β1, β2) subunits of hetero-dimeric soluble guanylyl cyclases and seven particulate guanylyl cyclases (GC-A ~ GC-G) have been identified thus far (reviewed in Garbers, 1992; Wedel & Garbers, 1997; Schulz *et al.*, 1998). Soluble guanylyl cyclases are globular proteins which are located in the cytoplasm. Dimerization of the α and β subunit is a requisite for cyclase catalytic activity. They are stimulated by binding of nitric oxide or carbon monooxide to a prosthetic heme group. Nitric oxide and carbon monooxide are low-molecular weight signaling substances with high permeability for plasma membranes. While, particulate guanylyl cyclases belong to a single-transmembrane protein, consisting of an extracellular domain and an intracellular domain, which are connected through a single transmembrane polypeptide. Particulate guanylyl cyclases share common structural features : an N-terminal signal peptide, an extracellular ligand-binding domain, a transmembrane region, and an intracellular domain consisting of two sub-domains, a kinase-homology domain and a guanylyl cyclase catalytic domain (Fig. 1). The primary structure of the guanylyl cyclase catalytic domain is homologous to soluble guanylyl cyclases, while the extracellular ligand-binding domain is unique to particulate guanylyl cyclases (Schulz *et al.*, 1990; Garbers, 1992). The extracellular ligand-binding domain functions as a receptor for small peptides which regulate cell functions. To date, six peptides have been identified as ligands for three particulate guanylyl cyclases, as shown in Fig. 1. GC-A and B are known as the receptors for three natriuretic peptides, ANP, BNP and CNP, which are endogenous peptides regulating uresis, natriuresis, and blood pressure in cardiovascular tissues. One other protein, the

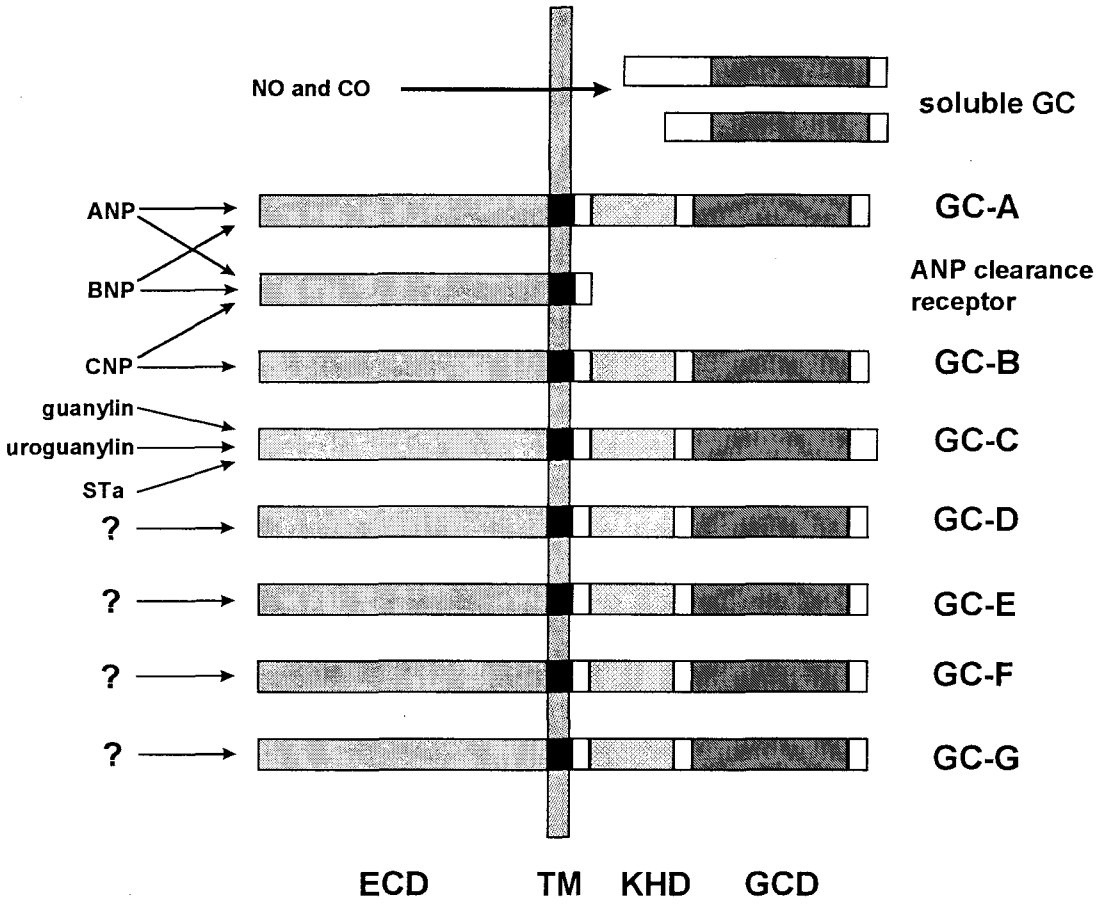

Fig. 1. The guanylyl cyclase family. ECD : the extracellular domain, TM : the transmembrane region, KHD : the kinase-homology domain, GCD : the guanylyl cyclase catalytic domain. The ligands of guanylyl cyclases : NO (nitric oxide) and CO (carbon monooxide) are activators for soluble guanylyl cyclases. ANP (atrial natriuretic peptide), BNP (brain natriutetic peptide), and CNP (C-type natriuretic peptide) belong to a peptide family which activates GC-A and GC-B. Guanylin and uroguanylin are endogenous peptides for GC-C, while STa (heat-stable enterotoxin) is a peptide family consisting of homologous bacterial toxins which stimulate GC-C. Soluble and particulate guanylyl cyclases appear to exist as dimers or higher ordered homomers (Garbers & Lowe, 1994).

ANP clearance receptor, is homologous within its extracellular ligand-binding domain to GC-A and GC-B but does not contain guanylyl cyclase activity. GC-C, which is the target molecule of this thesis, serves as a receptor protein for the polypeptide ligand ; heat-stable enterotoxin, guanylin, and uroguanylin (Currie *et al.*, 1991; Hamra *et al.*,

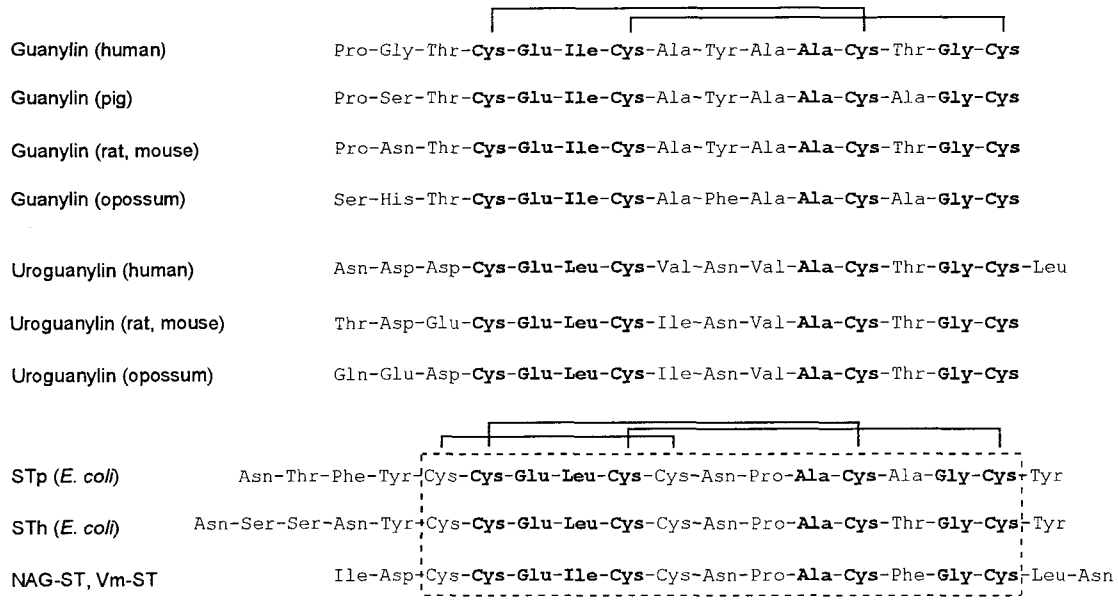

Fig. 2. Comparison of amino acid sequences of GC-C ligands. The highly homologous 13 amino acid sequence in STa (toxic domain) are boxed. The conserved amino acids (bold letters) between the subfamilies of guanylin (Currie *et al.*, 1992; de Sauvage *et al.*, 1992; Wiegand *et al.*, 1992; Hill *et al.*, 1997), uroguanylin (Hamra *et al.*, 1993; Kita *et al.*, 1994; Miyazato *et al.*, 1996), and bacterial STa's are shaded. Leu and Ile are thought to be conservative replacements for each other. STp and STh are produced by enterotoxigenic *E. coli* of porcine (Takao *et al.*, 1983) and human (Aimoto *et al.*, 1982) origin, respectively. NAG-ST and Vm-ST are elaborated by *V. cholerae* non-O1 (Takao *et al.*, 1985) and *Vibrio mimicus* (Arita *et al.*, 1991), respectively.

1993). Heat-stable enterotoxin (STa or STI) is a family of homologous peptides elaborated by enteric bacteria, which cause acute and secretory diarrhea in infants and domestic animals (Smith & Gyles, 1970; Giannella, 1981). Guanylin and uroguanylin are endogenous peptides which regulate electrolyte homeostasis in ntestines, kidney, and pancreas (reviewed in Forte & Currie, 1995). Thus, GC-C is mainly localized on the intestinal brush border membrane and in kidney cortex. The other particulate guanylyl cyclases are orphan receptors which exist in the olfactory neuroepithelium (GC-D) (Fulle *et al.*, 1995), the retina (GC-E and GC-F) (Yang *et al.*, 1995), or intestines and skeletal muscle (GC-G) (Schulz *et al.*, 1998). The biological roles of the orphan receptor guanylyl cyclases are presently unknown. Possibly, GC-A, B, C and G belong to one

subfamily of peptide receptor which maintains homeostasis, and GC-D, E, and F belong to another, which relates to sense perception (Wedel & Garbers, 1997; Schulz *et al.*, 1998).

GC-C was first identified as the receptor protein for a heat-stable enterotoxin (STa) (Schulz *et al.*, 1990) and, later, for the endogenous peptides, guanylin and uroguanylin (Currie *et al.*, 1991; Hamra *et al.*, 1993). The primary structures of STa, guanylin, and uroguanylin are highly homologous (Fig. 2). In fact, the tertiary structures of these peptide are reasonably similar to each other (Ozaki *et al.*, 1991; Skelton *et al.*, 1994; Marx *et al.*, 1998). An elevation in the intracellular cGMP level, as a result of the binding of one of these ligands to GC-C, leads to activation of a cGMP dependent protein kinase, which, in turn, induces the phosphorylation of a chloride ion channel, the cystic fibrosis transmembrane conductance regulator protein on the apical membrane in intestinal cells (Chao *et al.*, 1994; Pfeifer *et al.*, 1996). This signaling cascade ultimately results in the secretion of chloride and water from the inside of the cells to the outside. Thus, GC-C is involved in the regulation of chloride transport in electrolytes, that is, the homeostasis of intestinal fluid and electrolytes, in intestinal cells by means of interaction by guanylin or uroguanylin. On the contrary, GC-C, when targeted by STa, is immediately over-activated and, thus, the cGMP content in intestinal cells is greatly increased, resulting in the phosphorylation of the cystic fibrosis-related channel and, in turn, chloride secretion from inside the cells to the outside, a process which results in secretory diarrhea in infants.

The primary structure of the extracellular domain of GC-C is quite different from that of another particulate guanylyl cyclase, while the intracellular domain is highly homologous to them in terms of primary structure. A possible explanation for this unique structure is that signaling is initiated on the extracellular domain and then transferred to the intracellular domain via the binding of a specific ligand (STa, guanylin and uroguanylin), which is different from those which normally bind to other particulate guanylyl cyclases. Mechanistically, it is then possible that the extracellular domain activates the intracellular cyclase catalytic domain in the same manner as is operative for other particulate guanylyl cyclases in generating cGMP, a common cytoplasmic second messenger. In addition, GC-C exists as an oligomer regardless of the presence or

absence of a ligand and oligomerization of GC-C is essential for cyclase catalytic activity as has been observed in other particulate guanylyl cyclases (Vaandrager *et al.*, 1994; Garbers & Lowe, 1994; Runder *et al*, 1995). In signal transduction, the binding of a ligand to the extracellular domain induces a conformational change in the intracellular domain, thus leading to activation of the cyclase catalytic domain. The functional role of the oligomer in this signaling is not yet clear.

GC-C appears as multiple protein bands of 140-160 kDa in molecular weight on SDS-PAGE (Vaandrager *et al.*, 1993). The complexity in molecular weight is due to heterogeneity as the result of various levels of N-linked glycosylation at eight potential sites in the extracellular domain. The N-linked carbohydrate chains may play a role in subunit interactions, ligand binding as well as the structural stability of the protein. Thus, the structural requirements of the extracellular domain for ligand recognition and the propagation of signaling to the intracellular domain remain to be elucidated. In this thesis, the author's studies have been focused on the analysis of functions and structural characteristics of the extracellular ligand-binding domain of GC-C, in order to clarify the mechanism of the ligand-recognition and activation of particulate guanylyl cyclases. In chapter 1, the establishment of the expression system of GC-C by the Sf21 insect cell line and a baculovirus vector is described. The ligand-binding property and the oligomerization of the extracellular domain as a truncated and soluble form are discussed. In chapter 2, the synthesis of photo-affinity labeling STa analogs which specifically label the ligand-recognition site of GC-C is described. The relationship between the efficiency of photoaffinity-labeling and the location of the photo-crosslinking group in an STa analog have clearly revealed the interaction site to GC-C in STa. In chapter 3, the identification of the ligand-binding site of GC-C using the synthetic STa analogs is described. The photoaffinity-labeling method in combination with mass spectrometry permitted the characterization of the ligand-binding site in GC-C. In chapter 4, the role of N-glycosylation in the extracellular domain of GC-C is discussed. The experiments revealed that N-linked carbohydrate chains are indispensable for the ligand-binding function of GC-C in terms of structure stability. These experimental results give new insights on the ligand-recognition and signaling function of particulate guanylyl cyclases.

Chapter 1. Expression and characterization of guanylyl cyclase C from baculovirus and Sf21 insect cells

1.1 Introduction

Acquisition of a sufficient quantity of a purified sample is a requisite for a successful study on the relationship between structure and function of a protein. To date, several attempts at a large-scale preparation and purification of GC-C have been carried out by several research groups (Smith *et al.*, 1992; Nandi *et al.*, 1996). Nevertheless, these works did not wholly satisfy a demand for the structural analysis up to the present. GC-C is little expressed in the native tissues and is easily degraded by intrinsic protease activity and the high protease-sensitivity of GC-C caused the artificial molecular species in a preparation from native tissues, as have been reported in previous papers (Kuno *et al.*, 1986; Hirayama *et al.*, 1992; Vaandrager *et al.*, 1993; Cohen *et al.*, 1993). Thus, the establishment of an efficient expression system of the recombinant GC-C was needed. However, the expression of GC-C using *E. coli* failed in acquisition of the fully active form (Nandi *et al.*, 1996), since GC-C is a membrane-bound protein which consists of the multiple domains with post-translational modifications. On the contrary, GC-C which functions with compatibility to the native one in terms of the biological properties has been expressed in mammalian culture cell lines (Schulz *et al.*, 1990; de Sauvage *et al.*, 1992), but the low productivity in the culture mammalian cells are unsuitable for the production of large amounts of GC-C. To obtain large amounts of GC-C which functions as the receptor of a peptide, we expressed the extracellular domain (ECD) from a baculovirus system and generated large amounts of the protein, suitable for biochemical analysis. The expression system which consisted of baculovirus and insect cells has potential not only for the production of large amounts of a foreign protein with post-translational modifications but also for localization of the protein to a specific target, depending on its nature (Smith *et al.*, 1983; Luckow & Summers, 1988; Luckow & Summers, 1989). The recombinant GC-C showed the same binding characteristics to

STa as those of GC-C with the entire amino acid sequence. This chapter describes the over-expression of the ECD as well as the full-length GC-C from Sf21 insect cells by means of a baculovirus vector. The ECD, containing a C-terminal histidine (His_6) tail, was purified by means of the Con A and Ni-chelating affinity chromatography from the culture supernatant, thus permitting a sufficient quantity of the recombinant protein to be obtained for biochemical characterization.

1.2 Results

1.2.1 Expression of recombinant GC-C

The recombinant GC-C was expressed using a system consisting of baculovirus and insect cells. Western blot analysis revealed two products, one major 120-kDa protein and another minor 130-kDa protein, as detected by a polyclonal antibody raised against a peptide from the region 461-475 of porcine GC-C (Wada *et al.*, 1996b), as shown in Fig. 1-1A, lane 2. The 120-kDa protein was not photoaffinity-labeled by ^{125}I-BB-STp(4-17) (Fig. 1-1B, lane 2). In contrast, the 130-kDa protein was labeled and competitively inhibited in binding to ^{125}I-BB-STp(4-17) in the presence of an excess amount of STp(4-17) (Fig. 1-1B, lanes 2 and 3). Edman degradation showed that the N-terminal sequence of the 120-kDa protein was completely identical to the signal sequence of porcine GC-C, MKTPLLALAL-. Based on these findings, we conclude that the 120-kDa protein is probably not localized on the cell membranes due to insufficient glycosylation and that the native N-terminal signal sequence of porcine GC-C was incompletely processed by a signal peptidase and/or other signal recognition components of Sf21 insect cells, suggesting that most of the product had accumulated as the unprocessed 120-kDa protein in cells.

To improve the expression efficiency of the 130-kDa protein, the signal sequence of porcine GC-C was replaced by that of ecdysteroid UDP-glycosyltransferase (egt), which has been reported to increase the expression efficiency of secretory proteins in the baculovirus expression system (Murphy *et al.*, 1993). The expression vector for porcine GC-C was constructed as described in section 1.4.2 and expressed in Sf21 insect cells.

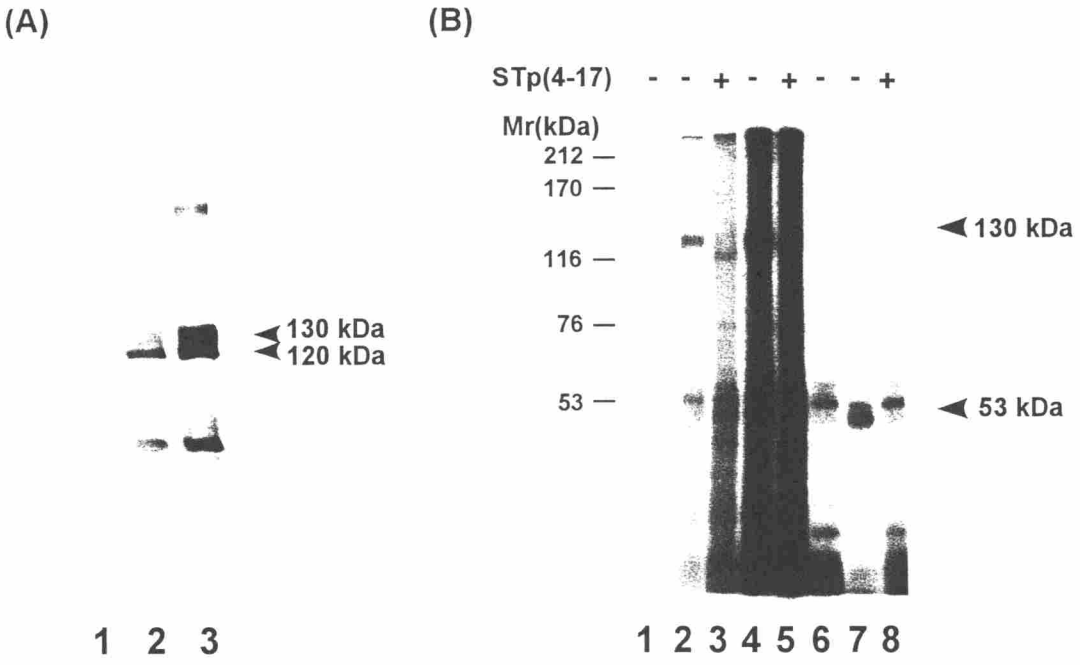

Fig. 1-1. (A) Western blot analysis of the recombinant GC-C expressed from Sf21 cells : lane 1, Sf21 cell lysates without the recombinant virus (control) ; lanes 2 and 3, those with the recombinant virus carrying the signal peptide of GC-C and of egt, respectively. (B) SDS-PAGE of the recombinant GC-C and ECD expressed from Sf21 cells : lane 1, Sf21 cells without the recombinant virus (control) ; lanes 2 and 3, GC-C ; lanes 4 and 5, GC-C(egt) ; lane 6, the culture supernatant of Sf21 cells infected by the recombinant virus of GC-C (control) ; lanes 7 and 8, ECD(egt) ; lanes 3, 5, and 8, in the presence of 10^{-5} M STp(4-17). SDS-PAGE was carried out on 10 % polyacrylamide gel and protein bands were visualized by (A) an anti-GC-C antibody or by (B) photoaffinity-radiolabeling with ^{125}I-BB-STp(4-17).

As a result of this, the expression efficiency of the 130-kDa protein dramatically increased, even though the quantity of the 120-kDa protein was nearly the same in both cases (Fig. 1-1A, lane 3). These results clearly showed that the mature GC-C (130-kDa protein) was expressed as a major protein in Sf21 insect cells as the result of replacing the signal sequence of porcine GC-C with that of egt (Fig. 1-1A, lane 3, and in Fig. 1-1B, lane 4). The 130-kDa protein had an N-terminal sequence (SSVSQ-), identical to that of the mature GC-C and was accompanied by a sequence which was probably a minor contaminant. In addition, treatment of the 130-kDa protein with PNGase F caused the protein to move from position corresponding to 130-kDa to 120-kDa on SDS-PAGE. The latter value is close to the molecular weight calculated from the predicted amino acid sequence (120,556) (data not shown). These results indicate that the 130-kDa protein was the mature GC-C which consists of the entire amino acid sequence and some sugar chains. The maximum binding of ^{125}I-STp(4-17) to the insect cells expressing GC-C with the signal peptide of GC-C or egt was 1.0 ± 0.3 pmol / 10^6 cells or 19 ± 2 pmol / 10^6 cells respectively (data not shown), indicating that the exchange of the signal sequence gave a 19-fold improvement in the expression efficiency of the mature GC-C.

1.2.2 Expression of ECD

To examine the interaction between GC-C and its ligand, ECD was expressed in Sf21 cells and secreted as a 53-kDa protein into the culture medium (Fig. 1-1B, lanes 7 and 8). The 53-kDa protein could be modified with sugar chains of approximately 7-kDa, because the molecular weight of EDC deduced from the amino acid sequence is 46,101. To isolate and purify ECD from a culture medium, the protein was linked to the His_6 tail at the C-terminus to give ECD6H which was purified using Ni-chelating affinity chromatography using the procedure described in section 1.4.5. The protein was purified by two-step affinity chromatography on Con A and Ni-chelating columns and obtained as a homogeneous product as evidenced by SDS-PAGE (Fig. 1-2). The molecular weight of ECD6H was slightly larger than that of ECD, as a result of the addition of the His_6 tail, and this was confirmed by SDS-PAGE and photoaffinity labeling analysis (data not shown). The purified ECD6H had an N-terminal sequence (SSVSQ-) which was identical to that deduced for the mature ECD.

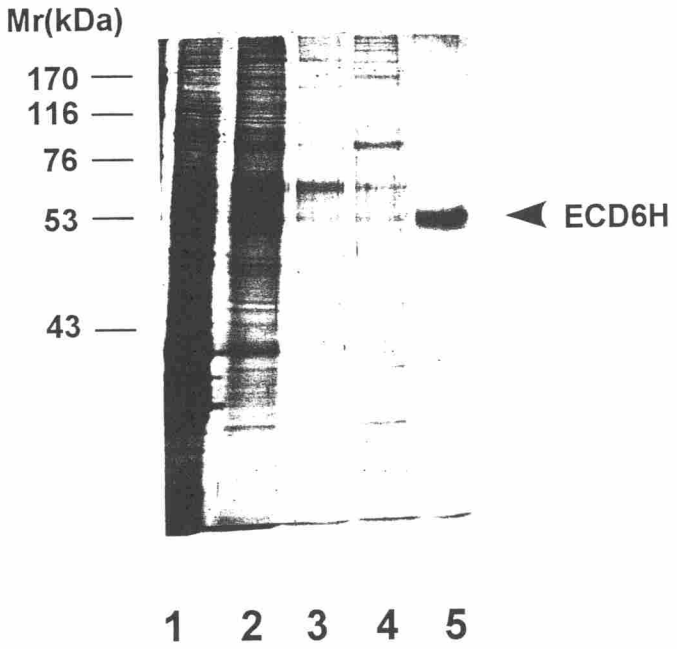

Fig. 1-2. SDS-PAGE of ECD6H. Lane 1, the culture supernatant of Sf21 cells infected with the recombinant baculovirus carrying the cDNA encoding ECD6H ; lane 2, the culture supernatant in lane 1 adsorbed on and eluted from a Con A agarose column ; lane 3, the passed-through fraction from the Ni-chelating agarose column of the eluate in lane 2 ; lanes 4 and 5, the fractions in lane 3 adsorbed on a Ni-chelating agarose column and eluted with 20 mM or 100 mM imidazole, respectively.

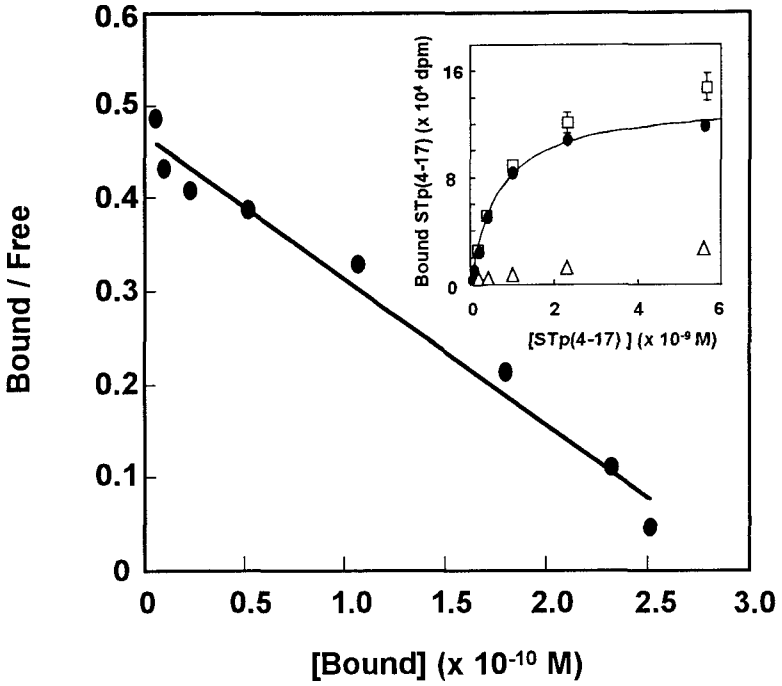

Fig. 1-3. Scatchard plot analysis of the binding of STa to recombinant GC-C. Inset : the saturation curve for the binding of ^{125}I-STp(4-17). The solid line is a theoretical curve for the binding of the ligand with the K_D value obtained from the Scatchard plot analysis. Open squares, closed circles, and open triangles represent the total binding, the specific binding, and the non-specific binding, respectively. Non-specific binding was estimated in the presence of 10^{-6} M STp(4-17). The data represent the averages of three data sets and the error bars indicate the standard deviation.

1.2.3 The binding of recombinant GC-C and ECD to STa

To estimate the ability of the recombinant GC-C to bind to STa, the dissociation constant (K_D) between the recombinant GC-C or ECD and STa was determined. The binding capability of the recombinant GC-C expressed on the cell membranes was examined in the presence of ^{125}I-STp(4-17) at various concentrations (1×10^{-10} - 2×10^{-8} M) (Inset in Fig. 1-3). The data relative to the binding experiments in the equilibrium state were analyzed using the software program LIGAND (Munson and Rodbard, 1980). A Scatchard plot analysis (Scatchard, 1949) of the data showed that the K_D value for the

Table 1-1 Ligand-binding ability and cyclase catalytic activity of GC-C and ECD

		K_D (M)	B_{max} (M)	cGMP (nmol/min) STa (-)	STa (+)
GC-C		$(6.4 \pm 0.2) \times 10^{-10}$	3.0×10^{-10}	0.42	3.1
ECD	High affinity	$(4.0 \pm 0.4) \times 10^{-10}$	4.5×10^{-10}	———	
	Low affinity	$(7.3 \pm 1.4) \times 10^{-8}$	1.1×10^{-9}		
ECD6H	High affinity	$(7.2 \pm 0.7) \times 10^{-10}$	5.8×10^{-10}	———	
	Low affinity	$(3.0 \pm 1.6) \times 10^{-8}$	1.5×10^{-9}		

K_D and B_{max} represent the dissociation constant and the maximum binding-capacity of STp(4-17). cGMP (nmol/min) represents cyclase activity in the cell membrane fraction (1 mg total protein) in the absence (STa (-)) or the presence (STa (+)) of 10^{-5} M STp(4-17).

interaction between the recombinant GC-C and STp(4-17) was 6.4×10^{-10} M (Fig. 1-3 and Table 1-1). This value is comparable to that of porcine GC-C expressed in 293T mammalian cell lines (K_D, 7.9×10^{-9} M) (Wada *et al.*, 1994). Deshmane *et al.* (1995) reported that rat GC-C expressed in COS-7 cells exhibited high (0.4×10^{-11} M), low_1 (1.5×10^{-10} M), and low_2 (2.2×10^{-9} M) affinity sites. In the present study, it was difficult to determine the multiple K_D values of the membrane-associated form of the recombinant porcine GC-C, because the influence of the non-specific binding of STa to the crude cell membranes could not be excluded in our assay system.

Figure 1-4A shows the Scatchard analysis and the saturation curve for the binding of STp(4-17) to ECD. The Scatchard plot of the data revealed the presence of a single class for the binding of STa to ECD with a K_D value of 4.0×10^{-10} M. This was close to the value for the recombinant GC-C (Table 1-1). The binding of ^{125}I-STp(4-17) to ECD was assayed at high concentrations of STp(4-17) in order to determine the K_D value for the low affinity binding site (Fig. 1-4B, inset). The Scatchard plot of the data was downward concave, suggesting the presence of a low-affinity binding site at higher ligand concentrations (Fig. 1-4B). The data, when analyzed according to the method of Klotz (1985), showed a doubly sigmoidal curve, indicating two classes of binding sites comprising high ($K_D = 4.0 \times 10^{-10}$ M) and low ($K_D = 7.3 \times 10^{-8}$ M) affinity sites with the B_{max} values, 4.5×10^{-10} M and 1.1×10^{-9} M, respectively (Fig. 1-4C and Table 1-1). The

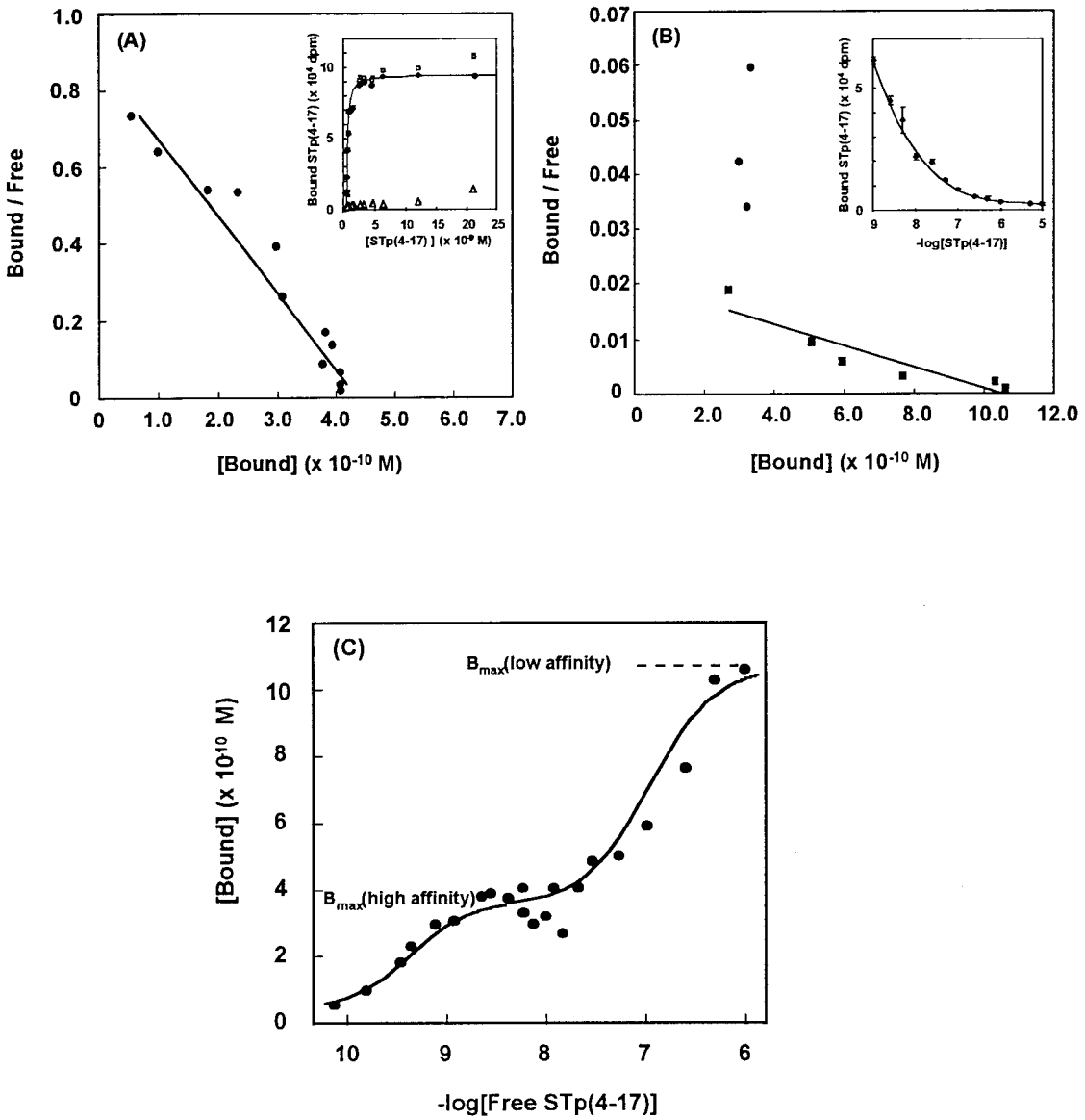

Fig. 1-4. A Scatchard plot analysis of the binding of STa to recombinant ECD. (A) The saturation binding and (Inset) the saturation curve of the binding of ^{125}I-STp(4-17). Open squares, closed circles, and open triangles represent the total binding, the specific binding, and the non-specific binding, respectively. The non-specific binding was estimated in the presence of 10^{-6} M STp(4-17). (B) The competitive binding and (Inset) the competitive inhibition by STp(4-17) in the binding of ^{125}I-STp(4-17). Closed circles and squares represent the high and low affinity bindings, respectively. (C) Klotz plot of the combined data of (A) and (B). The solid line is a theoretical curve for the binding of the ligand with the K_D values obtained from the Scatchard plot analysis. The data represent the averages of three data sets and the error bars indicate the standard deviations.

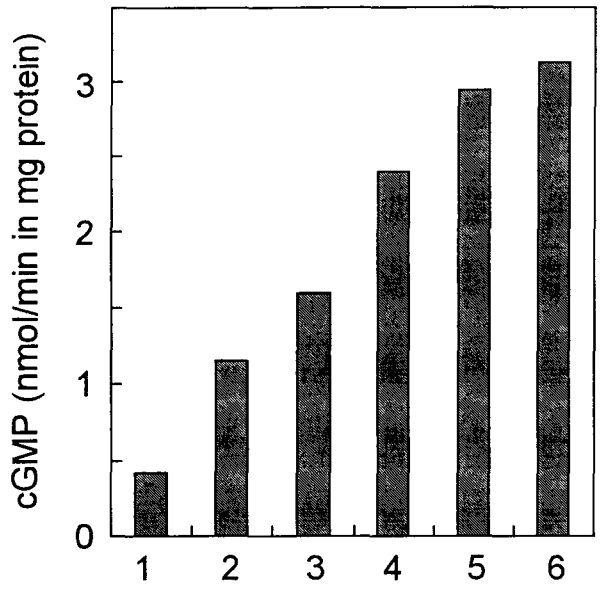

Fig. 1-5. The formation of cGMP induced by recombinant GC-C expressed on the cell membranes. Lane 1, in the absence of STp(4-17) ; lanes 2–6, in the presence of STp(4-17) : lane 2, 10^{-9} M ; lane 3, 10^{-8} M ; lane 4, 10^{-7} M ; lane 5, 10^{-6} M ; lane 6, 10^{-5} M.

K_D values for the high and low affinity sites of ECD6H were 7.2×10^{-10} M and 3.0×10^{-8} M, respectively, which were nearly the same values as those obtained for the case of ECD, regardless of the additional His_6 tail to the C-terminus of ECD (Table 1-1).

1.2.4 Guanylyl cyclase catalytic activity of recombinant GC-C

The membrane fractions of the Sf21 cells comprising the recombinant GC-C showed remarkably high cyclase catalytic activity in a ligand-dependent manner (Fig. 1-5). The accumulation of cGMP (0.42 nmol cGMP/min in 1 mg of membrane protein in the absence of STp(4-17)) was detected in the Sf21 cell membranes with the recombinant baculovirus containing GC-C, while cyclase catalytic activity was not significant in the membranes of the non-infected insect cells (less than 1 pmol cGMP/min in 1 mg of membrane protein). The maximum cyclase activity was approximately 7.5-fold higher (3.1 nmol cGMP/min in 1 mg of membrane protein in the presence of 10^{-5} M STp(4-17))

than the basal activity, as shown in Fig. 1-5.

1.2.5 Oligomerization of ECD

ECD6H was treated with DSS in the presence or absence of STp(4-17). Two protein bands appeared at 160 and 110 kDa on SDS-PAGE with silver staining, corresponding to the molecular weights of a trimer and dimer of ECD6H respectively, as shown in Fig. 1-6A. The 160-kDa protein was not observed in the absence of STp(4-17) or the presence of an inactive analog of STp, [Leu^{13}]STp(5-17) (Yamasaki *et al.*, 1990; Sato *et al.*, 1994) (Fig. 1-6A, lanes 2 and 4), while the protein band at 110-kDa was consistently observed regardless of the presence or absence of the ligand (Figs. 1-6A and 1-6B). The 160-kDa protein was not an artifact derived from the His_6 tail attached to the C-terminus of ECD, because the protein was observed even in the presence of 1 mM EDTA (data not shown). The 160-kDa protein was formed in the range from 10^{-8} M to 10^{-5} M of STp(4-17) or guanylin (Fig. 1-6B). The mid point for the formation of the protein was estimated to be approximately 10^{-7} M of STp(4-17), which was equivalent to the concentration of ECD6H. This protein was formed at a slightly higher guanylin concentration than that of STa. The difference in the concentration of the ligands appears to reflect their ability to bind to GC-C, because guanylin shows a lower affinity to GC-C than to STa (Hidaka *et al.*, 1993; Carpick *et al.*, 1993). The 160-kDa as well as the 53 kDa proteins were specifically labeled with ^{125}I-BB-STp(4-17), which were inhibited in the presence of an excess amount of guanylin or STp(4-17) (Fig. 1-6C).

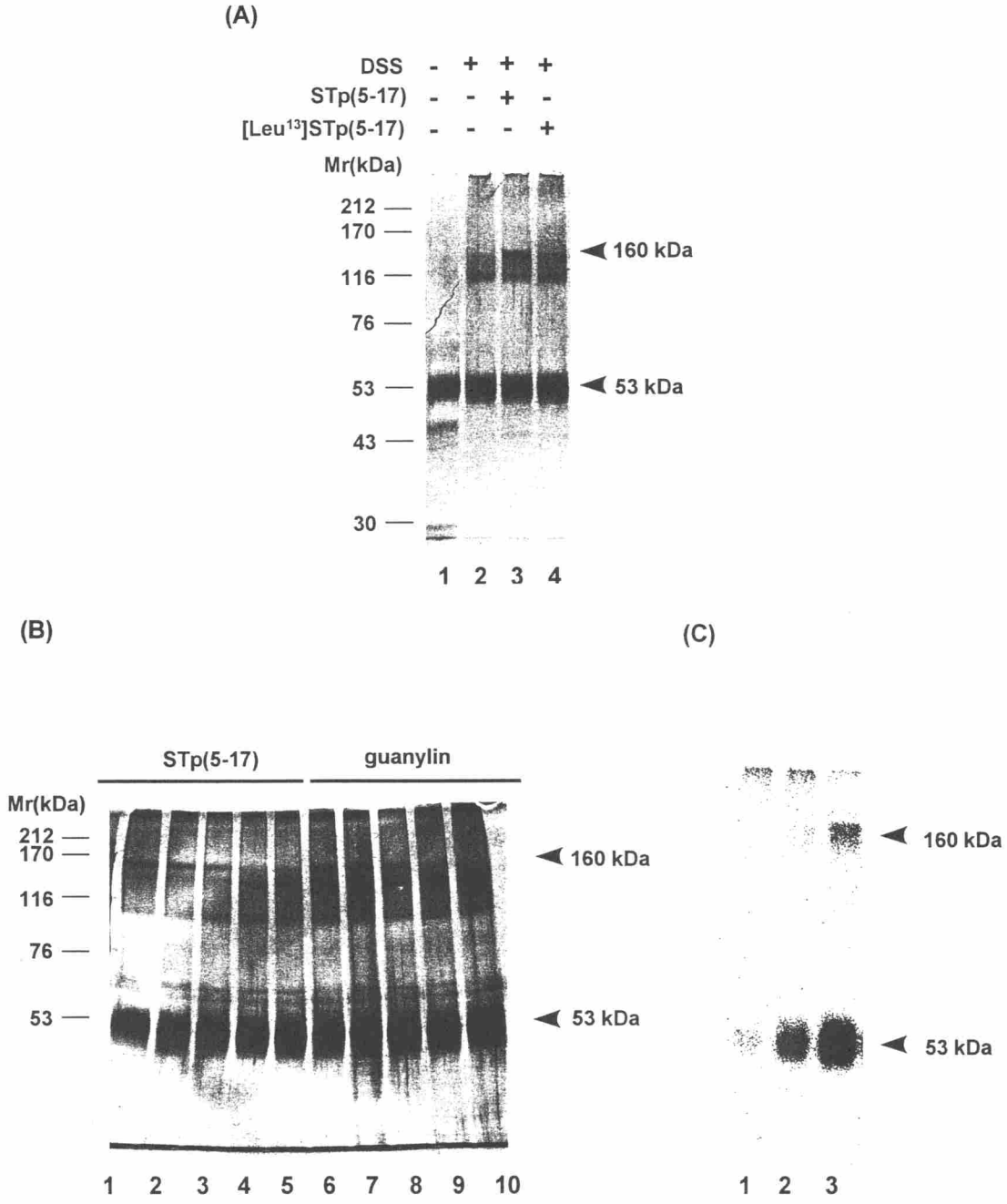

Fig. 1-6. (A) Cross-linking of recombinant ECD with DSS. Lane 1, purified ECD6H ; lanes 2 - 4, ECD6H treated with DSS ; lane 2, without STp(4-17) ; lane 3, in the presence of 10^{-6} M STp(4-17) ; lane 4, in the presence of 10^{-6} M [Leu^{13}]STp(5-17). (B). Cross-linking of recombinant ECD with DSS. Lanes 1-5, ECD6H treated in the presence of STp(4-17) and lanes 6-10, in the presence of guanylin : lanes 1 and 6, 10^{-5} M ; lanes 2 and 7, 10^{-6} M ; lanes 3 and 8, 10^{-7} M ; lanes 4 and 9, 10^{-8} M ; lanes 5 and 10, 10^{-9} M. (C). Cross-linking of recombinant ECD with DSS. Lane 1, ECD6H treated with ^{125}I-BB-STp(4-17) in the presence of 10^{-5} M STp(4-17) ; lane 2, in the presence of 10^{-5} M guanylin ; lane 3, in the absence of 10^{-5} M STp(4-17) or guanylin. SDS-PAGE was carried out on a 10 % (A) or 7.5 % (B)(C) polyacrylamide gel and visualized by a silver staining (A)(B) or an autoradiography (C).

1.3 Discussion

1.3.1 Establishment of over-expression system of GC-C

The expression system which consisted of baculovirus and insect cells has potential not only for the production of large amounts of a foreign protein with post-translational modifications but also for the localization of the protein to a specific target, depending on its nature. However, the expression level of a membrane-associated protein in the baculovirus- insect cell system is generally lower than those of soluble proteins, such as nuclear-localized proteins or virus-derived proteins (Jarvis *et al.*, 1993). Certainly, one of the particulate forms of GC, GC-A, which has a structural topology similar to GC-C, was expressed in insect cells using the baculovirus vector, but the yield of the bioactive GC-A was less than 1 pmol / 10^6 cells (Chinkers *et al.*, 1991). We found that the expression of the functional GC-C (130-kDa protein) using its native signal peptide was poor in the insect cells, in spite of the production of a large amount of the premature protein (120-kDa protein). In this case, it appeared that most of the nascent polypeptide spontaneously aggregated without being folded and/or localized to the cell surface and that recognition of the signal peptide on a target would be insufficient as a result of the aggregation of the recombinant protein. Indeed, it has previously been reported that the secretion of a foreign protein from insect cells infected with the baculovirus vector could be enhanced by conversion of the signal peptide of the protein to that of an original protein in the insect cells (Tessier *et al.*, 1991; Murphy *et al.*, 1993). The replacement of the signal peptide of the recombinant GC-C by that of egt (Murphy *et al.*, 1993) dramatically improved the yield of the functional GC-C expressed on the cell membranes with a 19-fold increase in yield. Thus, the replacement of a signal peptide represents an alternative for the expression of a sufficient amount of a protein, although the substitution of a signal peptide by one of another origin does not always improve the expression and secretion of a recombinant protein in the baculovirus-insect cell system (Javis *et al.*, 1993). The yield of the entire GC-C protein expressed in the insect cells and baculovirus system was approximately 5-10 nmol per liter of culture medium, which is slightly lower than that usually obtained in this system.

The dissociation constant for the interaction between the recombinant GC-C and

STp(4-17) was 6.2×10^{-10} M, which was similar to that of porcine GC-C expressed in mammalian cells (K_D, 7.9×10^{-9} M) (Wada *et al.*; 1994). The cyclase catalytic activity increased 7.5 fold by stimulation with STa (3.1 nmol cGMP/min in 1 mg of membrane protein in the presence of 1×10^{-5} M STp(4-17)) in the cell membranes which contained the recombinant porcine GC-C. This value was considerably higher than that of native Sf21 cell membranes (less than 1 pmol cGMP/min in 1 mg of membrane protein). The number of the binding sites to STa was 3.6 pmol in 1 mg of membrane protein, calculated from the B_{max} value in Table 1-1. Therefore, the cyclase catalytic activity per ligand-binding site was 0.86 nmol cGMP/min per pmol of binding-site, which is similar to that of porcine GC-C expressed in mammalian cells (0.48 nmol cGMP/min per pmol of binding-site) (Wada *et al.*, 1994). These results demonstrated that the recombinant GC-C expressed in insect cells had not only ligand-binding affinity but cyclase catalytic activity which is identical to native GC-C.

The truncated extracellular domain will be an advantageous model for an analysis of the interaction between GC-C and a ligand, which reflects the mechanism of the activation of the complete protein, providing that the extracellular domain could be expressed as a soluble form and easily obtained in a large scale. Indeed, the extracellular domains of single transmembrane receptors, such as an epidermal growth factor (EGF) receptor, were successfully expressed in the insect cells and baculovirus system (Lax *et al.*, 1991; Hurwitz *et al.*, 1991). In the present study, the extracellular domain of GC-C was secreted as a soluble protein in the culture medium of the insect cells and was easily purified with Con A and Ni-chelating affinity chromatography by means of the addition of the His_6 tail at the C-terminus of the protein. Recently, the extracellular domain of GC-C was prepared as a fusion protein with glutathione S-transferase by a recombinant technique using *Escherichia coli* (Nandi *et al.*, 1996). The authors showed that the fusion protein is able to bind STa and suggested that post-translational modifications such as N-linked glycosylation are not essential for the binding of the extracellular domain to STa. When we cleaved the sugar chains at the potential N-linked glycosylation sites from ECD, expressed from the insect cells and baculovirus system, by treatment with PNGase-F, the deglycosylated ECD did not show binding to STa (section 4.2.1). This suggests that N-linked glycosylation is required for the interaction between

ECD and STa.

1.3.2 Multiple ligand-binding affinity and oligomerization of ECD

GC-C expressed in COS-7 cells contains multiple affinity sites to STa with three K_D values, 0.4×10^{-11}, 1.5×10^{-10}, and 2.2×10^{-9} M, which were determined by analysis of ligand-binding kinetics, and the occupancy of the ligand to both the high and low affinity binding sites is necessary for activation of the cyclase catalytic domain (Deshmane *et al.*, 1995). The measured K_D values of ECD were 4.0×10^{-10} and 7.3×10^{-8} M. The possibility that an additional binding site is present, but hidden cannot be excluded, since the present method focused on the analysis of the binding equilibrium with a ligand and, as a result, was different from the method based on the ligand-binding kinetics in an earlier report (Deshmane *et al.*, 1995). In the case of the EGF receptor, the K_D value of the truncated extracellular domain was 30-40-fold larger than that of the complete receptor and showed the presence of high and low affinity ligand-binding sites (Basu *et al.*, 1989; Lax *et al.*, 1991; Hurwitz *et al.*, 1991). It is likely that the K_D values for ECD correspond to those of the high and middle affinity sites of GC-C expressed in COS cells similarly to the case of the extracellular domain of the EGF receptor.

An interaction between the subunits of GC-C is required for cyclase catalytic activity and involves the intracellular domain (Runder *et al.*, 1995). This conclusion is supported by the finding that in GC-A the interaction site is localized at a hinge region between the kinase-homology domain and the cyclase catalytic domain in the intracellular domain (Wilson & Chinkers, 1995). GC-C may also interact with each subunit through a hinge region similar to that of GC-A, since the intracellular domain shares high sequence homology among particulate guanylyl cyclases. We treated ECD with a bifunctional coupling reagent in the presence or absence of STa. Interestingly, the formation of an oligomer of ECD was observed only in the presence of a ligand, although the oligomer was formed at a lower level. This implies that the oligomerization of the extracellular domain might be directly coupled to the activation of the intracellular domain. Thus, the extracellular domain of GC-C, which was prepared as a soluble protein at the large-scale expression level from a baculovirus and insect cell system, could be of use for studies of, not only the interaction between the extracellular domain and ligands but the mechanism

of signaling from the extracellular domain into the intracellular domain of GC-C as well.

1.4 Materials and Methods

1.4.1 Materials

Chemicals were purchased from Nacalai tesque Inc. (Kyoto, Japan) or Katayama chemical industries, Inc. (Osaka, Japan). Restriction enzymes were obtained from TOYOBO (Tokyo, Japan). Grace's and SF900II insect media were from Gibco/BRL (NY, USA) and fetal bovine serum was from Dainippon Pharmaceutical Co. (Osaka, Japan). A TaKaRa ligation kit (Takarashudo, Co., Kyoto, Japan), Competent High JM109 (TOYOBO), and a Flexi Prep Kit (Pharmacia, Uppsala, Sweden) were used for the construction of plasmids. STp(4-17), [Leu^{13}]STp(5-17), and *p*-benzoylbenzoyl (BB)-STp(4-17) were synthesized as described previously (Aimoto *et al.*, 1983; Yoshimura *et al.*, 1984; Gariépy & Schhoolnik, 1986; Yamasaki *et al.*, 1990). Human guanylin was synthesized according to procedures described previously (Hidaka *et al.*, 1993). Na^{125}I (carrier free) was purchased from DuPont NEN (MA, USA) and used for iodination of Tyr^{4} in STp(4-17) and BB-STp(4-17) (section 2.3.5). Con A and Ni-NTA agarose were from VECTOR (CA, USA) and QIAGEN (Hilden, Germany), respectively.

1.4.2 Constructions of transfer vectors carrying cDNA's of porcine GC-C and ECD

The transfer vectors carrying the cDNA encoding porcine GC-C or ECD were constructed as depicted in Fig. 1-7. That is, linker 1 (Table 1-2) encompassing restriction enzyme sites, the Kozak sequence (Kozak, 1986), and the start and stop codons were inserted into pUC19 at the *Pst*I/*Bam*HI site, resulting in the construction of pUC19-1. The cDNA fragments (bases 87 - 703 and 704 - 1373) of porcine GC-C (Wada *et al.*, 1994) obtained by digestion with *Bsp*HI and *Kpn*I or *Kpn*I and *Apa*I, respectively, were inserted together into the linker 1 on pUC19-1 at the *Nco*I/*Apa*I site to obtain pUC19-2. The sticky end of the *Nco*I site is compatible with that of *Bsp*HI. The 2.7 kb fragment (bases 704 - 3374) prepared by the treatment of the cDNA with *Kpn*I and *Hind*III was added to the *Not*I site derived from the multicloning sites of

Table 1-2 Oligonucleotide linker

Linker 1	M G P Q * * GCCACC ATG GGGG GGC CCT CAA TAG TAG G ACGTCGGTGG TAC CCCC CCG GGA GTT ATC ATC CCTAG
Linker 2	M T I L C W L A L L S T L T A V N A S S C ATG ACT ATT CTC TGC TGG CTT GCA CTG CTG TCT ACG CTT ACT GCT GTA AAT GCG TCC AGT GCA TGA TAA GAG ACG ACC GAA CGT GAC GAC AGA TGC GAA TGA CGA CAT TTA CGC AGG AC
Linker 3	G P Q G H H H H H H * CT CAA GGG CAC CAC CAC CAC CAC CAC TAA G CCG GGA GTT CCC GTG GTG GTG GTG GTG GTG ATT CCT AG

Amino acid sequences coded by the oligonucleotides are presented above the oligonucleotide sequences. Asterisks (*) indicate stop codons.

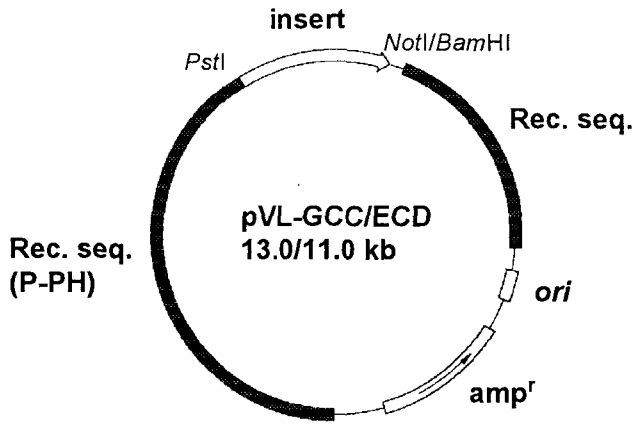

Fig. 1-7. The construction of the transfer vectors including the complete region of porcine GC-C or ECD(1-407). The cDNA's encoding GC-C or ECD were inserted into *PstI*/*NotI* sites (pVL-GCC) or *PstI*/*Bam*HI sites (pVL-ECD and pVL-ECD6H), respectively, in the multicloning sites of pVL1392. Rec.seq. and P-PH indicate the recombination sequence and the polyhedlin promoter, respectively.

pBluescript (Stratagene). The 0.7 kb *Pst*I/*Kpn*I fragment (Kozak sequence and bases 87 - 703 obtained from pUC19-2) and the 2.7 kb *Kpn*I/*Not*I fragment (bases 704 - 3374 with *Not*I linker) were ligated together to a baculovirus transfer vector (pVL1392) at the *Pst*I/*Not*I site. On the other hand, the 1.4 kb *Pst*I/*Bam*HI fragment (bases 87 - 1373 containing the start and additional stop codons) of pUC19-2 was inserted into pVL1392 at the *Pst*I/*Bam*HI site. These, respectively, provided the transfer vectors of GC-C or ECD flanking with the cDNA encoding the signal sequence of GC-C, pVL-GCC or pVL-ECD.

The signal peptide of porcine GC-C was replaced by that of egt as follows. The 0.6 kb *Pst*I/*Kpn*I fragment (bases 138 - 703), derived from pBS-M1GCC (Wada *et al.*, 1996a), was ligated together with linker 2 to pUC19-1 at the *Nco*I/*Kpn*I site to construct pUC19-3. The 0.7 kb *Pst*I/*Kpn*I fragment (the start codon, the signal sequence of egt, and bases 87 - 703) of pUC19-3 was ligated with the 2.7 kb *Kpn*I/*Not*I fragment (bases 704 - 3374 with *Not*I linker) into pVL1392 at the *Pst*I/*Not*I site. The 0.7 kb *Pst*I/*Kpn*I fragment of pUC19-3 was ligated together with the 0.7 kb *Kpn*I/*Bam*HI fragment (bases 704 - 1373 and the stop codon) of pUC19-2 into pVL1392 at the *Pst*I/*Bam*HI site. The mutation, which occurred at the linking site of the signal sequence, was repaired by PCR, resulting in the construction of the transfer vectors, pVL-GCC(egt) and pVL-ECD(egt).

The cDNA fragment encoding ECD with the His6 tail (GHHHHHH, single letter code for amino acid residues) at the C-terminus was constructed by insertion of linker 3 into pUC19-1 at the *Apa*I/*Bam*HI site (pUC19-4), which corresponded to the plasmid replaced at the latter part of linker 1 in pUC19-1. The 0.7 kb *Pst*I/*Kpn*I fragment of pVL-ECD(egt) and the 0.7 kb *Kpn*I/*Bam*HI fragment of pUC19-4 were inserted together into pVL1392 at the *Pst*I/*Bam*HI site, providing the transfer vector, pVL-ECD6H(egt).

1.4.3 Preparation of recombinant proteins

The recombinant baculovirus was prepared by the homologous recombination between the transfer vectors and a linearized viral DNA (BaculoGold, Phar-Mingen) according to the manufacturer's specifications. Sf21 insect cells were cultured in Grace's medium with 10 % fetal bovine serum and gentamycin (30 μg / ml) at 27 °C and maintained as stock cultures in 75 cm^2 flasks. The recombinant virus, of which the titer

was 5-10 multiples of infection, was infected to the cells (5×10^7, 80 % confluent state) in a 175 cm^2 flask for 1 h. The infected cells were scraped into a fresh SF-900II medium and then cultured to express the recombinant protein in a spinner flask for 2 d.

1.4.4 Preparation of membranes

All procedures were carried out at 4 °C. The cells which expressed the recombinant protein were harvested by scraping into PBS(-) and washed twice with the same buffer. The cells were then resuspended in buffer A (20 mM HEPES (pH 7.4), 100 mM NaCl, 10 % glycerol, 0.02 μg/ml leupeptine, 0.4 mM phenylmethanesulphonyl fluoride, 1 mM EDTA), and homogenized by sonication. Unbroken cells were removed by centrifugation at 1,000 × g for 15 min, and the supernatant was recentrifuged at 20,000 × g for 1 h and washed twice with buffer A. The pellet was suspended at 0.5-1 mg / ml of the protein concentration in buffer A for further use. Protein concentration was determined using bovine serum albumin as a standard protein in conjunction with the Bio-Rad protein assay kit.

1.4.5 Purification of ECD6H

The culture supernatant (400 ml) was separated from the cells by centrifugation and was mixed with Con A immobilized agarose (5 ml) in a batch. The Con A agarose was filtered and washed with 5 bed volumes of buffer B (20 mM HEPES (pH7.4) and 100mM NaCl). The adsorbed protein was eluted with 5 bed volumes of buffer B containing 500 mM α-methyl-D-mannoside. The non-adsorbed fraction was treated repeatedly by the same procedure and the eluted fractions were pooled. The eluate containing ECD6H was stirred with Ni-NTA resin (2 ml) for 2 h and the resin was then washed with 5 bed volumes of buffer B containing 20 mM imidazole. ECD6H was eluted from the resin with 5 bed volumes of buffer B containing 100 mM imidazole. The fraction containing ECD6H was concentrated by Centricon-10 (Amicon). The results of the purification are summarized in Table 1-3.

Table 1-3 Purification of ECD6H

	Protein (mg)	^{125}I-STp(4-17) binding (cpm)	Recovery (%)	Purification fold
Culture medium	1720	3.7×10^8	100	1
Con A affinity chromatography	22	1.3×10^8	34	27
Ni-chelating affinity chromatography	0.52	1.7×10^8	4.7	156

1.4.6 Western blot analysis

The recombinant porcine GC-C was analyzed according to a previously published procedure (Wada *et al.*, 1996b) and detected with Renaissance Western Blot Chemiluminescence Reagent (DuPont NEN).

1.4.7 Analysis of N-terminal amino acid sequence

Recombinant GC-C (120 and 130 kDa) and ECD6H (53-kDa), prepared and purified as described above, were run on SDS-PAGE and blotted onto a polyvinylidene difluoride membrane. After staining with coomassie brilliant blue, the corresponding protein bands on the membrane were cut out and subjected to N-terminal sequence analysis with an Applied Biosystems Model 474A Sequencer.

1.4.8 Photoaffinity-labeling of recombinant proteins and binding assay to STa

The cells infected with the recombinant baculovirus (5×10^4 cells / tube) or the culture supernatant (10 μl) were incubated with ^{125}I-BB-STp(4-17) (8.0×10^5 cpm) in PBS(-) (60 μl) in the presence or absence of 1 μM STp(4-17) at 37 °C for 1 h in the dark. The mixture was exposed to UV light (254 nm, Model UVG-54, UVP inc., CA) for 30 min on ice, then boiled for 3 min in the SDS-PAGE sample buffer as described previously (Wada *et al.*, 1994) and then separated by SDS-PAGE. After drying the gel, the binding proteins were analyzed by autoradiography on a Fujix Bio-image analyzer

BAS 2000 (Fuji film, Tokyo).

In saturation and competitive binding experiments, the cell membrane fraction (5 μg protein), which expressed recombinant GC-C, was incubated with ^{125}I-STp(4-17) (1×10^{-10} - 2×10^{-8} M) or with ^{125}I-STp(4-17) (5×10^{-9} M) in the presence of STp(4-17) (1×10^{-8} M - 1×10^{-5} M), respectively, in PBS(-) (60 μl) at 37°C for 1 h. After incubation, the radio-iodinated STp analog which had bound to the membranes was collected on a Whatman GF/C glass-filter pretreated with 1 % polyvinyl-pyrrolidone as described previously (Hasegawa *et al*, 1997). In the case of ECD or ECD6H, the culture medium (10 μl) was diluted to PBS(-) (60 μl) in the presence of STp(4-17) (various concentrations) as described above. The free ligand was removed by filtration on a TLK-3000 ultra-free filter (Millipore) at 4 °C, followed by 2 washings with cold PBS(-) (150 μl) and centrifugation (1,000 × g, 10 min). The radioactivity of the filter was measured with a γ-well counter. All experiments were performed in triplicate at each peptide concentration.

1.4.9 cGMP assay

The membrane fraction (10 μg) of the Sf21 cells expressing recombinant GC-C was suspended in buffer (20 mM HEPES (pH7.4), 7.5 mM creatine phosphate, 5 U creatine kinase, 4 mM $MgCl_2$, 0.1 mM isomethylbutylxantine), mixed with GTP (1mM) and STp(4-17) (various concentrations), and incubated at 37 °C for 20 min. The reaction was stopped by the addition of 0.12 M HCl (900 ml), followed by boiling for 3 min. The cGMP concentration was estimated by a radioimmunoassay kit (YAMASA).

1.4.10 Chemical cross-linking of ECD6H

A solution of purified ECD6H (100 μl) was incubated with ligand (various concentrations) at 37 °C for 1 h and then mixed with 50 mM DSS in DMSO (2 μl). After 15 min, the reaction was stopped by the addition of the SDS-PAGE sample buffer. The reaction product was separated by SDS-PAGE and detected by silver staining or photoaffinity radio-labeling as described above.

Chapter 2. Development of photoaffinity-labeling with identification of the receptor-binding site in a ligand of guanylyl cyclase C

2.1 Introduction

A narrow and well-defined part of total protein surface is presumed to be involved in selective and high affinity interaction with a specific ligand, and this part is referred to as the binding site. The complete understanding of how particulate guanylyl cyclases carry out their biological function requires a detailed understanding of how the binding sites on both a ligand and the receptor is constituted. For this purpose, an affinity-labeling technique was applied to analysis the interaction sites between STa and GC-C.

The affinity-labeling reagent for identification of the interaction sites needs to meet following requirements : (i) an affinity-labeling reagent should be converted from low reactive state to high reactive state in biological condition after the binding to GC-C ; (ii) the reactive group for the cross-linking reaction needs to position in close proximity to the interaction site for GC-C in the STa analogous molecule, and simultaneously, the reactive group should not inhibit binding affinity of the carrier STa analog to GC-C; (iii) the specificity of the cross-linking reaction should be low enough to make a stable covalent bond to any amino acid residues. Photoaffinity-labeling using an azido group is possibly a method satisfying these requirements (Bayley & Knowles, 1977; Eberle & de Graan, 1985). In this chapter, development of the photoaffinity-labeling method using synthetic STa analogs is described.

STp is produced by one strain of enterotoxigenic *E. coli* and consists of 18 amino acid residues, as shown in Fig. 2-1 (Takao *et al.*, 1983). The region from Cys^{5} to Cys^{17}, commonly referred to as the toxic domain, is highly homologous among members of the STa family. This region contains three disulfide linkages, between Cys^{5} and Cys^{10}, Cys^{6} and Cys^{14}, and Cys^{9} and Cys^{17}, which occur in all of the STa's known to date and which are essential for expression of the full enterotoxigenic activities of STa (Hidaka *et al.*,

1988). The X-ray crystallography of the toxic domain of STp shows that it consists of three structural segments: a 3_{10} helix in the N-terminal region (Cys^5-Cys^9), a type I β-turn in the central region (Asn^{11}-Cys^{14}), and a type II β-turn in the C-terminal region (Cys^{14}-Cys^{17}) (Ozaki *et al.*, 1991; Sato *et al.*, 1994). Based on the structure-function relationships of STa's it has been concluded that the central segment which contains the β-turn structure represents a contact region for the receptor protein (Yamasaki *et al.*, 1990; Ozaki *et al.*, 1991; Okumura *et al.*, 1994). To determine the most suitable site of the reactive group for photoaffinity labeling, we have synthesized three STa analogs which contain a photoreactive amino acid, *p*-azido-L-phenylalanine (Pap), and which gives rise to a covalent bond between the STa analogs and the receptor protein on UV radiation. Pap was introduced into positions 8, 11, and 15 in STp(4-17), which are located, respectively, at the N-terminal, the central, and the C-terminal segments, as shown in Fig. 2-1. The binding ability and the cross-linking efficiency of the photo-reactive STp analogs were estimated by analyzing their interaction with rat intestinal membranes which contain the receptor protein. The results showed that only the Pap residue in the central segment binds to the receptor protein by UV radiation, providing evidence that it is this region of the STa molecule (including the asparagine residue at position 11) which represents the recognition site of the receptor protein.

2.2 Results and Discussion

2.2.1 Design of the photo-affinity labeling STa analogs

A photoaffinity-labeling method is an effective technique to obtain direct information related to interaction sites between a ligand and a receptor. In this chapter, the photoreactive peptides, which could cross-link to the receptor protein of STa, were prepared to identify the binding site on STp for the receptor protein. Structural analyses of the toxic domain of STp by X-ray crystallography showed that the toxic domain consists of three structural segments, which are a 3_{10} helix in the N-terminal region, a type I β-turn in the central region, and a type II β-turn in the C-terminal region, and which are tightly connected to one another by disulfide bonds (Ozaki *et al.*, 1991; Sato *et*

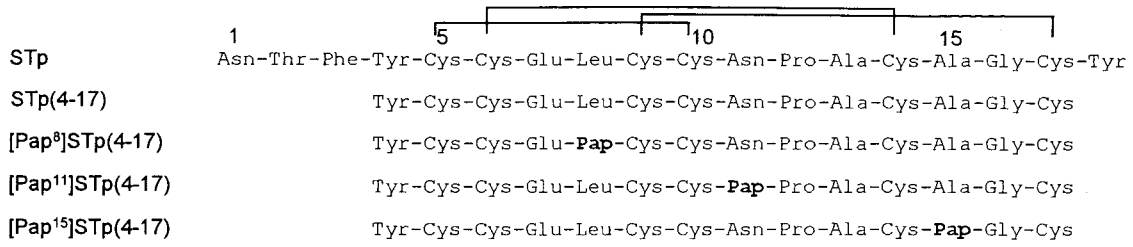

Fig. 2-1. Primary structures of STp and the synthetic analogs. Solid lines above indicate the positions of disulfide linkages.

al., 1994). These structural segments are exposed to different orientations on the STp molecule. Based on this information, the photochromophor, Pap, was introduced at positions 8, 11, and 15 in STp(4-17), as shown in Fig. 2-1. Thus, the Pap residues are oriented in different directions from the surface of the ST molecule and replace Leu^{8} or Asn^{11} or Ala^{15}. These three photoreactive STp analogs are capable of interacting with different sites of the receptor protein, only one of which represents the binding site.

2.2.2 Synthesis of photoreactive STp analogs

Aph was used as the building block for the preparation of precursors of the photoreactive STp analogs, because Aph is easily introduced into a peptide using standard solid-phase techniques and converted to a photolabile and cross-reactive arylnitrene (Schwyzer & Caviezel, 1971). The scheme for synthesis of the STp analog with Aph at position 11, for example, is shown in Fig. 2-2. The reversed-phase HPLC of the STp analogs thus synthesized showed several peaks, which had the same molecular weight and amino acid composition as the expected values, after the formation of intramolecular disulfide linkages, as shown in Figs. 2-3A~C. The CD spectra of these fractions were compared with that of the native type of STp(4-17), as shown in Fig. 2-4. The fractions indicated by arrows in Figs. 2-3A~C had similar spectral patterns to that of STp(4-17), while the other one which is indicated by an asterisk in Fig. 2-3B and contained an isomeric peptide was different. Characteristic negative bands were observed centered at 198 nm in the far-UV CD spectra of not only STp(4-17) but the

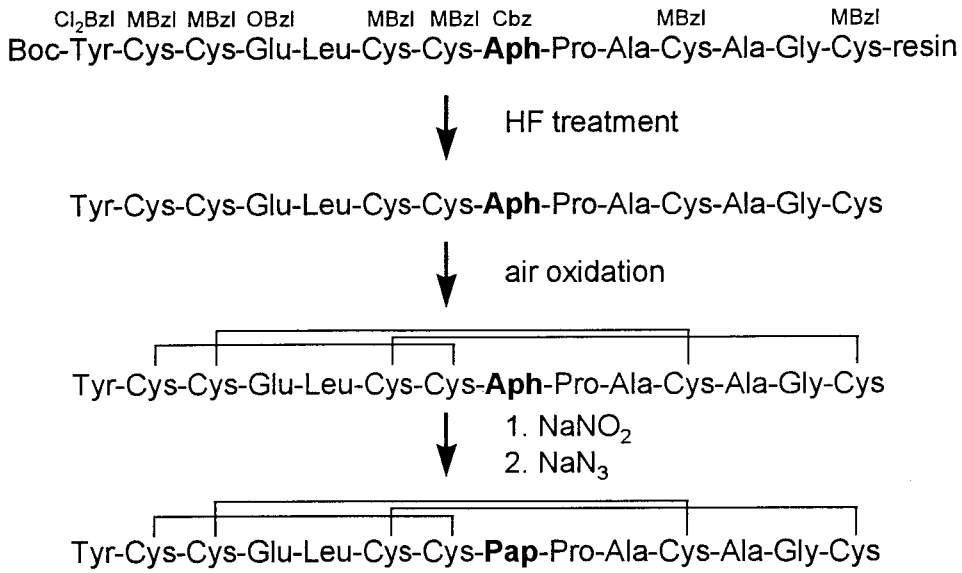

Fig. 2-2. Scheme for synthesis of [Pap[11]]STp(4-17). Aph and Pap represent *p*-amino-*L*-phenylalanine and *p*-azido-L-phenylalanine residues. Boc; *t*-butyloxycarbonyl, Cl2Bzl; O-2,6-dichlorobenzyl, MBzl; S-4-methylbenzyl, OBzl; benzyl ester, Cbz; carbobenzoxy are protecting groups.

STp analogs with an Aph residue. Moreover, shoulder peaks at around 210 nm, derived from the β-turn structure in the central region of STp(4-17) (Ozaki *et al.*, 1991; Sato *et al.*, 1994), were observed in the spectra of the STp(4-17) analogs. These provide supporting evidence that the STp analogs thus synthesized and purified had the same conformation and therefore the same arrangement of disulfide linkages as those of native STp. The results were confirmed by the finding that the peptides in the fractions indicated by arrows in Figs. 2-3A~C completely inhibited the specific binding of ^{125}I-STp(4-17) to the receptor protein on rat intestinal membranes in their concentrations of 1 μM, while those in other fractions did not (data not shown). The results were further confirmed by the assessment of the immunological reactivities of synthetic STp analogs with an anti-STa monoclonal antibody, MAb 53-4 (Takeda *et al.*, 1993), in competitive ELISA (Yamasaki *et al.*, 1990). The monoclonal antibody recognizes leucine residue at position 9 and the conformation of native STh(1-19) (Yamasaki *et al.*, 1990; Takeda *et*

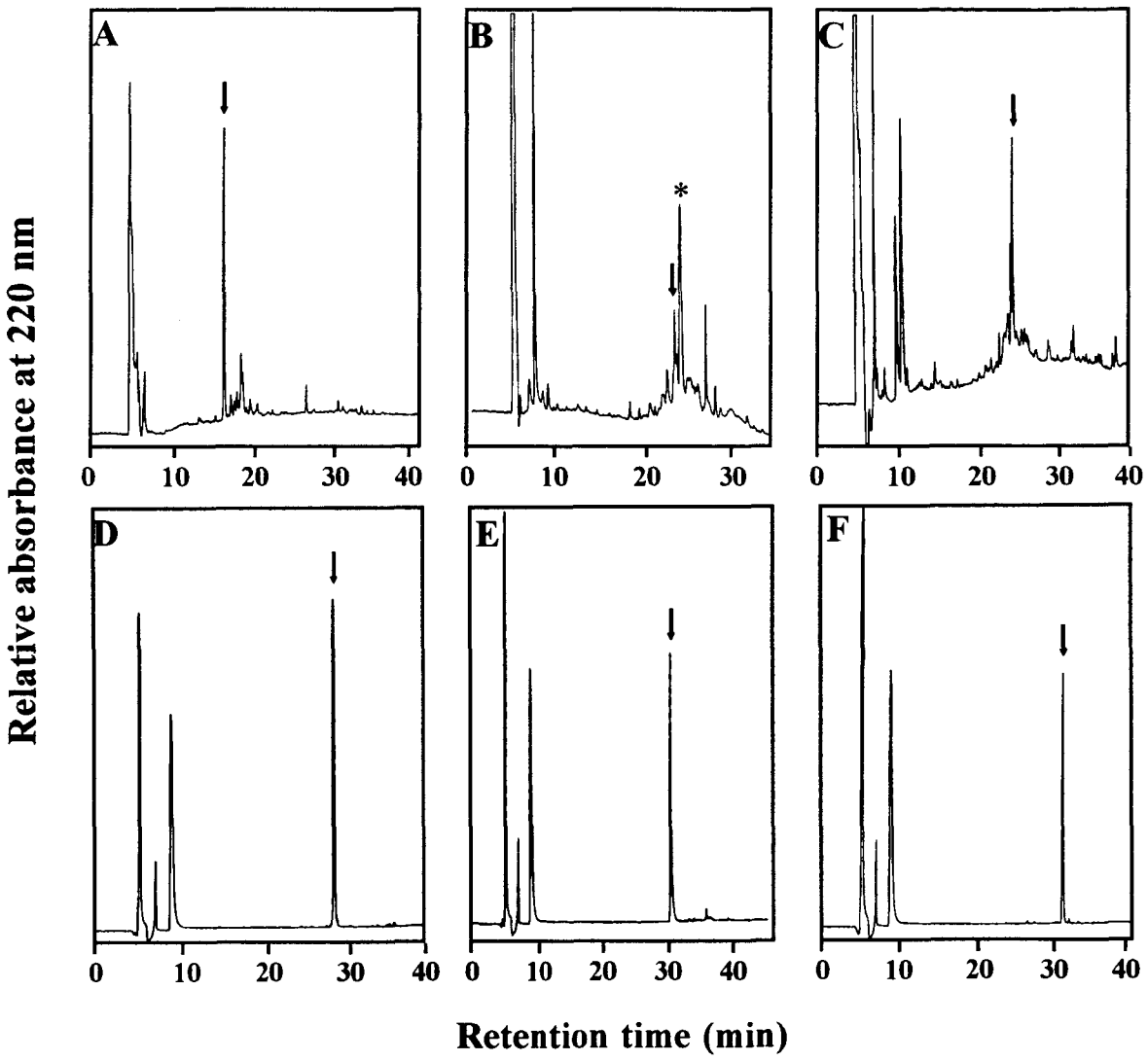

Fig. 2-3. Reversed-phase HPLC profiles of the peptides containing Aph. (A) [Aph^{8}]STp(4-17); (B), [Aph^{11}]STp(4-17); (C), [Aph^{15}]STp(4-17). HPLC analyses were performed using a linear gradient in 0.05 % TFA in A and C, and in 10 mM $AcONH_4$ buffer (pH 5.7) in B. Arrows show peaks corresponding to the desired peptides. An asterisk indicates the peak fraction of an inactive isomer of [Aph^{11}]STp(4-17) and its CD spectrum is shown in Fig.2-4. Reversed-phase HPLC profiles of the peptides containing Pap. (D) [Pap^{8}]STp(4-17); (E) [Pap^{11}]STp(4-17); (F) [Pap^{15}]STp(4-17). HPLC analyses were performed using a linear gradient in 0.05 % TFA.

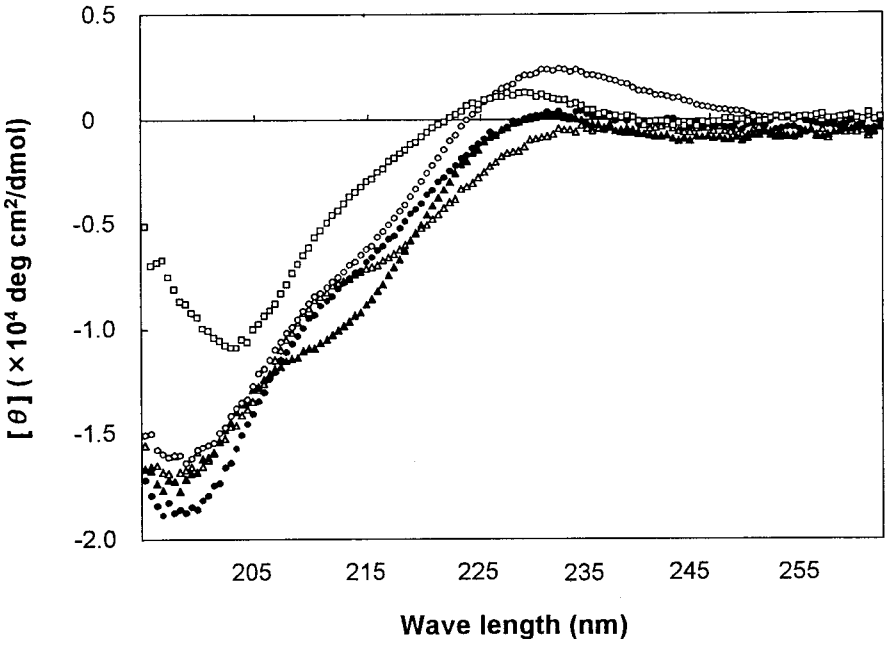

Fig. 2-4. CD spectra of the STp analogs. [Aph[8]]STp(4-17) (closed triangles), [Aph[11]]STp(4-17) (open triangles), [Aph[15]]STp(4-17) (open circles), STp(4-17) (closed circles), and an inactive isomer of [Aph[11]]STp(4-17) (open squares).

al., 1993). STp(4-17) and the synthetic STp(4-17) peptides ([Aph[8]]STp(4-17), [Aph[11]]STp(4-17), and [Aph[15]](4-17)) in the fractions indicated by arrows in Figs. 2-3A~C) showed IC_{50} values of 0.4, 200, 50, and 0.4 pmol per well of an ELISA plate, respectively, in the binding reaction MAb 53-4 with STh(1-19) immobilized on wells. The weak reactivity of [Aph[8]]STp(4-17) was reasonable, because the epitope of MAb 53-4 is centered to Leu[9] in the N-terminal region of STh(1-19) (corresponding to Leu[8] of STp) (Takeda *et al.*, 1993). The reactivity of [Aph[11]]STp(4-17), which was lower than those of STp(4-17) and [Aph[15]]STp(4-17), might be affected by the close proximity of Aph[11] to the epitope of MAb 53-4. On the other hand, the isomeric peptide of [Aph[11]]STp(4-17) indicated by an asterisk in Fig. 2-3B did not inhibit the binding of the

antibody even in the amount of 1,200 pmol per well.

The correct disulfide linkages of STp(4-17) are formed spontaneously in the air oxidation (Aimoto *et al.*, 1983; Yoshimura *et al.*, 1984). The STp(4-17) analogs with the Aph residue at position 8 or 15 ([Aph^{8}]STp(4-17) and [Aph^{15}]STp(4-17), respectively) were obtained as major peaks, while the STp(4-17) analog with Aph at position 11 ([Aph^{11}]STp(4-17)) was obtained as a minor peak, as shown in Figs. 2-3A~C. The side chain of the asparagine residue at position 11 binds to an amide bond of the main chain of STp by hydrogen bonding and contributes to the stability of the β-turn structure in the central region of STp (Ozaki *et al.*, 1991; Sato *et al.*, 1994). The replacement of asparagine at position 11 by Aph may eliminate the possibility for hydrogen bonding at this residue and the Aph residue with a large side chain may affect the folding process of STp, resulting in the production of a peptide with the correct arrangement of disulfide linkages as a minor product.

The Aph residue in the purified peptides was converted into Pap, using the previously described procedure (Schwyzer & Caviezel, 1971). Figures 2-3D~F show the reversed-phase HPLC profiles of the reaction mixtures. The final Pap-containing peptides were prepared with no side reactions and were characterized by fast atom bombardment mass spectrometry and amino acid analysis.

2.2.3 Photoaffinity labeling of photo-reactive STp analogs to STp receptor on rat intestinal membranes

In a number of laboratories, the photoaffinity-labeling experiments for detecting the receptor protein specific for STp on rat intestinal cell membranes revealed that several molecular species ranging from 50 to 140 kDa are produced (Kuno *et al.*, 1986; Hirayama *et al.*, 1992; de Sauvage *et al.*, 1992; Vaandrager *et al.*, 1993). In our experiments, we found a protein of 70-77 kDa as a major band and one of 125-140 kDa as a minor band on SDS-PAGE (Hirayama *et al.*, 1992). The 70-77 kDa receptor protein was targeted for photoaffinity-labeling in this experiment, because it shows nearly the same characteristics in the photoaffinity-labeling experiment as that of 125-140 kDa protein and proteins from 50 to 80 kDa represent proteolytic products of the 125-140 kDa receptor protein (de Sauvage *et al.*, 1992; Vaandrager *et al.*, 1993; Cohen *et al.*,

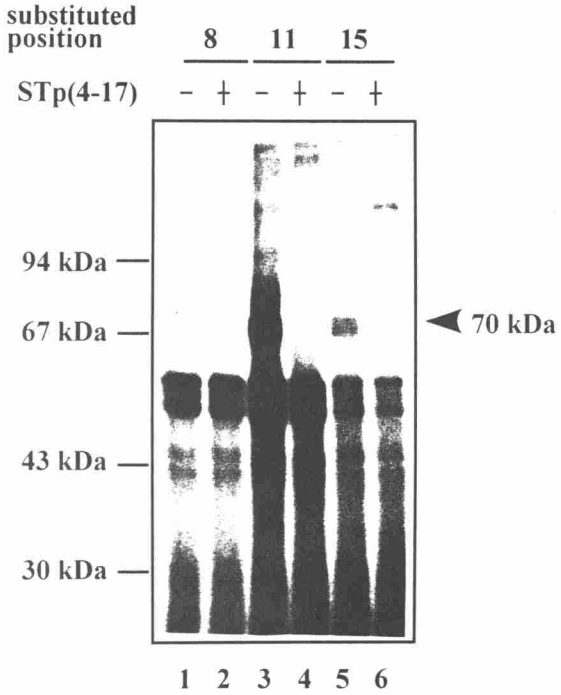

Fig. 2-5. Photo-affinity labeling using the synthetic STp analogs. Photoaffinity labeling of rat intestinal membranes by ^{125}I-[Pap^{8}]STp(4-17) (lanes 1 and 2), ^{125}I-[Pap^{11}]STp(4-17) (lanes 3 and 4), and ^{125}I-[Pap^{15}]STp(4-17) (lanes 5 and 6). Molecular masses of the standard proteins (Pharmacia, Uppsala, Sweden) are indicated at the left side.

1993).

The photoreactive STp(4-17) analogs ([Pap^{8}]STp(4-17), [Pap^{11}]STp(4-17), and [Pap^{15}]STp(4-17)) were radioiodinated at the N-terminal tyrosine residue by treatment with $Na^{125}I$ using the chloramine-T method and purified by reversed-phase HPLC (data not shown). These radioiodinated analogs were reacted with the STa receptor on rat intestinal membranes, prepared as described in section 2.3.4, and cross-linked to the receptor protein by UV radiation. These three analogs showed protein bands at approximately 70-kDa on SDS-PAGE, which were specifically radiolabeled (odd-numbered lanes in Fig. 2-5) in the absence of non-radiolabeled STp(4-17) and diminished in the presence of an excess of non-radiolabeled STp(4-17) (even-numbered lanes in Fig. 2-5). However, the photoreactive STp(4-17) analogs showed a different degree of cross-linking efficiency in the binding reaction to the 70-kDa protein. [Pap^{11}]STp(4-17) was linked most intensively to this specific protein, while the protein bands labeled by the other two analogs were faint on an autoradiographic image. These results showed the order of the cross-linking efficiencies of [Pap^{11}]STp(4-17) > [Pap^{15}]STp(4-17) > [Pap^{8}]STp(4-17) .

2.2.4 Binding affinity of STp analogs

To determine if the difference in the intensities of these protein bands arose from the degree of the binding affinities of the STp analogs ([Pap^{11}]STp(4-17), [Pap^{15}]STp(4-17), and [Pap^{8}]STp(4-17)) to the receptor protein or from the position of the photo-reactive arylnitrene residue in these STp analogs, the binding affinities of these three STp analogs were compared to the receptor protein by examining their competitive inhibition on the binding of radioiodinated STp(4-17) to the receptor protein. The IC_{50} value of [Pap^{11}]STp(4-17) was approximately 30-fold higher than that of STp(4-17), whereas those of [Pap^{8}]STp(4-17) and [Pap^{15}]STp(4-17) were comparable to that of STp(4-17), as shown in Fig. 2-6. The order of the binding affinity to the receptor protein was [Pap^{8}]STp(4-17) $\geq$ [Pap^{15}]STp(4-17) $>>$ [Pap^{11}] STp(4-17). That is, the binding affinity of [Pap^{11}]STp(4-17) was lower than those of [Pap^{8}]STp(4-17) and [Pap^{15}]STp(4-17), despite the fact that [Pap^{11}]STp(4-17) was cross-linked much more effectively to the receptor protein than [Pap^{8}]STp(4-17) and [Pap^{15}]STp(4-17), as described above.

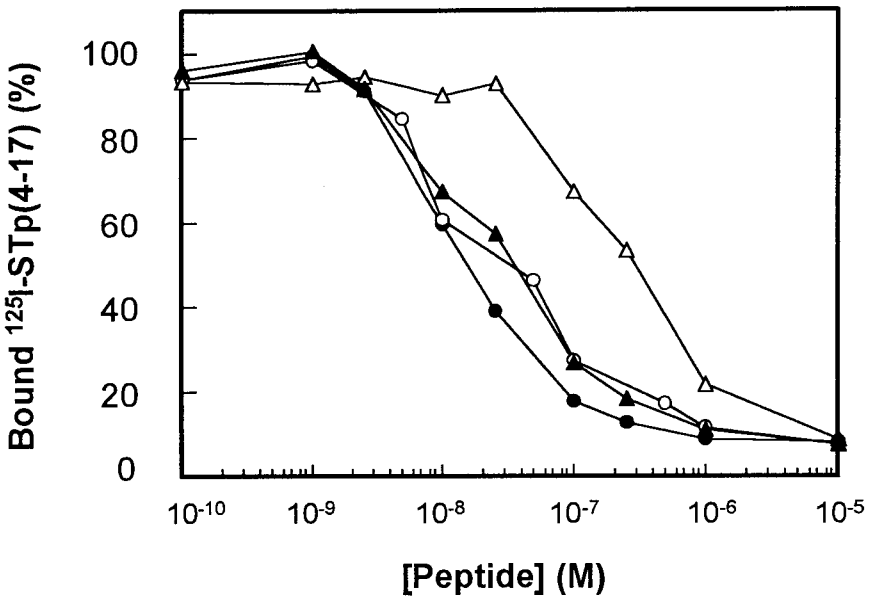

Fig. 2-6. Estimation of receptor-binding affinity of the STp analogs. Curves for the inhibition by the STp analogs of the binding of ^{125}I-STp(4-17) to the receptor (Values shown represent the mean of duplicate data sets): [Pap^{8}]STp(4-17) (closed triangles), [Pap^{11}]STp(4-17) (open triangles), [Pap^{15}]STp(4-17) (open circles), and STp(4-17) (closed circles).

These results suggest that the Pap^{8} and Pap^{15} residues, respectively, in the N-terminal and C-terminal segments of STp do not participate at all, or participate weakly, in direct binding to the receptor protein, or that the Pap at position 11 in the central segment of the STp molecule is spatially in close proximity to the receptor protein and, therefore, is capable of interacting with the ligand binding site(s) on the receptor protein, because the cross-linking efficiency of a photochemical reaction depends strongly on the distance between the photochromophor and the surface of a target molecule (Bayley & Knowles, 1977; Eberle & de Graan, 1985).

The central segment of STp forms the β-turn structure with a hydrophobic core and is exposed to the outside of the STp molecule (Ozaki *et al.*, 1991; Sato *et al.*, 1994). Moreover, three amino acid residues (Asn^{11}-Pro^{12}-Ala^{13}) of the central region are conserved among the STa family, as seen in Fig. 2-1. The replacement of these three

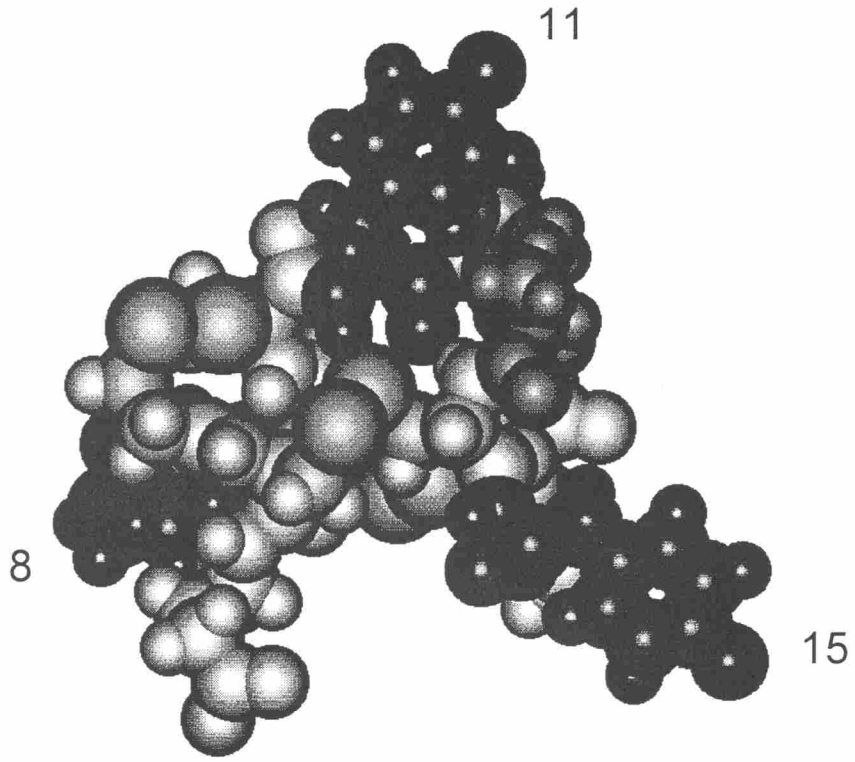

Fig. 2-7. Structure model of the STp analogs. CPK-model of STp(5-17) substituted by Pap residue at positions 8, 11, and 15, based on the native structure determined by X-ray crystallography (Ozaki *et al.*, 1991). The residues in gray were Pro^{12}-Ala^{13}, which were critical for the toxic activity or receptor binding (Yamasaki *et al.*, 1990; Okumura *et al.*, 1994).

amino acid residues by others dramatically decreases binding activity to the receptor. The size of the aliphatic side chains of Pro-Ala greatly influences binding to the receptor (Yamasaki *et al.*, 1990; Okumura *et al.*, 1994). The CPK-modeling of [Pap^{11}]STp(4-17) shows that the side chain of the amino acid residue at position 11, located on the surface of the hydrophobic core, is present adjacent to the side chain of the Ala^{13} residue, as shown in Fig. 2-7. This close proximity of the side chains of two amino acid residues, Pap^{11} and Ala^{13}, may increase the efficiency of the cross-linking of [Pap^{11}]STp(4-17) to the receptor protein, although the steric effect of the photoreactive group may reduce the receptor-binding activity. On the other hand, the efficiencies of the cross-linking of

[Pap^{8}] STp(4-17) and [Pap^{15}]STp(4-17) to the receptor protein were considerably lower than that of [Pap^{11}]STp(4-17) in spite of their high binding affinity to the receptor. The side chains of Pap^{8} and Pap^{15} residues may protrude to the other side of the STp-binding pocket in the STa receptor after binding.

These results, taken together, suggest that the environment around the amino acid residue at position 11 in STp is critical for binding with the receptor protein and/or that the site on the STa molecule which binds to the receptor protein is limited to a narrow region in the central segment of STp, including the amino acid residue at position 11.

2.3 Materials and Methods

2.3.1 Peptide synthesis

The reagents used for peptide synthesis were purchased from Peptide Institute Inc. (Minoh, Japan) and nacalai tesque, inc. (Kyoto, Japan). Boc-Aph(Z)-OH was prepared by methods described previously (Schwyzer & Caviezel, 1971). Peptides were synthesized by standard solid-phase procedures using Boc blocking groups. Details of the procedure for the synthesis of peptides, protection of the side chains of functional amino acid residues, removal of the peptides from the resin, and their conversion from a linear form to an oxidized form are described in the papers of reference (Aimoto *et al.*, 1983; Yoshimura *et al.*, 1984; Yamasaki *et al.*, 1990). The resulting peptides were purified by reversed-phase HPLC, as described below. [Aph^{8}]STp(4-17) and [Aph^{15}]STp(4-17) were prepared in a similar yield to STp(4-18) reported previously (Yoshimura *et al.*, 1984). The yield of [Aph^{11}]STp(4-17) was approximately one-tenth of those of the two other peptides.

The conversion of Aph to Pap in STp analogs was carried out as follows: A purified peptide carrying an Aph residue (100 nmol) was dissolved in 0.1 M HCl (200 μl) and mixed with 1 M $NaNO_2$ (10 μl), and the mixture was then kept on ice for 15 min. The reaction was stopped by adding 1 M NH_2SO_3H (12 μl). The mixture was then incubated with 1 M NaN_3 (8 μl) at 0 °C for 5 min. The final product, containing a Pap residue, was purified by reversed-phase HPLC and its purity confirmed by amino acid analysis and fast atom bombardment mass spectrometry.

2.3.2 High-performance liquid chromatography (HPLC)

The synthetic peptides were purified on a reversed-phase column (Cosmosil $_5C_{18}$, 8 × 300 mm) (nacalai tesque, inc., Kyoto, Japan) using an HPLC delivery system consisting of a Waters M600 pump (Milford, MA), a Hitachi 655A variable-wavelength UV monitor, and a D-2000 chromatointegrator (Hitachi, Tokyo, Japan). HPLC was carried out at a flow rate of 2 ml/min with a linear gradient of 10-50 % CH_3CN in 0.05 % TFA over 40 min. The peptides thus purified were rechromatographed under the same conditions as described above except that 10 mM ammonium acetate buffer (pH 5.7) was used instead of 0.05 % TFA. The eluates from the HPLC column were monitored by their absorbance at 220 nm.

2.3.3 Circular Dichroism (CD)

CD spectra of peptides (10 mM) in the far-UV region (195-260 nm) were measured in 10 mM potassium phosphate buffer (pH 7.4) in a 10 mm path length cuvette at room temperature on a Model J-700 spectropolarimeter (JASCO, Tokyo, Japan).

2.3.4 Membrane preparation

Rat brush border membranes were prepared essentially by procedures described previously with some modifications (Hirayama *et al.*, 1992). All procedures were carried out at 4 °C. Protein concentrations were determined using Bio-rad protein assay kit. Rat small intestine was rinsed in an ice-cold 0.9% NaCl aqueous solution and homogenized with a Polytron homogenizer (Kinematica AG, Lucerne, Switzerland). The homogenate was diluted with 50 mM Tris-HCl buffer (pH 7.6) containing 1 mM EDTA, 1 mM PMSF, 10 mM MgCl2, and 0.25 M sucrose, and was then stirred for 15 min. The homogenate was centrifuged at 1,000 × g for 20 min, and the supernatant was then recentrifuged at 100,000 × g for 60 min. The resulting membrane pellets were resuspended in the same buffer as above and washed twice with the same buffer. The final membrane sample was suspended in the same buffer but without $MgCl_2$ and sucrose, and stored at -20 °C until used.

2.3.5 Photoaffinity and cross-linking with ^{125}I-[Pap]STp analogs

Peptides were radiolabeled with ^{125}I according to the modified chloramine-T method (Hunter & Greenwood, 1962). A peptide (6 nmol) was dissolved in 150 mM phosphate buffer (pH 7.5) (10 μl) and mixed with 3.5 mM chloramine-T (5 μl) and Na125I solution (0.5 mCi/peptide, carrier free, DuPont). After incubation for 30 s, the reaction was stopped by adding a saturated aqueous solution of L-ascorbic acid and the radiolabeled peptide was immediately purified by reversed-phase HPLC.

The membrane sample (100 μg) was incubated with ^{125}I-[Pap^{8} or ^{11} or ^{15}]STp(4-17) (8.0×10^5 cpm) in 60 μl of PBS(-) in the presence or absence of STp(4-17) at 37 °C for 1 h in the dark. The mixture was exposed to UV light (254 nm) for 30 min on ice and boiled for 3 min in the sample buffer (1.8 % SDS, 30 mM Tris-HCl (pH 7.6), 4 % glycerol, 1.5 mM EDTA, 5 % DTT and 0.05 % bromophenol blue), and the reaction mixture then applied to SDS-PAGE. After drying, the gel was subjected to an autoradiographic analysis with Fujix Bio-image analyzer BAS 2000 (Fuji film, Tokyo, Japan)

2.3.6 Receptor binding assay

The membrane sample (100 μg) was incubated with ^{125}I-labeled STp(4-17) (2.5×10^5 cpm) and non-radiolabeled STp analogs of various concentrations in PBS(-) (60 μl) at 37 °C for 1 h in the dark. After incubation, the membranes were collected on GF/C glass fiber filter (Whatman) pretreated with 1 % polyvinyl-pyrrolidone, and washed twice with 5 ml of PBS(-) to remove the free ligand. The radioactivity of the membranes was measured using an ARC-361 γ-well counter (Aloka, Tokyo, Japan). All experiments were performed in duplicate at each peptide concentration.

2.3.7 Enzyme-Linked Immunosorbent Assay (ELISA)

Competitive ELISA was performed in the reaction of synthetic peptides with a monoclonal antibody, MAb 53-4, which recognizes Leu^{9} in STh(1-19) (Yamasaki *et al.*, 1990; Takeda *et al.*, 1993). STh(1-19) (1 μg/ml of PBS) (0.1 ml) was immobilized into wells of a Falcon microtest III flexible assay plate (Becton Dickinson and Co., Oxnard, CA., U.S.A.) by incubation at 37 °C for 2 h. The wells were washed thrice with PBS

and treated with PBS (0.15 ml) containing 1% bovine serum albumin at 37 °C for 1 h. After washing the wells thrice with PBS containing 0.05 % Tween20 (PBS(T)), a samples (50 μl) and a solution of MAb 53-4 (50 μl) appropriately diluted with PBS(T) were mixed and added to each well. After incubation at 37 °C for 1h, the wells were then washed thrice with PBS(T). Subsequently, a PBS(T) solution (0.1 ml) of horseradish peroxidase-conjugated goat anti-mouse immunoglobulin G (Zymed Laboratories, Inc., San Francisco, CA, U.S.A.) was added to each well and incubated at 37 °C for 1 h. After washing thrice with PBS(T), 0.1 % *o*-phenylenediamine in 100 mM citrate buffer (pH 4.5) containing 0.015 % hydrogen peroxide (0.1 ml) was added. The optical density at 450 nm was measured in a spectrophotometer.

Chapter 3. Identification of photoaffinity labeling of the specific site on the extracellular domain of guanylyl cyclase C involved in ligand binding

3.1 Introduction

GC-C is a single-subunit protein molecule (1050 residues) with a unique structure consisting of an extracellular domain (ECD, ~ 407 resisues), responsible for ligand binding and an intracellular domain (~ 619 resisues), for guanylyl cyclase catalysis, which are connected through a single transmembrane polypeptide (~ 24 resisues). Signaling of a specific ligand (STa, guanylin and uroguanylin) is initiated by its binding to ECD on the outside of cell membranes and the signal is then transferred to the intracellular domain in the cytoplasm through the transmembrane polypeptide located in cell membranes. In one scenario for this process, the binding of a ligand to ECD induces a conformational change in the intracellular domain, thus, leading to activation of the cyclase catalytic region in the intracellular domain. However, the precise mechanism of the conformational change and activation of the intracellular domain in this signaling is not yet clear.

In our earlier work (Wada *et al.* 1996a), the site-directed mutational analysis of the ECD of porcine GC-C suggested that two regions, which are sensitive to point mutations, exist in ECD ; one is a highly conserved region from residue-91 to residue-155 (numbers denote the positions of amino acid residues relative to the N-terminus of porcine GC-C) in the amino acid sequences of GC-C's determined thus far and the other in the sequence from residue-274 to residue-407, located near the transmembrane portion. In particular, a mutation in the sequence from a residue at position 347 to that position 401, which is close to the transmembrane portion, caused a significant reduction in both the binding activity to a ligand and guanylyl cyclase catalytic activity. These results strongly suggest that the region on ECD for interacting with STa is focused on or located in these residues, the mutation of which strongly affects the biological properties of GC-C.

To develop a better understanding of the mechanism by which a signal is transmitted from a ligand, bound to the extracellular domain of GC-C, to the intracellular domain through the transmembrane portion, we attempted to identify the specific region in the ECD which involved in ligand-binding by designing a photoaffinity-labeling analog of STa (biotinyl($NH(CH_2)_4CO)_2$[Gly^4,Pap^{11}]STp(4-17)) with Pap residue (*p*-azido-L-phenylalanine) at position 11 and a biotin moiety at the N-terminus. In chapter 2, we demonstrated that [Pap^{11}]STp(4-17) can be linked to ECD in a highly efficiency manner. Thus, it was expected, when this ligand undergoes UV-induced binding to ECD, that a ligand-labeled peptide fragment could be salvaged from the enzymatic digest of the photoaffinity-labeld ECD by using avidin-immobilized matrix. MALDI TOF mass spectrometry was used to map the binding region on ECD for biotinyl($NH(CH_2)_4CO)_2$[Gly^4,Pap^{11}]STp(4-17). The region is specifically limited to the amino acid sequence from residue-387 to residue-393 which is located near the transmembrane portion. This finding was confirmed by site-directed mutagenesis, in that substitution by an Ala residue for Thr-389 or Phe-390 or Trp-392 in the sequence, respectively, greatly effects the binding ability to the ligand, as well as cyclase activity of GC-C. These results will provide novel insight into elucidation of the recognition and activation mechanism of GC-C by a ligand.

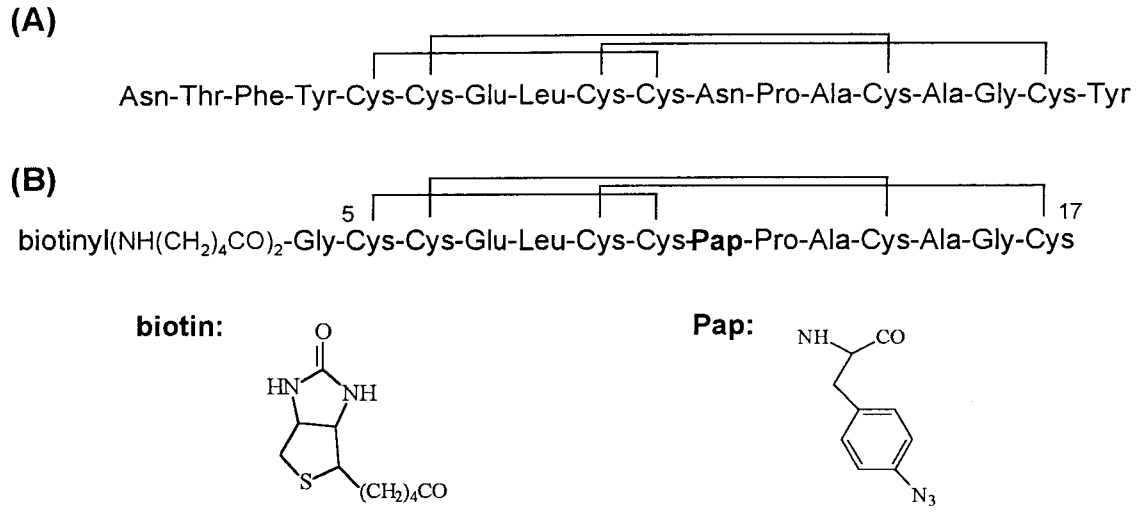

Fig. 3-1. Amino acid sequence of : (A) STp produced by a porcine strain of enterotoxigenic *E. coli* and (B) biotinyl(NH(CH2)4CO)2[Gly^4,Pap^{11}]STp(4-17). Solid lines indicate the position of disulfide linkages. The chemical structures of biotin which is connected with a dipentylamido linker and Pap (*p*-azido-L-phenylalanine) are depicted.

3.2 Results

3.2.1 Synthesis of biotinyl(NH(CH$_2$)$_4$CO)$_2$[Gly^4,Pap^{11}]STp(4-17)

A novel STa analog (biotinyl(NH(CH$_2$)$_4$CO)$_2$[Gly^4,Pap^{11}]STp(4-17), Fig. 3-1) was designed as a probe for mining a peptide fragment which encompasses the ligand-binding site on ECD of GC-C. The peptide ligand had two functional groups; one, a photo-sensitive amino acid (*p*-azido-L-phenylalanine, Pap) with azido group, which is easily converted to nitrene with UV light ($\lambda \cong 300$ nm) and which is covalently bound to electron-rich groups such as N-H, O-H, etc. on the receptor molecule (Bayley & Knowles, 1977; Eberle & Graan, 1985). This amino acid was introduced at position 11 of STp(4-17), as described in chapter 2.. The other, a biotinyl group noncovalently binds to avidin with an extremely high-affinity (K_D, $\sim 10^{-15}$ M) and is widely used for biochemical applications such as affinity chromatography, detection of antigen-antibody

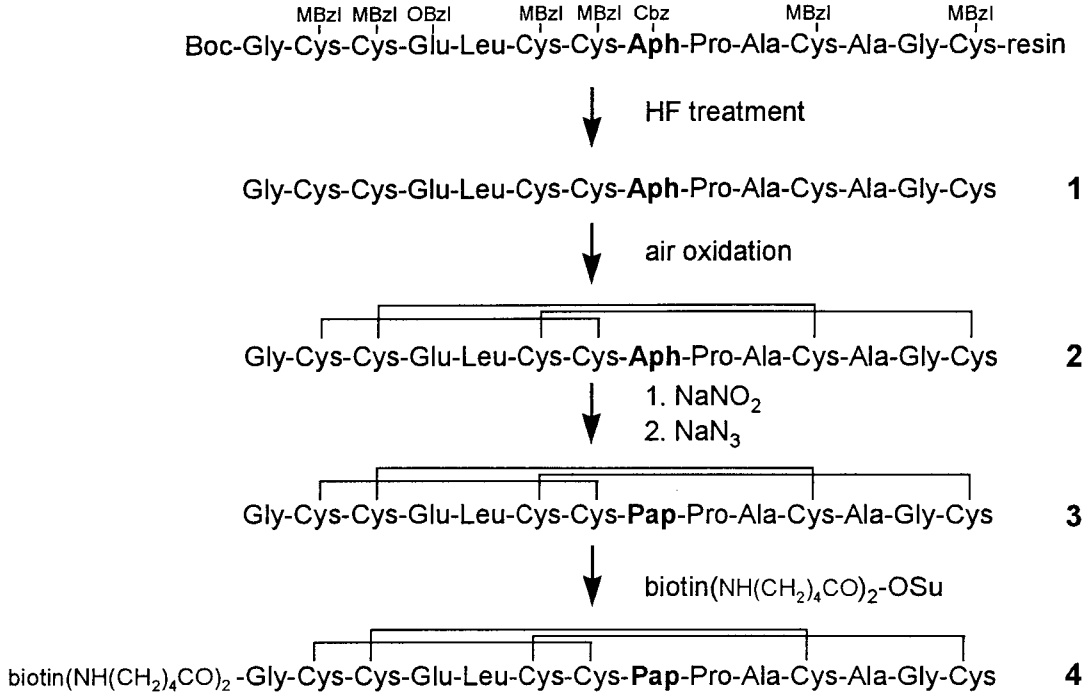

Fig. 3-2. Scheme for the synthesis of biotinyl(NH(CH2)4CO)2[Gly^4,Pap^{11}]STp(4-17).

reactions, etc. This group was attached at the N-terminus of [Pap^{11}]STp(5-17) through a dipentylamido linker and a Gly residue space (Fig. 3-1).

The strategy for the synthesis of biotinyl(NH(CH2)4CO)2[Gly^4,Pap^{11}]STp(4-17) is shown in Fig. 3-2. The synthetic intermediates and final product (**1** to **4** in Fig. 3-2) were purified by reversed-phase HPLC and the peak fractions (shown by arrows in Fig. 3-3 A~D) were confirmed to be target peptides by mass spectrometry, amino acid analysis, and the binding assay to ECD. After the elongation by a solid-phase synthesis and the cleavage from a resin, the linear peptide (**1**) was isolated by reversed-phase HPLC (Fig. 3-3A). The air-oxidation of the aimed peptide gave several peaks, which had the same molecular weight as the expected value (Fig. 3-3B). Only the peptide in the peak fraction indicated by the arrow in Fig. 3-3B completely inhibited the specific binding of ^{125}I-STp(4-17) to ECD6H at a concentration of 1×10^{-6} M, while other fractions showed no binding (data not shown). The CD spectra of the peptide (**2**), in the

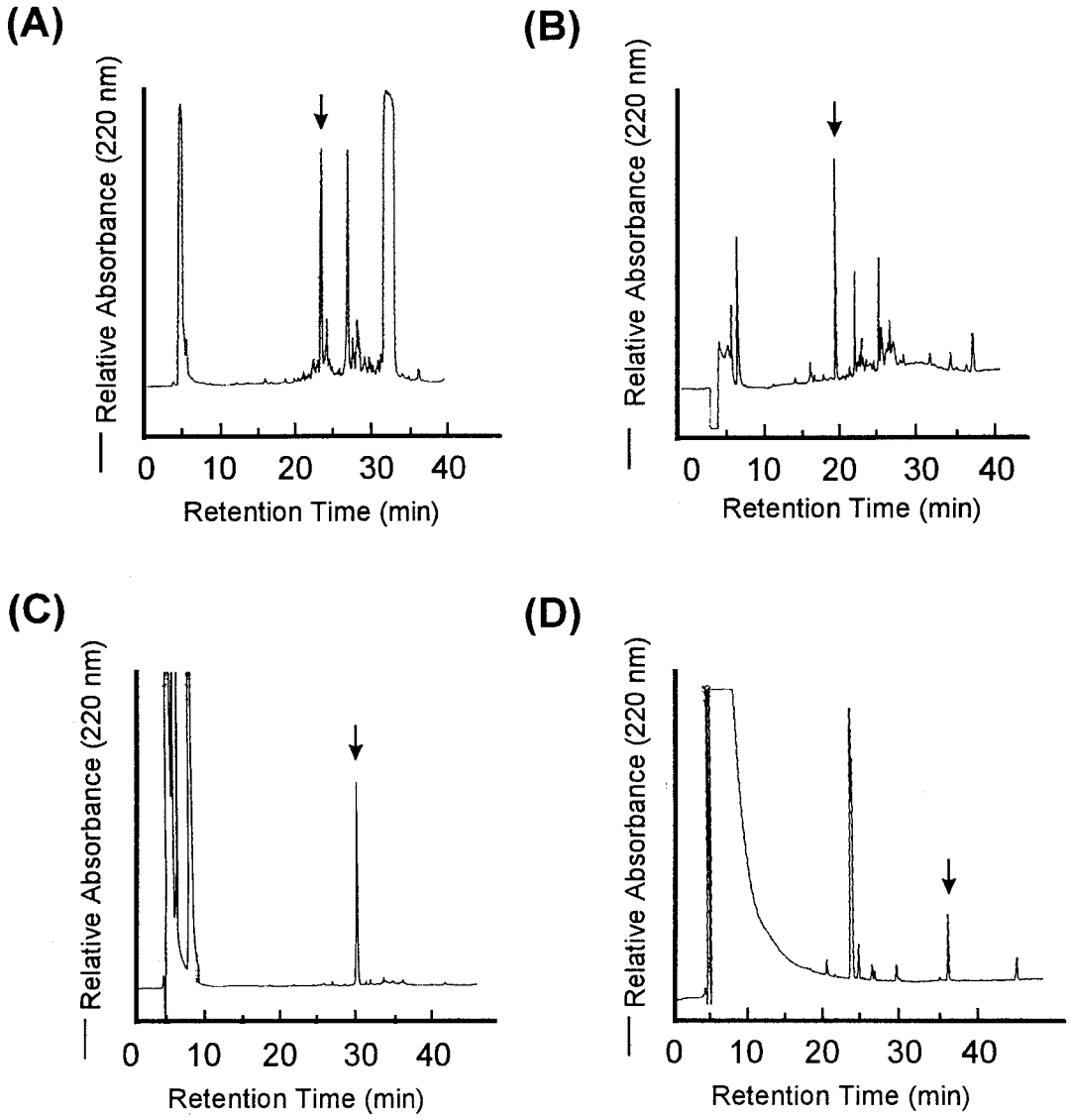

Fig. 3-3. HPLC profiles of the synthetic peptides : (A) Elongation of [Gly^{4},Aph^{11}]STp(4-17) with a linear sequence (1) on a resin by solid-phase synthesis and removal and deprotection of the peptide from the resin with treatment of anhydrous hydrogen fluoride, (B) Air oxidation in 1 % NH_4HCO_3 of 1 to [Gly^{4},Aph^{11}]STp(4-17) (2) with disulfide linkages, (C) Treatment of 2 with sodium nitrite and conversion to [Gly^{4},Pap^{11}]STp(4-17) (3), and (D) Introduction of biotinyl group at the N-terminus of 3 to give biotinyl-[Gly^{4},Pap^{11}]STp(4-17) (4). Reversed-phase HPLC was performed using a linear gradient of acetonitrile in 0.05 % TFA in Cosmosil $_5C_{18}$ column (8 × 250 mm). Arrows show peak fractions 1 to 4.

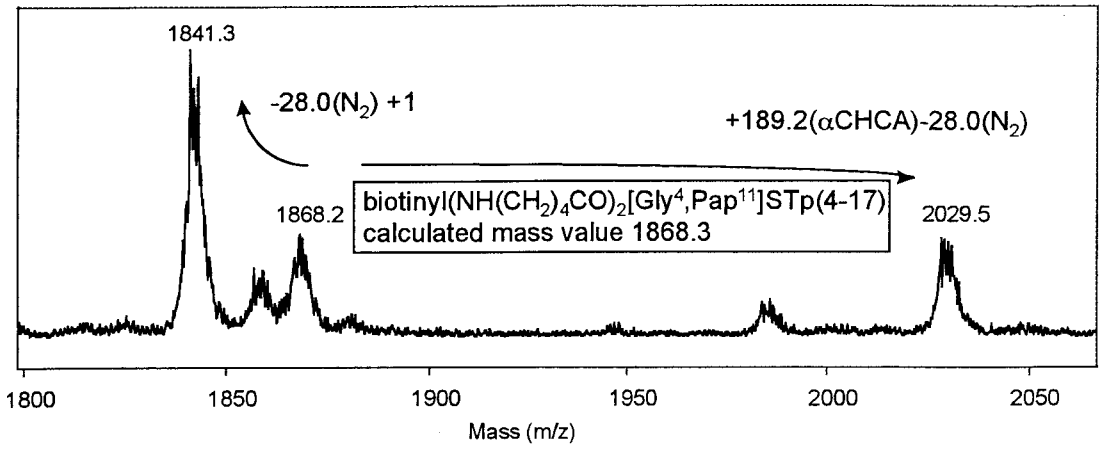

Fig. 3-4. MALDI-TOF mass spectrum of biotinyl(NH(CH$_2$)$_4$CO)$_2$[Gly^4,Pap^{11}]STp(4-17).

far-UV region (λ = 195 - 260 nm) were similar to those of STp(4-17) (data not shown). The conversion of an amino group to an azido group on Aph was done in the same procedures described in section 2.3.1 and yielded [Gly^4,Pap^{11}]STp(4-17) (**3**). The final product, biotinyl(NH(CH$_2$)$_4$CO)$_2$[Gly^4,Pap^{11}]STp(4-17) (**4**), was contained in the fraction with the arrow in Fig. 3-3D and exhibited the mass value and amino acid composition as expected values. The mass spectrum of biotinyl(NH(CH$_2$)$_4$CO)$_2$-[Gly^4,Pap^{11}]STp(4-17) revealed the expected mass signal at m/z = 1868.2 (the calculated mass value, 1868.25), as shown in Fig. 3-4. The signals observed at 1841.3 and 2029.5 likely arose from degradation products produced via the removal of two nitrogen atom (N_2) from a Pap moiety and the addition of one or two hydrogen atom(s) or a matrix, α-cyano-4-hydroxycinnamic acid (αCHCA) (the calculated mass values are 1840.3 and 2029.5, respectively). This observation is consistent with the fact that nitrogen laser radiation (λ = 337 nm) for ionization is capable of activating an azido group in the STa analog. Furthermore, biotinyl(NH(CH$_2$)$_4$CO)$_2$[Gly^4,Pap^{11}]STp(4-17) was confirmed to be efficiently adsorbed on avidin-immobilized agarose and entirely separated from it by heating at 100 °C for 10 min (data not shown).

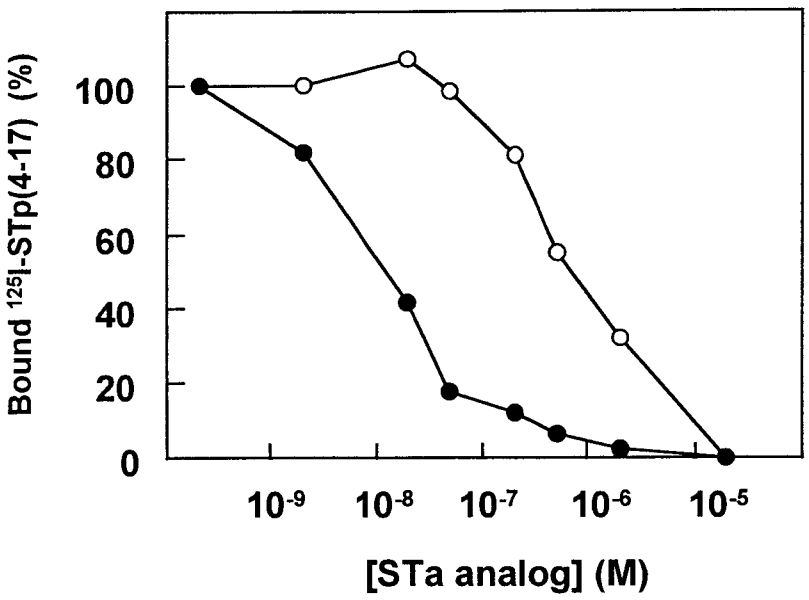

Fig. 3-5. Binding of biotinyl(NH(CH$_2$)$_4$CO)$_2$[Gly^4,Pap^{11}]STp(4-17) (open circles) and STp(4-17) (closed circles) to ECD6H. Curves show inhibition of the binding of ^{125}I-STp(4-17) to ECD6H by the STp analogs. Each point represents the mean values of triplicate data set.

3.2.2 Binding affinity of biotinyl(NH(CH$_2$)$_4$CO)$_2$[Gly^4,Pap^{11}]STp(4-17) to ECD6H

To confirm whether biotinyl(NH(CH$_2$)$_4$CO)$_2$[Gly^4,Pap^{11}]STp(4-17) can bind sufficiently to GC-C, we examined the binding activity of biotinyl(NH(CH$_2$)$_4$CO)$_2$-[Gly^4,Pap^{11}]STp(4-17) to ECD6H, using a competitive ligand-binding assay in the presence of a constant amount of ^{125}I-STp(4-17). Figure 3-5 shows the competitive binding curves in the binding equilibrium between ECD6H and biotinyl(NH(CH$_2$)$_4$CO)$_2$-[Gly^4,Pap^{11}]STp(4-17) or STp(4-17) with IC_{50} value of 8×10^{-7} M and 2×10^{-8} M, respectively, indicating that the binding potency of biotinyl(NH(CH$_2$)$_4$CO)$_2$-[Gly^4,Pap^{11}]STp(4-17) to ECD6H is 40-fold lower than that of STp(4-17). Previous experiments demonstrated that [Pap^{11}]STp(4-17), in which a Pap residue was introduced at position 11 in STp(4-17), retained the high efficiency of photoaffinity-labeling to GC-C, although it diminished the binding potency of STp(4-17) to GC-C to a level about 30-

fold lower than that of STp(4-17) (see section 2.2.4). Therefore, we concluded that biotinyl($NH(CH_2)_4CO)_2$[Gly^4,Pap^{11}]STp(4-17), as well as [Pap^{11}]STp(4-17) are good candidates for the efficient photoaffinity-labeling of ECD6H and that the optimum concentration of the analog for a photoaffinity-labeling experiment is 5×10^{-6} M based on the findings shown in Fig. 3-5.

3.2.3 Photoaffinity-labeling of ECD6H with biotinyl($NH(CH_2)_4CO)_2$-[Gly^4,Pap^{11}]STp(4-17) and isolation of a labeled peptide fragment

ECD6H was prepared from the protein expression system consisting of Sf21 insect cells and the baculovirus vector according to the procedure described in section 1.4.3. ECD6H was partially purified by Con A affinity chromatography and concentrated to more than 40 pmol/ml. Then, ECD6H was incubated with 5×10^{-6} M of biotinyl($NH(CH_2)_4CO)_2$[Gly^4,Pap^{11}]STp(4-17) at 37 °C for 1 h under the dark condition prior to the photo-crosslinking reaction and, then, allowed to react by UV radiation (λ = 304 nm) for 30 min on ice. UV radiation of the purified ECD6H with occupation by biotinyl($NH(CH_2)_4CO)_2$[Gly^4,Pap^{11}]STp(4-17) result in extensive non-reversible binding of the ligand ; Fifty % of the ECD6H was occupied with the ligand and the other 50 % was free and bound to ^{125}I-STp(4-17) after removal of the free ligand, in comparison with the ECD6H treated under the same conditions except for the absence of biotinyl($NH(CH_2)_4CO)_2$[Gly^4,Pap^{11}]STp(4-17) (data not shown). This suggested that half of the ECD6H was involved in crosslinking with the ligand and that it was no longer available for crosslinking with biotinyl($NH(CH_2)_4CO)_2$[Gly^4,Pap^{11}]STp(4-17).

After the further purification by Ni-chelating affinity chromatography, the photoaffinity-labeled ECD6H was treated with PNGase F for removal of carbohydrate moieties and, then, digested by *Achromobacter lyticus* lysyl-endopeptidase. The digest was passed through a column of the avidin-immobilized matrix and adsorbed peptides were separated from the avidin-immobilized matrix by heating. The eluate from the avidin-immobilized matrix was measured directly by MALDI TOF mass spectrometry. Figure 3-6 shows a typical mass spectrum of the eluates from the avidin-immobilized matrix, obtained in the presence or absence of biotinyl($NH(CH_2)_4CO)_2$-[Gly^4,Pap^{11}]STp(4-17). The mass values of two major signals (signals 1 and 2),

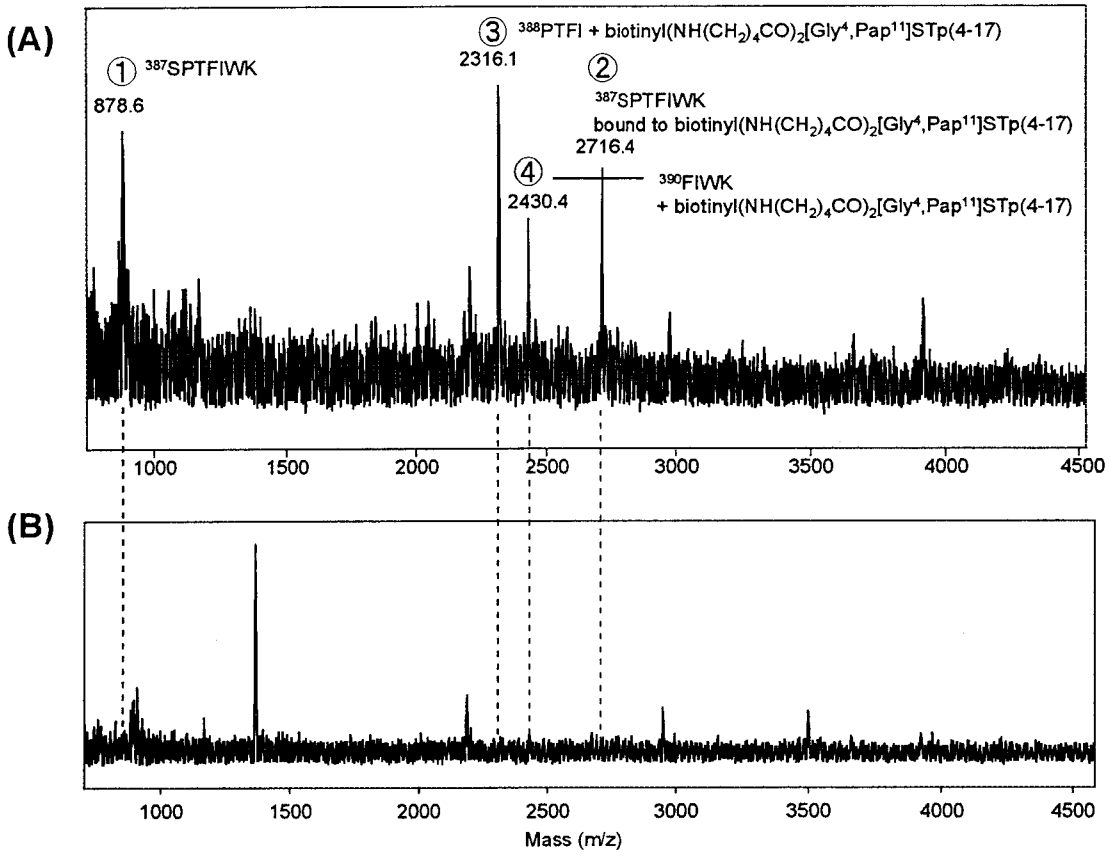

Fig. 3-6. MALDI-TOF mass spectra of : (A) the eluate from avidin-immobilized agarose applied to the digest of ECD6H labeled by biotinyl(NH(CH$_2$)$_4$CO)$_2$-[Gly^4,Pap^{11}]STp(4-17) and (B) the digest of ECD6H in the absence of biotinyl(NH(CH$_2$)$_4$CO)$_2$[Gly^4,Pap^{11}]STp(4-17).

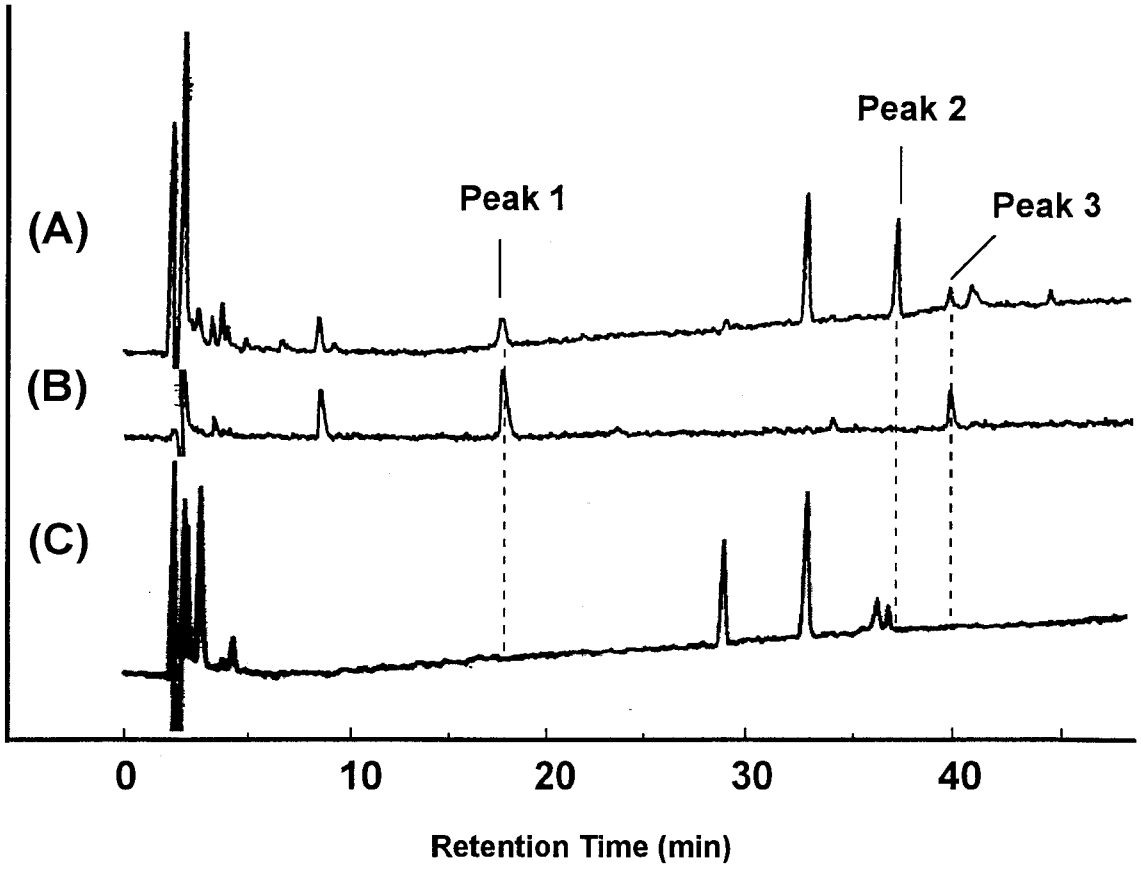

Fig. 3-7. Reversed-phase HPLC of the eluate from the avidin-immobilized agarose applied to (A and B) the digest of ECD6H labeled by biotinyl(NH$(CH_2)_4$CO)$_2$[Gly^4,Pap^{11}]STp(4-17) in Fig. 3-6A and (C) the digest of ECD6H in the absence of biotinyl(NH$(CH_2)_4$CO)$_2$[Gly^4,Pap^{11}]STp(4-17) in Fig. 3-6B. The peak fractions were detected by UV absorbance at 220 nm (A and C) or 280 nm (C). HPLC was performed using a linear gradient of acetonitrile in 0.05 % TFA in Develosil ODS-UG-5 column (5 × 150 mm, Nomura Chemical).

Table 3-1 Mass value of peptife fragments of ECD6H

Fragment [a]	Mass (linked to ST) [b]
(1-32) + (91-131)	9898.2
33-68	5760.8
69-90	4222.7
132-143	3240.4
144-153	3199.3
154-171	4043.7
(172-196) + (220-236)	6536.8
197-200	2331.9
201-219	4224.8
237-269	5567.7
270-289	3970.8
290-295	2512.0
296-314	4021.7
315-319	2487.0
320-327	2773.1
328-367	6316.7
368-369	2147.8
370-378	2946.3
379-386	2789.1
387-393	2716.1
394-396	2235.8
397-414	3880.6

[a]Disulfide linkages consist of Cys^{72}-Cys^{77}, Cys^{179}-Cys^{226}, and combinations of Cys^{7}, Cys^{94}, Cys^{101}, Cys^{128} (Matsumoto *et al.*, unpublished data).

[b]Expected mass value of peptide fragments which was hypothetically bound to biotinyl-$(NH(CH_2)_4CO)_2$[Gly^4,Pap^{11}]STp(4-17).

observed at m/z = 878.6 and 2716.4, were in complete agreement with the calculated mass values for the peptide fragment (residue-387 to residue-393) of ECD (calculated mass value for SPTFIWK, 878.47) and the same peptide fragment bound to biotinyl$(NH(CH_2)_4CO)_2$[Gly^4,Pap^{11}]STp(4-17) (calculated mass value for SPTFIWK + biotinyl$(NH(CH_2)_4CO)_2$[Gly^4,Pap^{11}]STp(4-17) - N_2, 2716.10), respectively. Moreover, the mass values of the other two signals (signals 3 and 4) observed at m/z = 2316.1 and 2430.4 were quite close to the values of PTFI (residue-388 to residue-391) and FIWK (residue-390 to residue-393) bound to biotinyl$(NH(CH_2)_4CO)_2$[Gly^4,Pap^{11}]STp(4-17) (calculated mass values, 2314.9 and 2431.0, respectively). These fragments could arise via the unexpected cleavage of the labeled peptide, detected as signal 2. Table 3-1 notes all the expected mass values of the possible cross-linked adducts between the peptide fragments of ECD6H and biotinyl$(NH(CH_2)_4CO)_2$[Gly^4,Pap^{11}]STp(4-17). The mass

values of the signals observed in Fig. 3-6 conform to a peptide with the sequence (residue-387 to residue-393) bound to biotinyl($NH(CH_2)_4CO)_2$[Gly^4,Pap^{11}]STp(4-17) but did not fit those of any other sequences, as seen in Table 3-1. These results are supported by the observation that the signals (1 to 4 in Fig. 3-6A) were not detected in the digest of ECD6H which was treated in the absence of biotinyl($NH(CH_2)_4CO)_2$-[Gly^4,Pap^{11}]STp(4-17) by the same procedures as described above (the control experiment), as shown in Fig. 3-6B.

The eluate from the avidin-immobilized matrix was subjected to reversed-phase HPLC analysis (Fig. 3-7A). Peak fractions 1 and 2 gave signals at m/z = 879.3 and 1841.1, which corresponded to those for the peptide (SPTFIWK, residue-387 to residue-393 ; calculated mass value, 878.5) and the degradation material of biotinyl($NH(CH_2)_4CO)_2$[Gly^4,Pap^{11}]STp(4-17) with two nitrogen atoms removed and one hydrogen atom added (calculated value, 1841.3), respectively. A minor peak fraction (peak 3), which was eluted at a longer retention time than peak fractions 1 and 2, gave a mass values of 879.5 corresponding to that of the peptide sequence (SPTFIWK, residue-387 to residue-393). This is consistent with being derived from the peptide fragment bound to biotinyl($NH(CH_2)_4CO)_2$[Gly^4,Pap^{11}]STp(4-17), since the covalent bond between the peptide fragment and the photoaffinity-labeling reagent would be expected to be very labile. The signals of the remaining biotinyl($NH(CH_2)_4CO)_2$[Gly^4,Pap^{11}]STp(4-17) and the peptide fragment bound to biotinyl($NH(CH_2)_4CO)_2$[Gly^4,Pap^{11}]STp(4-17) were not observed. The mass measurement of this peptide bound to biotinyl($NH(CH_2)_4CO)_2$[Gly^4,Pap^{11}]STp(4-17) might be difficult due to the small amount of material available. However, a weak signal was occasionally observed at a mass value 1841 in the mass measurement of the extracts from avidin-immobilized agarose (data not shown). Peak fractions 1 and 3 showed the UV absorption at 280 nm, as shown in Fig. 4-7B, indicating the presence of aromatic amino acids in the peptides in these fractions, which is consistent with the above observation that peak fractions 1 and 3 consist of a peptide with the sequence SPTFIWK. Furthermore, in the control experiment, these peak fractions could not be observed in the eluate of ECD6H, which was treated in the absence of the photoaffinity-labeling reagent but under same conditions as those in the presence of the reagent, as shown in

Fig. 3-7C.

3.2.4 Site-directed mutational analysis of the ligand-binding site

We next attempted to confirm if the ligand binding region is truly localized within the amino acid sequence (387 - 392) in ECD. For this purpose, six mutant protein were prepared (Fig. 3-8), in which each of the amino acid residues in the sequence (residue-387 to residue-393, shown in parenthesis in Fig. 3-9) were individually replaced by an Ala residue, by employing recombinant GC-C expression system using 293T human embryonic kidney cells. The effect of amino acid substitutions on the binding affinity of GC-C to a ligand were then examined in the context of ligand-binding ability and cyclase catalytic activity. The expression of the mutant proteins was confirmed by western-blotting and staining with an anti-GC-C antibody raised against a synthetic peptide covering the C-terminal region (amino acid residues 1036 to 1050) of porcine GC-C (Vaandrager *et al.*, 1993), as shown in Fig. 3-8A. The recombinant GC-C gave two protein bands on SDS-PAGE (lane 1 in Fig. 3-8A), in which the heterogeneity of molecular weight of GC-C was likely caused by differences in the extent of N-linked glycosylation, as has been reported in a previous paper (Vaandrager *et al.*, 1993). The mutant proteins two protein bands on SDS-PAGE, which were stained by an antibody-detection reagent, similarly to the wild type of GC-C (lanes 3~8), suggesting all the mutant proteins were expressed in the same quantity as that of the wild-type of GC-C.

The mutant proteins were photoaffinity-labeled with ^{125}I-ANB-STp(4-17), as shown in Fig. 3-8B. Among the six mutant proteins, one mutant protein (S387A) showed a binding potency identical to that of the wild-type GC-C. On the contrary, two mutant proteins (P388A and I391A) showed a reduced binding ability to ^{125}I-ANB-STp(4-17), and the remaining three mutant proteins (T387A, F390A, and W392A) were nearly completely devoid of binding ability to ^{125}I-ANB-STp(4-17). These results indicate that the substitution by an Ala residue of the amino acid residues at T387, F390, and W392 caused a complete deficiency in binding ability to a ligand.

The response of the guanylyl cyclase activation of the mutant proteins for exposure to STp(4-17) was examined by assaying the cGMP in the 293T cells which express these mutant proteins and were compared with that for the wild-type GC-C, as shown in Fig.

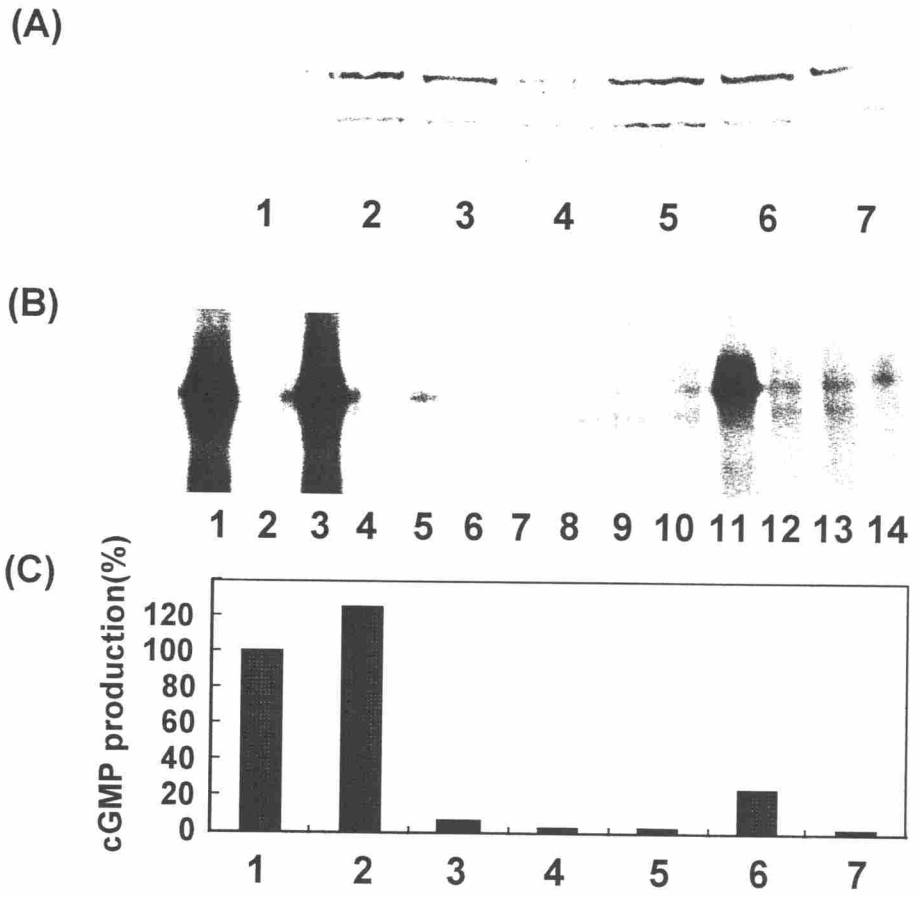

Fig. 3-8. Analysis of site-directed mutant proteins in the region (387 - 392) of GC-C expressed in 293T cells : (A) SDS-PAGE and western blot analysis of the mutant proteins of GC-C contained in the 293T cell membrane fraction. Proteins were visualized by an anti-GC-C antibody raised against a synthetic peptide with the sequence of the C-terminal region of GC-C. Lanes 1, wild-type ; lane 2, S387A ; lane 3, P388A ; lane 4, T389A ; lane 5, F390A ; lane 6, I391A ; lane 7, W392A. (B) SDS-PAGE of the same mutant proteins in (A) photoaffinity-radiolabeled with ^{125}I-ANB-STp(4-17). Lanes 1 and 2, wild-type ; lanes 3 and 4, S387A ; lanes 5 and 6, P388A ; lanes 7 and 8, T389A ; lanes 9 and 10, F390A ; lanes 11 and 12, I391A ; lanes 13 and 14 ; W392A. Odd and even lanes show the mutant proteins photoaffinity-labeled without and with 10^{-5} M STp(4-17), respectively. (C) cGMP production of the 293T cells expressing the mutant proteins of GC-C in the presence of 10^{-5} M STp(4-17). Each lane corresponds to the same number of lane in (A).

3-8C. The cGMP production of the wild-type GC-C after incubation for 20 min in the presence of 1×10^{-5} M of STp(4-17) was 400 pmol cGMP / 5×10^{-5} cells and in the absence of STp(4-17) was less than 10 pmol cGMP / 5×10^{-5} cells. cGMP formation for each of the mutant proteins was correlated to the binding ability to STa, even though all the mutant proteins, when stimulated by STa, exhibited cGMP formation to some degree. The mutant protein (S387A) gave rise to cGMP at a level similar to that of the wild-type GC-C. On the contrary, the mutant proteins (P388A and I391A) showed 6.0 and 24 % cGMP formation and the other three mutant proteins (T389A, F390A, and W392A) showed only 0.5-1 % in comparison with the wild-type GC-C, respectively. This indicates that the mutant proteins (T389A, F390A, and W392A) have practically no ability to bind to STa (1×10^{-5} M). Collectively, these experiments indicate that the substitution by an Ala residue for amino acid residues Thr-389, Phe-390, and Trp392 in GC-C abolish their ability to bind to a ligand and, hence, the cyclase catalytic activity of GC-C.

3.3 Discussion

Biotinyl($NH(CH_2)_4CO)_2$[Gly^4,Pap^{11}]STp(4-17) was designed with two functional groups, one of which functions as a reagent for photoaffinity-labeling and the other for non-covalent, high affinity binding in order to examine the specific region on ECD which is involved in binding to STa and obtain further insight into the precise mechanism of the interaction between GC-C and its ligand. We previously demonstrated that Asn^{11}-Pro^{12}-Ala^{13} in STp (Fig. 3-1) constitutes the binding region to GC-C and Ala^{13} occupies a critical position in STp in the context of its binding to GC-C (Yamasaki *et al.*, 1990; Ozaki *et al.*, 1991; Okumura *et al.*, 1994). We then confirmed that [Pap^{11}]STp(4-17), substituted by a Pap residue in place of Asn^{11}, located near a key amino acid residue Ala^{13}, is an efficient probe for photoaffinity-crosslinking of STa to GC-C (see chapter 2). In addition, we showed that the extracellular domain (ECD) of GC-C, which is expressed from a system consisting of insect cells and recombinant baculovirus, retains a ligand-binding ability which is similar to that of GC-C could be prepared as a soluble,

homogeneous protein (see chapter 1). These previous experiments enabled us to design and use the STp analog with the photoaffinity-labeling group for examining the region on ECD which is involved in binding to STa.

To determine the region on ECD which is involved in binding to STa and to identify the peptide fragment covering the binding region, we used the following four steps strategy ; covalent binding of ECD to an STa analog with a photoaffinity-labeling functional group, digestion of the ECD which is covalently coupled with the STa analog, isolation of the photoaffinity-labeled fragment from the digest by affinity chromatography, and the identification of the labeled fragment by mass spectrometry. In addition, we attempted to examine the biochemical properties of the mutant proteins of GC-C, which were prepared by site-directed mutagenesis of the amino acid residues in the binding region. For this purpose, we first synthesized an STp analog (biotinyl($NH(CH_2)_4CO)_2$[Gly^4,Pap^{11}]STp(4-17)) directed to the specific target on ECD, as shown in Fig. 3-2. By replacement of Asn^{11} by a Pap residue, this STa analog proved to have high potential for the photoaffinity-labeling of ECD. And it not only covalently linked to the ECD but permitted the isolation of a peptide fragment from the digest of the photoaffinity-labeled ECD by affinity chromatography, taking advantage of the non-covalent binding between biotin and avidin, by the attachment of a biotin moiety at the N-terminus of the STa analog. In general, the binding of a photoaffinity-labeled ligand to its receptor protein seems to proceed with considerably low efficiency, as shown in another case (Pandey *et al.*, 1986). Therefore, an expedient technique should be developed to detect the photoaffinity-labeled receptor protein or its fragment from a photoaffinity-labeled reaction mixture. In the present case, the photoaffinity-labeled peptide fragment was successfully recovered by the attachment of a biotin moiety at the N-terminus of the ligand from the digest of the photoaffinity-labeled ECD6H but in a tiny amount. Mass spectrometry identified the peptide fragment, which encompassed the amino acid sequence from residue-387 to residue-393 (SPTFIWK) positioned near the transmembrane portion of GC-C, in the digest of the ECD6H photoaffinity-labeled with biotinyl($NH(CH_2)_4CO)_2$[Gly^4,Pap^{11}]STp(4-17). Moreover, the peptide fragments which are bound to the STa analog with the sequences from residue-388 to residue-391 (PTFI) and that from residue-390 to residue-393 (FIWK) were observed by mass spectrometry

Table 3-2 Comparison of amino acid sequence of the ligand-binding site of GC-C in various species

Species	(Identity[a])	Sequence
pig	(100 %)	SPTFIWK
bovine	(86 %)	SPTFIWK
human	(77 %)	SPTFTWK
guinea pig	(73 %)	HPTFTWK
rat	(70 %)	SPNFIWK
Africa clawed frog	(43 %)	SPNFIWK
Japanese medaka	(36 %)	SPTFIW-
rat GC-A	(20 %)	HKLY-WP

[a] Identity of amino acid sequence of the extracellular domain

(Fig. 3-6). These findings strongly suggest that the ligand binds to the amino acids, Phe or Ile, at positions 390 and 391 respectively which are common in the three peptide fragments observed on mass spectra. The result is supported by the site-directed mutational analysis, which show that mutations of the amino acid residues at positions Pro-388, Thr-389, Phe-390, and Trp-392 caused a complete loss of binding ability to the ligand.

It is intriguing that the amino acid sequences of the ligand-binding region which was found in porcine GC-C in this experiment are highly conserved in all species determined thus far (Schulz *et al.*, 1990; Singh *et al.*, 1991; de Sauvage *et al.*, 1991; Wada *et al.*, 1994; MacFarland, 1995; Kruhoeffer *et al.*, 1996; Goraczniak *et al.*, 1997; Mantoku & Suzuki, 1997) (Table 3-2), even though the amino acid sequences of the extracellular domains in an amphibian (*Xenopus laevis* : Africa clawed frog) and a fish (*Oryzias latipes* : Japanese medaka) show low homology for the complete proteins. In our earlier work (Wada *et al.*, 1996a), the site-directed mutational analysis of the extracellular domain of porcine GC-C revealed that the amino acid replacement (residues-347 to 348, 363 to 365, 373 to 375, and 399 to 401) in a region (residue-347 to residue-401), which is close to the transmembrane region and surrounds the peptide

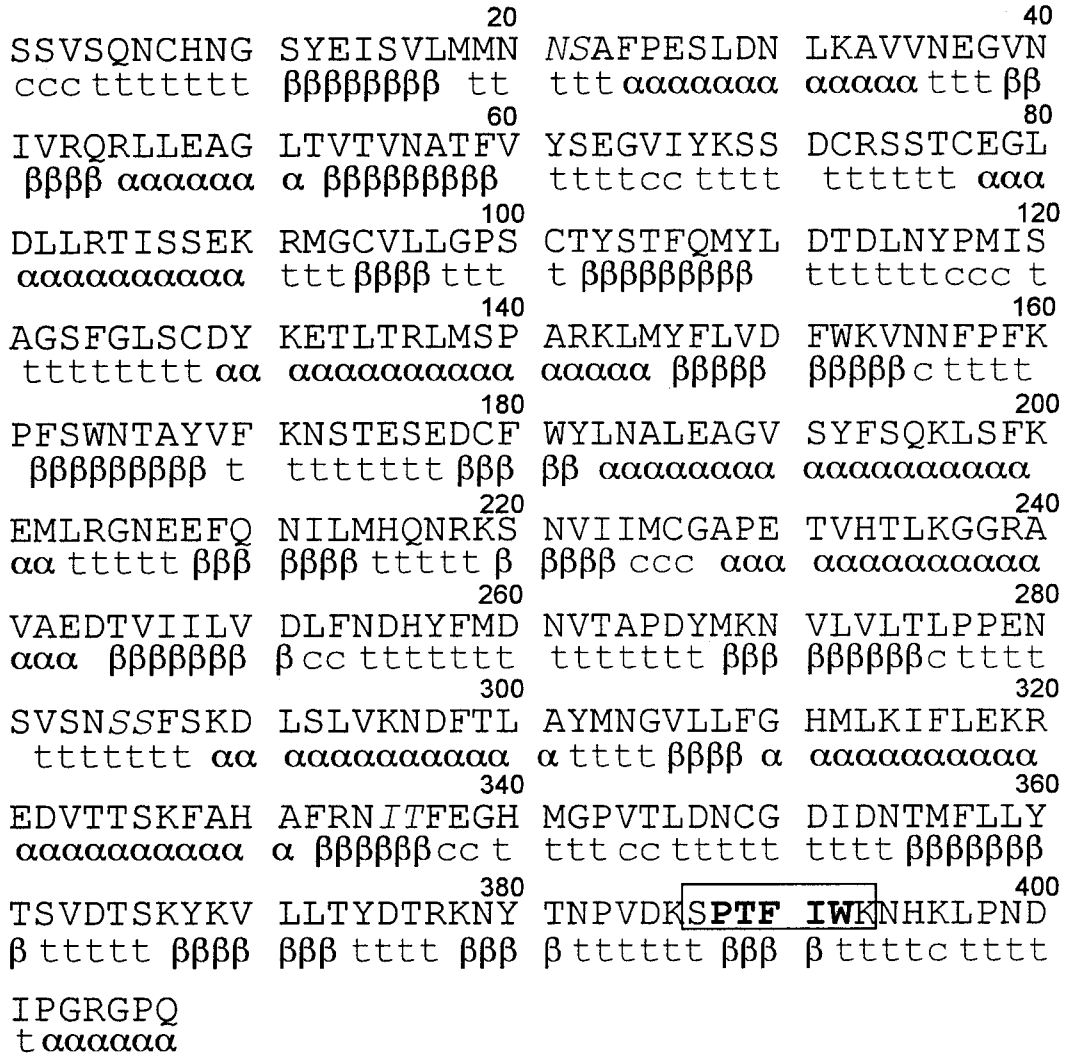

Fig. 3-9 Amino acid sequence and predicted secondary structure of the ECD of porcine GC-C. α, β, t, and c represent assignments of α-helix, β-strand, turn, and random coil. Boxed sequence is the fragment bound to biotinyl-$(NH(CH_2)_4CO)_2$[Gly^4,Pap^{11}]STp(4-17).

fragment found in this study, causes a strong reduction in both the binding ability to STa and guanylyl cyclase catalytic activity. These previous results are consistent with the observations described above.

The binding region in GC-A to atrial natriuretic peptide (ANP) was identified in positions from 181 to 188, which occupy a quite different region on primary structure from that of GC-C (McNicoll *et al.*, 1996). Another paper demonstrated that the Leuresidue at position 364 in GC-A, located near the transmembrane region, functions in binding to atrial natriuretic peptide (Duda *et al.*, 1991). These two regions are located apart from each other at different positions on the amino acid sequences but may be in close proximity to one another on the tertiary structure, and, thus, these two regions perhaps may simultaneously interact with atrial natriuretic peptide. In our previous paper, we demonstrated that the mutation of Arg-136 and Met-138 caused a complete loss in the binding of GC-C to STa (Wada *et al.*, 1996a). This region is located quite far from the binding region of ECD to biotinyl($NH(CH_2)_4CO)_2$[Gly^4,Pap^{11}]STp(4-17) found in this study. These observations again suggest that these two regions may well be in close proximity on the tertiary structure on ECD, as assumed in the case of GC-A.

Prediction of the secondary structure of ECD, as examined according to the method of Chou & Fasman (1974) suggests that ECD is composed from two subdomains ; an α/β region (residue-1 to residue-331) and a β-rich region (residue-332 to residue-401), as described in Fig. 3-9. The α/β region consists of alternative α-helixes and β-strands and contains all four intramolecular disulfide bridges, suggesting that this subdomain, which consists of 80 % of the amino acid residues of the extracellular domain, functions in constructing the basic architecture of the entire structure. On the contrary, the β-rich region has a low propensity for α-helix in contrast to high propensities for β-strand and turn and is comprised of hydrophilic amino acid residues including a sole Cys residue which is not involved in a disulfide linkage (Matsumoto *et al.*, unpublished data), implying that this subdomain is flexible. The X-ray crystallography of the complex of human growth hormone and its receptor protein suggest that the ligand-binding region on the receptor protein is constituted mainly by turn structures (de Vos *et al*, 1992). The same may be said of GC-C, since the Ser-387 to Pro-388 present in the ligand-binding region is likely to form a turn structure and, in

particular, Pro-388 could be an element of turn structure. Indeed, Pro-388 was identified to be a significant amino acid residue, as evidenced by the site-directed mutational analysis of GC-C (Fig. 3-8). Further, the result is in agreement with the conclusions that the region around this site points to a high content of hydrophilic amino acid residues, as can seen in Fig. 3-9, suggesting that this region is located on the surface of the molecular. The side chains of Pro-388, Thr-389, Phe-390, and Trp-392 may constitute a hydrophobic pocket on the molecular surface and the driving force to bind to a ligand, since the previous studies have suggested the possibility that the interaction between ECD and STa is compensated by hydrophobicity in their interaction sites (Yamasaki *et al.*, 1990; Ozaki *et al.*, 1991; Okumura *et al.*, 1994).

To identify the functional site of GC-C for interacting with STa, we undertook a series of experiments : (i) establishment of a mean for supplying a sufficient amount of ECD, (ii) preparation of a photoaffinity-labeling ligand appropriate for binding to ECD, and (iii) developing a method for mining a peptide fragment(s) from ECD linked to the photoaffinity-labeling ligand. In this paper, the photoaffinity-labeling STa analog, biotinyl($NH(CH_2)_4CO)_2$[Gly^4,Pap^{11}]STp(4-17), which carries the photo-reactive group, *p*-azido-L-phenylalanine, and biotin moiety, was successfully used for identifying the specific region of ECD which is involved in binding to STa. The result clearly indicates that an STa analog is linked to the region (residue-387 to residue-393) located nearly at the transmembrane portion of GC-C.

The results presented here can be generalized to other GC's such as the receptors of atrial natriuretic peptides, because the intracellular domain of GC-C is highly homologous to other GC's in terms of primary structure, although the extracellular domain of GC-C has a quite different amino acid sequence from that of other GC's (Schulz *et al.*, 1990) and therefore the extracellular domain of GC-C activates the intracellular domain in the same manner as in other GC's, when generating cGMP, a common cytoplasmic second messenger. It would then be interesting to see whether a principle of the transmission of a ligand signal from an extracellular domain into an intracellular domain in GC's, perhaps analogous to other GC-C, emerge based on not only the present study but others as well. In any event, the determination of the binding site of GC-C for interacting with its ligand will provide new insights into the elucidation

of the recognition and activation mechanism of GC-C by a ligand. The issue of how the extracellular domain transmits a signal to the intracellular cyclase catalytic domain, on binding with a ligand represents the next important subject.

3.4 Materials and Methods

3.4.1 Materials

The reagents used for peptide synthesis were purchased from Peptide Institute Inc. (Minoh, Japan) and Nacalai tesque, Inc. (Kyoto). T4 DNA ligase and restriction enzymes were from Takarashuzo Co. (Kyoto) and New England Biolabs, Inc. (Bervely, MA), respectively. Other reagents and solvents were purchased from Sigma Chemical Co. (St. Louis, MO) and Katayama Chem. Inc. (Osaka) and all were reagent grade. $Na^{125}I$ (carrier free) was purchased from DuPont NEN (MA) and used for the iodination of STp(4-17) (see section 2.3.5). Culture of Sf21 insect cells and 293T human embryonic kidney cells was described in section 1.4.3 and previous papers (Wada *et al.*, 1994; 1996a; 1996b). The expression and purification of ECD6H from Sf21 insect cells were described in section 1.4.5. A polyclonal anti-GC-C antibody was raised against the synthetic peptide corresponding to C-terminal region (amino acid residues 1036 to 1050) of porcine GC-C.

3.4.2 Synthesis of biotinyl($NH(CH_2)_4CO)_2$[Gly^4,Pap^{11}]STp(4-17)

Peptides were synthesized using standard solid-phase procedures using Boc chemistry. STp(4-17) and N-5-azido-2-nitrobenzoyl(ANB)-STp(4-17) were synthesized as described previously (Kubota *et al.* 1989). Details of the procedures for synthesis of intermediates, protection of the functional side chains of amino acid residues, removal of peptides from the resin, conversion from linear forms of peptides to their oxidized form, conversion of Aph to Pap, and purification on reversed-phase HPLC have been described in section 2.3.1. In the final step of synthesis, the biotin group was attached to the N-terminus of [Gly^4,Pap^{11}]STp(4-17) by the following procedure : [Gly^4,Pap^{11}]STp(4-17) (100 nmol) was mixed with Biotin-$(AC_5)_2$-OSu (Dojin Chem.

Lab. Inc., Kumamoto) and trimethylamine (50 eq. each of the amount of the peptide) in DMF (200 μl). After standing for 2 h at room temperature, the reaction product (biotinyl($NH(CH_2)_4CO)_2$[Gly^4,Pap^{11}]STp(4-17)) was isolated by reversed-phase HPLC. The binding activity of biotinyl($NH(CH_2)_4CO)_2$[Gly^4,Pap^{11}]STp(5-17) to GC-C was determined by a competitive inhibition assay to the binding of ^{125}I-STp(4-17), as described in section 1.4.8.

3.4.3 Photoaffinity-labeling of ECD6H with biotinyl($NH(CH_2)_4CO)_2$-[Gly^4,Pap^{11}]STp(4-17)

The expression and purification of ECD6H (ECD with a hexa-histidine sequence attached to the C-terminus) from Sf21 insect cells were carried out according to methods described in section 1.4.3. That is, the recombinant baculovirus carrying the cDNA of ECD6H was infected into Sf21 insect cells (5×10^7 cells, 80 % confluent state) in a 175 cm^2 flask for 1 h. The infected cells were scrapped and further cultured in spinner flasks (5×10^5 cells/ml) for 2 days. The culture supernatant (1200 ml) was treated batchwise with 10 ml bed volumes of Con A-immobilized agarose. The Con A agarose was filtered and washed with buffer A (50 mM Tris (pH7.5), 100 mM NaCl, 1mM $CaCl_2$, 1mM $MgCl_2$) (50 ml). The adsorbed protein was eluted with buffer A (50 ml) containing 500 mM α-methyl-D-mannoside. The non-adsorbed fraction was treated repeatedly by the same procedure and the eluted fractions were pooled. The eluate was concentrated to 20 ml using an Ultrafiltration Cell (Amicon Inc., MA). The solution contained about 800 pmol of the purified ECD6H. The purified ECD6H was mixed biotinyl($NH(CH_2)_4CO)_2$[Gly^4,Pap^{11}]STp(5-17) (100 nmol) and kept at 37 °C in the dark for 1 h. The solution was then exposed to UV irradiation (302 nm, Model UVM-57, UVP Inc., CA) for 30 min on ice. After the photoaffinity-labeling, the labeled protein was purified by using Ni-chelating affinity chromatography and separated from excess ligand and extraneous materials, according to the procedure described in section 1.4.5. Tris(hydroxymethyl)aminomethane was added into the reaction mixture as a scavenger to inhibit non-specific cross-linking reaction as well as for buffering the pH of the reaction solution (Bayley & Knowles, 1977). These purification procedures yielded about 260 pmol of the purified ECD6H, based on the starting, crude ECD6H (2 nmol),

as judged from the ligand-binding capacity of the purified ECD6H without photoaffinity-labeling (control experiments).

3.4.4 Digestion of photoaffinity-labeled ECD6H

The solution which contained the photoaffinity-labeled ECD6H, described above, was concentrated to 0.1 ml on a Centricon-10 (Amicon) and directly diluted with 1 ml of buffer (100 mM Tris (pH 9.0) and 8M urea) and incubated at 4 °C for 2 h. The solution was then diluted with 100 mM Tris (pH 9.0) (5 ml) containing 0.01 % SDS and concentrated to 0.5 ml on a Centricon-10. PNGase F (0.4 U) was added to the solution for removal of carbohydrate chains at the N-linked glycosylation sites and allowed to stand at 37 °C for 2 h. The resulting solution was then incubated with *Achromobacter lyticus* lysyl-endopeptidase (3 μg) at 37 °C for 16 h.

3.4.5 Isolation of photoaffinity-labeled peptides

The above digested ECD6H solution was mixed with avidin-immobilized agarose (50 μl bed volume) and incubated for 30 min at room temperature. The avidin-immobilized agarose was collected on an Ultrafree-MC 0.1 mm filter unit (Millipore Inc.). The agarose was washed twice with 100 mM Tris (pH 9.0) (300 ml) containing 100 mM NaCl and, then, with sufficient 0.05 % TFA to remove salts. The peptides bound on the agarose were separated by heating in a mixture of 0.05 % TFA and 50 % acetonitrile for 15 min at 100 °C. The supernatant, containing the peptides, was concentrated in vacuo and identified by mass measurements with Voyager Elite-XL MALDI TOF mass spectrometer (Perspective Inc.) using α-Cyano-4-hydroxycinnamic acid as a matrix.

3.4.6 Site-directed mutagenesis of porcine GC-C

The preparation of the constructs of the recombinant GC-C and its mutant proteins was carried out according to the procedures, reported previously (Wada *et al.*, 1996a), with minor modifications. These recombinant proteins were transiently expressed on 293T human embryonic kidney cells, which were grown in DMEM medium (Sigma) supplemented with 10% fetal bovine serum, using the Superfect transfection reagent

according to the manufacturer's specifications (QIAGEN). Briefly, the 1.0 kb cDNA fragment between *Kpn*I sites and *Hind*III was isolated from pCG-STaR. The cDNA fragment was subcloned into pBluescript SK(-) and used as a template for the PCR reaction as follows : The first PCR fragment was prepared by using a universal primer (M13-20) and sense primers for the mutation (summarized in Table 3-3), and the second PCR fragment was prepared by another universal primer (M13 reverse) and the anti-sense primers. The third PCR fragment was constructed with the universal primers (M13-20 and M13 reverse) using the first and second PCR fragments as templates. The third PCR fragment was digested with *Kpn*I and *Hind*III to subclone to *Xba*I/*Hind*III sites of pBluescript SK(-) together with the cDNA fragment between the *Xba*I site and *Kpn*I sites. These fragments were individually inserted into the pCG vector. The vectors were ligated with a 1.7 kb cDNA fragment which encodes for the C-terminal portion of GC-C with *Hind*III sites at both ends. The DNA sequences of the vectors constructed in this study were confirmed by an Applied Biosystems 373A DNA Sequencing System using an ABI PRISM Dye terminator cycle sequencing kit (PERKIN ELMER).

Table 3-3 Primers used for the mutation of GC-C

Mutant protein	Oligonucleotide
S387A	CCGGTGGATAAGG**CC**CCCCACATTCATC
P388A	GTGGATAAGAGC*G*CCACATTCATCTGG
T389A	GATAAGAGCCCC*G*C*C*TTCATCTGGAAG
F390A	AAGAGCCCCACA**GC**CATCTGGAAGAAC
I391A	AGCCCCACATTC**GC**CTGGAAGAACCAC
W392A	CCCACATTCGCC**GC**GAAGAACCACAAA

Asterisks (*) idicate position of the mutated nucleotides.

3.4.7 Assay of cGMP production of GC-C mutant proteins

The cGMP production of the mutant proteins of GC-C, expressed on 293T cells, was assayed as described previously (Wada *et al.*, 1994). Namely, the 293T cell expressing the mutant proteins were mixed with STp(4-17) and incubated at 37 °C for 10 min. The reaction was terminated by the addition of 10 % trichloroacetic acid. The cells were then rapidly frozen at -80 °C and thawed at room temperature. The cell debris was removed by centrifugation at 15,000 rpm (18,500 × g) for 15 min. The resulting supernatant was extracted three times with water-saturated ether. The cGMP concentration was estimated by a radioimmunoassay kit according to the manufacture's specifications (YAMASA). The other assays have been described in sections 4.4.6 and 4.4.7.

Chapter 4. The relevance of N-glycosylation to the binding of ligands to guanylyl cyclase C

4.1 Introduction

Like other particulate guanylyl cyclases such as the natriuretic peptide receptors, GC-C contains a high content of N-linked carbohydrate chains on the extracellular domain (ECD). There exist seven or eight putative N-linked glycosylation sites (Asn-Xaa-Thr/Ser, Xaa is any amino acid residue expect for Pro) in the primary structure of ECD, as shown in Fig. 4-1. This is consistent with the observation that when it is expressed in mammalian cells, GC-C is observed as multiple protein bands in the molecular weight range of 140-160 kDa on SDS-PAGE, while the molecular weight of GC-C is calculated to be 121-kDa, based on the amino acid sequence (Schulz *et al.*, 1990; Vaandrager *et al.*, 1993). Carbohydrate moieties at N-linked glycosylation sites in several proteins are known to be involved as determinants in physicochemical and biochemical functions such as folding, stability, targeting, ligand binding as well as molecular recognition (reviewed in Marshall, 1972; Kobata, 1992; Lis & Sharon, 1993). The carbohydrate moieties on ECD of GC-C might well play a role in ligand recognition, subunit interaction, and the propagation of signaling to the intracellular domain. However, their precise role has not yet been elucidated in detail.

This chapter reports an examination of the effect of deletion of the N-linked glycosylation sites to the biochemical functions of GC-C. For this purpose, we generated mutant proteins of ECD and GC-C, which lacked a carbohydrate moiety at each of the N-glycosylation sites on ECD, by using a system consisting of Sf21 insect cells and recombinant baculovirus or 293T human embryonic cells and analyzed the biochemical properties of the mutant proteins which were obtained. We found that deletion of a carbohydrate moiety at each of the N-linked glycosylation sites had no effect on the level of expression or on the ligand-binding affinity (K_D) of GC-C but the deletion of a carbohydrate moiety at N379 (the mutant protein is referred to N379A, in which Asn residue is replaced by Ala residue) abolished both ligand-binding capacity

(B_{max}) and cyclase catalytic activity. The mutant protein (N379A) was also more susceptible to denaturation in aqueous urea. We conclude that the N-linked glycosylation at N379 of GC-C is required for both the stability of the protein itself, as well as the recognition of the protein by its ligand.

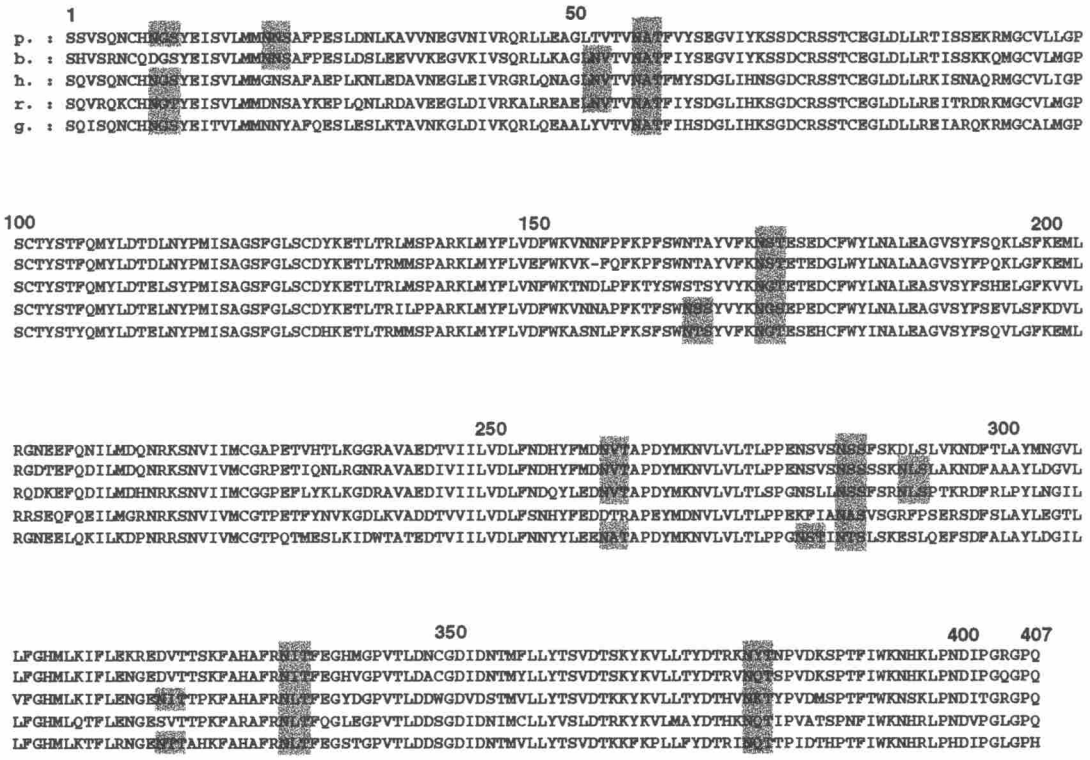

Fig. 4-1. Amino acid sequence around the putative N-linked glycosylation sites of GC-C's: pig (p.) (Wada *et al.*, 1994), bovine (b.) (Goraczniak *et al.*, 1997), human (h.) (Singh *et al.*, 1991; de Sauvage *et al.*, 1991), rat (r.) (Schulz *et al.*, 1990), and guinea pig (g.) (Kruhoeffer *et al.*, 1996). N-linked glycosylation sites are shown as shaded areas.

4.2 RESULTS

4.2.1 Deglycosylation of ECD

To examine the effect of deglycosylation on the biochemical properties of GC-C in detail, we first set up a system consisting of insect cells and recombinant baculovirus to express the ECD of porcine GC-C as a secretory protein into a culture medium, as described in chapter 1. As prepared, the protein had a molecular weight of 53-kDa but this value might include approximately 7-kDa of carbohydrate, since the molecular weight of ECD, as deduced from the amino acid sequence, is 46,101. The isolation and purification of ECD was easily carried out as a soluble protein from the culture medium by the attachment of the hexa-histidine tag (His_6) at the C-terminus (ECD6H). The purified ECD6H had the N-terminal sequence SSVSQ- (a single letter code is used to designate amino acid residues), which was completely identical to that deduced for the mature ECD, and showed a binding ability to STa which was similar to that of GC-C with the complete amino acid sequence (see section 1.2.2). Thus this extracellular domain of GC-C, which was expressed from a recombinant baculovirus and insect cell system, offers an approach to elucidate the biochemical characteristics of GC-C.

Treatment of the purified ECD6H with PNGase F in the absence of denaturant gave a major protein band at 45-kDa on SDS-PAGE with a minor unprocessed protein at 53-kDa (Fig. 4-2A). The molecular weight of the 45-kDa protein was close to that calculated from the amino acid sequence of ECD6H (46,981). Western blot analysis revealed that the 45-kDa protein can be detected by the His_6-tagged proteins detection kit (Ni-NTA alkaline-phosphatase conjugates, QIAGEN) but not Con A-conjugated HRP (Figs. 4-2B and 4-2C, respectively). Moreover, the purified ECD6H was efficiently photoaffinity-labeled by ^{125}I-BB-STp(4-17), while the 45-kDa protein was unlabeled (Fig. 4-2D). These results clearly show that the 45-kDa protein is completely deglycosylated form of ECD6H and, moreover, that ECD6H is deprived of its ability to bind to STa by treatment with PNGase F, indicating that N-linked glycosylation of ECD is required for the binding of ECD to STa.

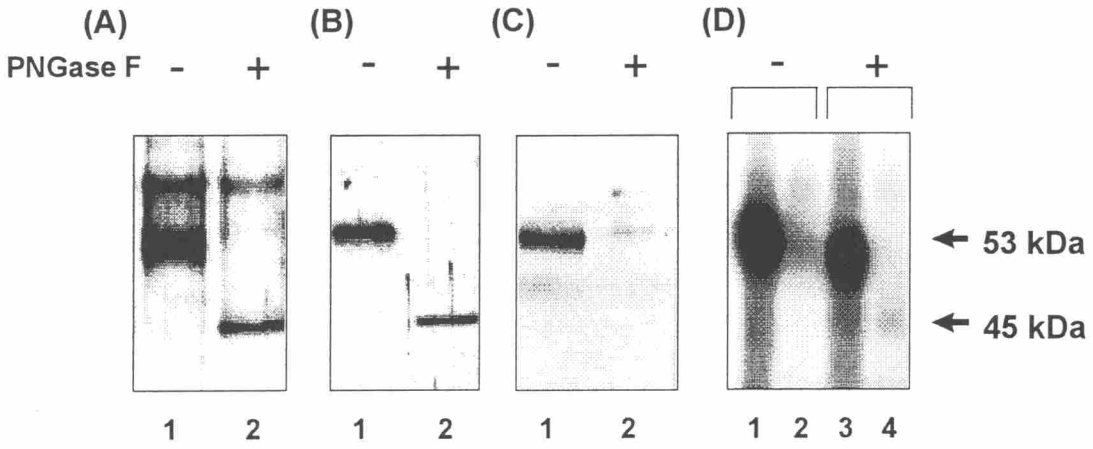

Fig. 4-2. SDS-PAGE and western blotting of ECD6H expressed from Sf21 cells, purified by Con A and Ni-chelating affinity chromatography, and visualized by (A) silver stain, (B) His_6-tagged protein detection kit, and (C) staining with Con A-conjugated HRP. PNGase F (-) and (+) show without or with the treatment of PNGase F. (D) ECD6H was treated without (lanes 1, 2) or with (lanes 3, 4) PNGase F and followed by photoaffinity-label with ^{125}I-BB-STp(4-17) in the absence (lanes 1, 3) and presence (lanes 2, 4) of 10^{-5} M STp(4-17).

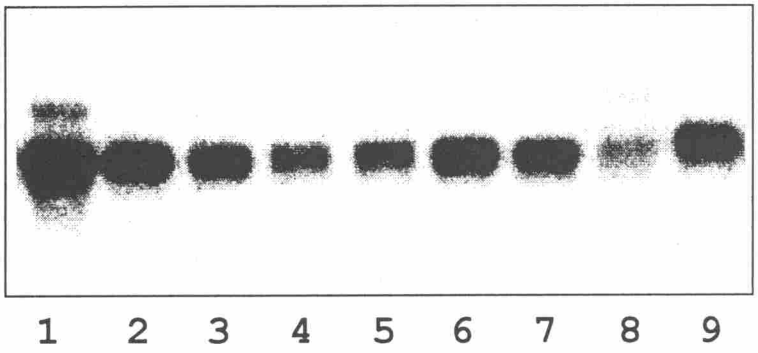

Fig. 4-3. SDS-PAGE of the mutant proteins of ECD purified by Con A affinity chromatography and labeled by ^{125}I-BB-STp(4-17) : lane 1, N9A; lane 2, N20A; lane 3, N56A; lane 4, N172A; lane 5, N261A; lane 6, N284A; lane 7, N334A; lane 8, N379A; lane 9, ECD.

4.2.2 Preparation of mutant proteins of ECD

Porcine GC-C contains eight potential N-linked glycosylation sites at N9, N20, N56, N172, N261, N284, N334, and N379 on the extracellular domain (numbers denote the positions of the amino acid residues relative to the N-terminus of porcine GC-C) (Fig. 4-1). To determine the influence of deglycosylation at each of the N-linked glycosylation sites on the biochemical properties of ECD, we created eight types of mutant proteins of ECD, which were devoid of a carbohydrate chain at each of these specific residues by amplifying the cDNA's in which the nucleotide sequence coding for the Asn residue was replaced by that for an Ala residue at one of these sites, using the procedures described in section 4.4.2. The mutant proteins were partially purified from the culture media by

affinity chromatography on a Con A-immobilized agarose column. The purified proteins were photoaffinity-labeled by ^{125}I-BB-STp(4-17), run on SDS-PAGE, and analyzed by autoradiography (Fig. 4-3). All the mutant proteins migrated slightly faster on SDS-PAGE than ECD, demonstrating that this was due to the loss of a carbohydrate chain at each modification site and, thus, that the Asn residues are glycosylated at all eight of the potential N-linked glycosylation sites. Those mutant proteins were specifically inhibited from binding to ^{125}I-BB-STp(4-17) in the presence of an excess of STp(4-17), indicating that the mutant proteins were photoaffinity-labeled by ^{125}I-BB-STp(4-17) at the same site which binds to STp(4-17) (data not shown). Among these mutant proteins, we found five mutant proteins (N9A, N20A, N56A, N284A, and N334A) were found which showed visible bands on SDS-PAGE at the same density as that of ECD in photoaffinity labeling with ^{125}I-BB-STp(4-17) and three mutant proteins (N172A, N261A, and N379A) were more weakly stained than ECD, as seen in Fig. 4-3. These results suggest that the mutation at positions N172, N261 and N379 resulted in a significantly decreased binding ability of the mutant proteins to STa or the reduction of the expression efficiency of the mutant proteins. If ECD suffered a great loss in its ability to bind to STa as the result of eliminating a carbohydrate chain, it may be inferred that some or all of carbohydrate chains at positions, N172, N261, and N379, are involved in the interaction between ECD and STa.

4.2.3 Binding characteristics of mutant proteins of ECD to STa

We estimated the binding affinities of the mutant proteins to STa in comparison with that of ECD by examining the abilities of the mutant proteins to bind to STa. Figure 4-4A, which shows some typical examples of the binding of ^{125}I-STp(4-17) to the mutant proteins as well as ECD, indicates that these bindings are concentration-dependent. A Scatchard analysis (Scatchard, 1949) of these data revealed that the mutant proteins possessed almost the same degree of the binding affinity to STa (K_D : dissociation constant in equilibrium ligand-binding) as that of ECD, and that this binding is similar to those for GC-C expressed in insect cells, 293T cells (Wada *et al.*, 1994), and intestinal cells (Katwa *et al.* 1991), as shown in Table 4-1. On the contrary, the mutant proteins showed a wide range in B_{max} values in binding to STa (Fig. 4-4B and

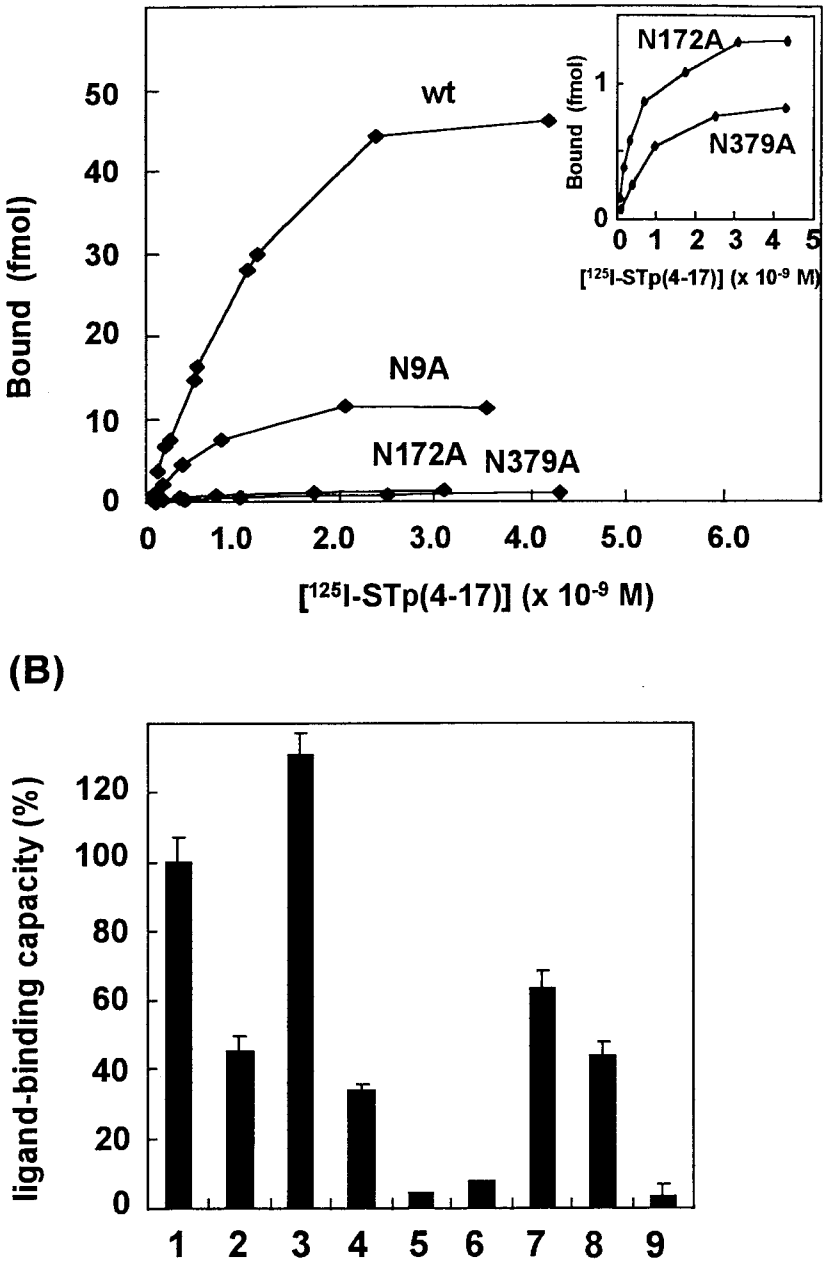

Fig. 4-4. (A) Equilibrium binding of the mutant ECD proteins to ^{125}I-STp(4-17) : The mutant proteins was incubated with ^{125}I-STp(4-17) at 37 °C for 1h, filtered and the radioactivity on the filter was then determined. The non-specific binding was determined at each point in the presence of 10^{-5} M STp(4-17). The values represent the mean of triplicate determinations. The data were analyzed by using the LIGAND program (Munson & Rodbard, 1980) to determine the K_D and the B_{max} according to the method of Scatchard. (B) Comparison of the binding capacities of the mutant proteins to ^{125}I-STp(4-17) to that of ECD. The B_{max} values from the analysis of equilibrium binding of ^{125}I-STp(4-17) to the mutant ECD proteins were compared.

Table 4-1 Ligand binding of mutant proteins of ECD

Mutant proteins	K_D (x 10^{-9} M)	B_{max} (x 10^{-10} M)
wild-type	0.72	5.8
N9A	0.86	2.6
N20A	1.2	7.8
N56A	0.85	2.0
N172A	0.56	0.25
N261A	0.47	0.45
N284A	1.2	3.7
N334A	1.0	2.6
N379A	1.1	0.19

K_D and B_{max} represent dissociation constant and maximum binding capacity of binding to STp(4-17), respectively

Table 4-1), which is consistent with the result of the photoaffinity-labeling experiment, as shown in Fig. 4-3. In a simple monovalent binding model, the B_{max} value reflects the total number of receptor molecules in the interaction between a receptor and its ligand (Lauffenburger & Linderman, 1993). We then compared the expression efficiencies of the mutant proteins to that of ECD using the His_6-tagged proteins, which were easily purified from their culture supernatants using Ni-chelating affinity chromatography. Judging from these protein bands on SDS-PAGE, which were visualized by staining with coomasie brilliant blue, the mutant proteins (N172A and N379A) were obtained in yields nearly equivalent to ECD6H as well as the mutant protein N9A as a control, the SDS-PAGE band of which exhibited a density which was the same level as that of ECD6H (Inset in Fig. 4-5). In addition, western blot analysis revealed that the mutant proteins (N172A and N379A) detected in the culture supernatants exhibited nearly the same densities as those of ECD6H or N9A, detected by the His_6-tagged protein detection kit (data not shown). Figure 4-5 shows that the binding quantities of ^{125}I-STp(4-17) to N172A and N379A were decreased to 12 % and 2 % , respectively, of that to ECD6H, while that to N9A was maintained at nearly the same level as that to ECD6H. These data indicate that the small B_{max} values of the mutant proteins (N172A and N379A) were

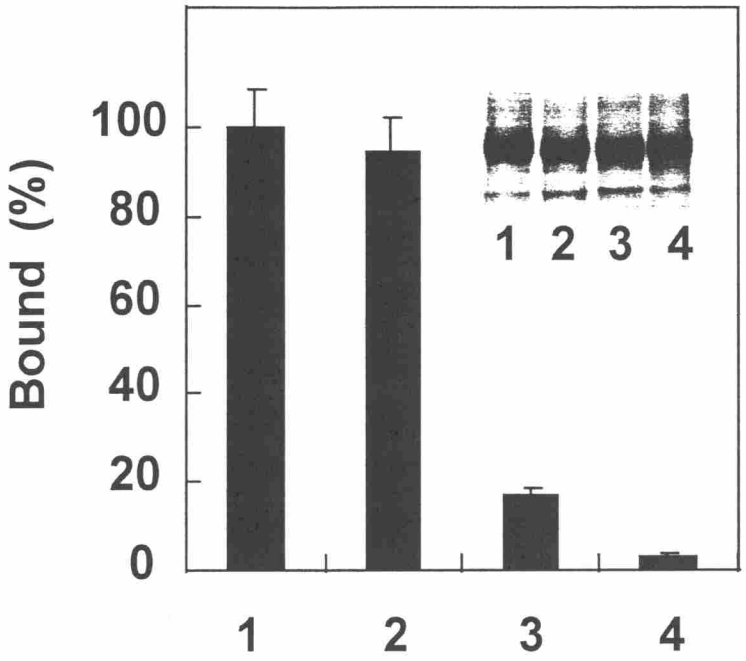

Fig. 4-5. Binding quantities of purified mutant proteins to STp(4-17). ^{125}I-STp(4-17) (1.8 nM) was incubated with ECD6H, N9A, N172A, and N379A, which were purified by Con A and Ni-chelating affinity chromatography, and the radioactivity of the peptide bound to each mutant proteins was measured. Each value represents the mean of triplicate determinations as a relative value. The purity and quantities of the mutant proteins were analyzed from the protein bands on SDS-PAGE visualized by coomasie brilliant blue staining (inset). Lane 1, ECD6H; lane 2, N9A; lane 3, N172A; lane 4, N379A.

due to the weaker binding ability but not to a lower expression efficiency of the mutant proteins than those of ECD or N9A. Thus, deglycosylation at N172 or N379 appears to result in the modification of the functional structure of ECD, resulting in a significant decrease in its ability to bind to the ligand.

4.2.4 Estimation of the stability of ECD6H and its mutant proteins to denaturant

To better understand why the mutant proteins (N172A and N379A) are deprived of binding ability to STa, we assayed the residual binding activity to STa of ECD6H and three mutant proteins (N9A, N172A, and N379A) after incubation for 30 min in aqueous urea ranging from 0 to 8 M, using the methods described in section 4.4.8. Figure 4-6A shows that the mid points of ECD6H, N9A, N172A, and N379A, which correspond to 50 % of the apparent binding of the original protein under non-urea conditions, are at 4.7, 4.4, 3.5, and 1.4 M urea, respectively. The mutant protein, N9A, had nearly the same stability as that of ECD6H, while the mutant proteins, N172A and, in particular, N379A, showed considerably less stability to denaturation in urea than ECD, suggesting that the carbohydrate chain at position N379 is critical for and play a role in protecting the functional structure of ECD to STa from a denaturant such as urea.

4.2.5 Characterization of mutant proteins of GC-C expressed in 293T cells

In order to confirm whether the modulation of the biochemical properties of ECD induced by mutation at the N-linked glycosylation sites truly resides in the intact protein, GC-C, we constructed three mutant genes coding for porcine GC-C (GC-C(N9A), GC-C(N172A), and GC-C(N379A)), in which the code for the Asn residue was individually replaced by that for an Ala residue at the same positions as those described above in the case of ECD. We also prepared other three mutant proteins, GC-C(S11A), GC-C(T174A), and GC-C(T381A), in which the code for a Ser or Thr residue, positioned at the N-linked glycosylation consensus sequence (Asn-Xaa-Thr/Ser) (Marshall, 1972), was replaced by an Ala residue, thereby preventing the Asn residues at positions N9, N172, and N379 from accepting a carbohydrate chain. As observed in the case of ECD, these mutant proteins run at a position corresponding to a slightly smaller molecular weight on SDS-PAGE than that of the original protein, due to the loss of a carbohydrate

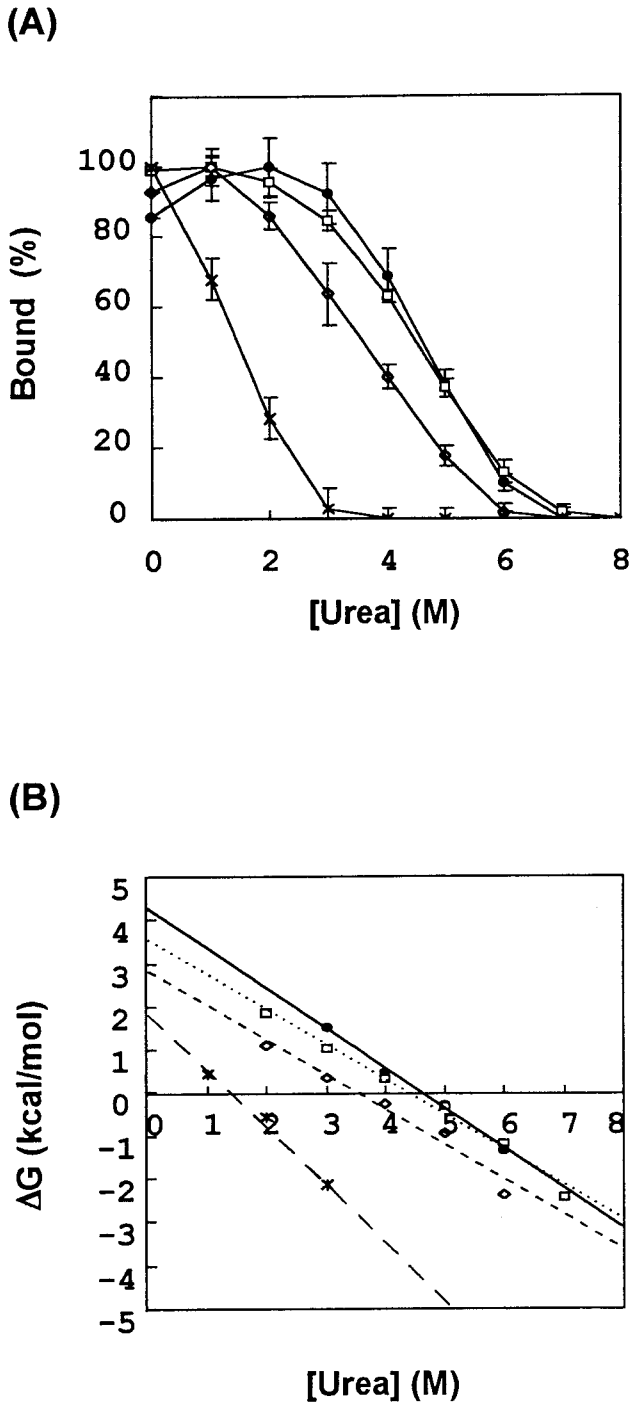

Fig. 4-6. Stability of mutant proteins of ECD in aqueous urea. (A) ^{125}I-STp(4-17) (1.8 nM) was incubated with ECD6H, N9A, N172A, and N379A, which were purified by Con A and Ni-chelating affinity chromatography and kept in aqueous urea, and the radioactivity of the peptide bound to the mutant proteins was determined. Each value represents the mean of triplicate determinations as a relative values. (B) The ΔG values in each concentration of urea were calculated from the data of (A), as described in section 4.3.

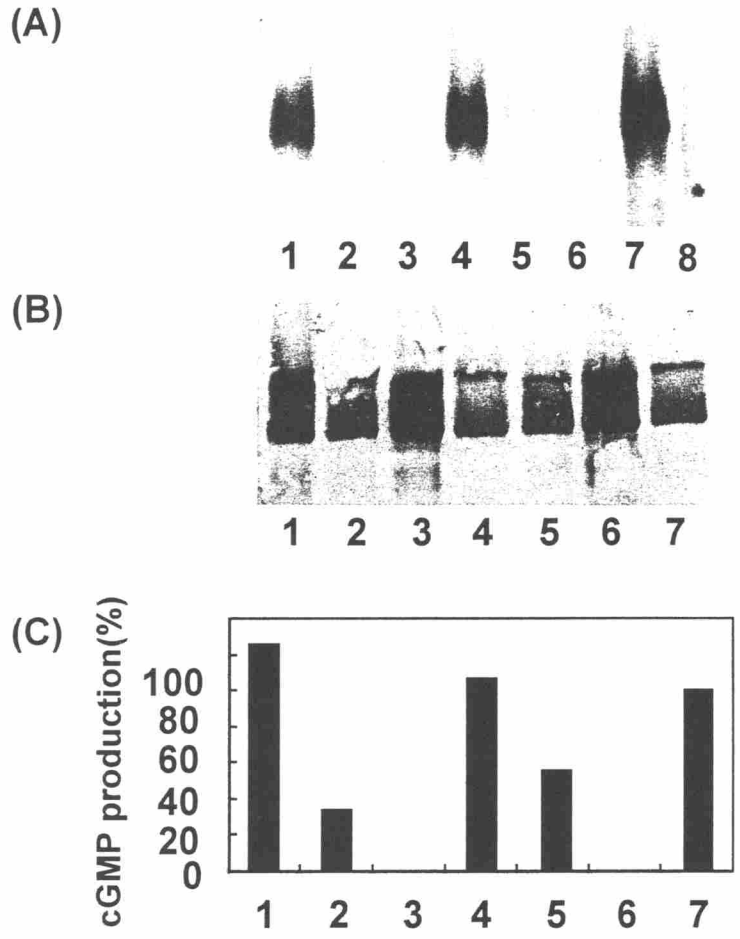

Fig. 4-7. Characterization of mutants of GC-C expressed in 293T cells. (A) SDS-PAGE of mutant proteins of GC-C photoaffinity-radiolabeled with ^{125}I-BB-STp(4-17). (B) SDS-PAGE of mutant proteins of GC-C visualized by an anti-GC-C antibody. (C) Guanylyl cyclase activity (cGMP production) of the mutant proteins of GC-C, expressed on 293T cells, in the presence of 10^{-5} M STp(4-17). Lane 1, N9A; lane 2, N172A; lane 3, N379A; lane 4, S11A; lane 5, T174A; lane 6, T381A; lane 7, GC-C. Lane 8 in (A) contains GC-C photoaffinity-labeled in the presence of 10^{-5} M STp(4-17).

chain at the mutation site.

The binding activities to STa were assayed by treatment of the mutant protein expressed on 293T cell membranes with ^{125}I-BB-STp(4-17). As can be seen in Fig. 4 7A, radiation with UV and SDS-PAGE revealed that GC-C(N9A) (lanes 1) was labele by ^{125}I-BB-STp(4-17) similarly to that of GC-C (lane 7), while GC-C(N172A) (lane 2 was labeled on it very weakly and GC-C(N379A) (lane 3) not at all, indicating that th deletion of a carbohydrate chain at positions N379 significantly affected the bindin ability of GC-C to STa. These results were further confirmed by the observation tha the mutant proteins, GC-C(S11A), GC-C(T174A), and GC-C(T381A), exhibited similar behavior on binding with the ligand to those of the corresponding mutan proteins, GC-C(N9A), GC-C(N172A), and GC-C(N379A), respectively, as seen in lane 4~6 in Fig. 4-7A. The expression efficiencies of GC-C and the mutant proteins wer then examined by immuno-blotting with an anti-GC-C antibody. All the mutant protein exhibited an expression level similar to that of GC-C, as judged from the densities of th immuno-stained protein bands on SDS-PAGE in Fig. 4-7B. Thus, deglycosylation a positions of N379 resulted in a significant loss of ligand-binding ability for the case o GC-C, as was also found for ECD.

We next measured the cyclase catalytic activities of the mutant proteins of GC-C which were prepared in 293T cells by transfection of the mutant genes. The cGMI production of GC-C(N9A), induced by stimulation with STa (in the presence of 10 μM STp(4-17)), was at the same level as that of GC-C, while GC-C(N172A) modestl increase cGMP production and GC-C(N379A) did not at all, as shown in Fig. 4-7C The same phenomena were observed in the mutant proteins, GC-C(S11A), GC-C(T174A), and GC-C(T381A), as can be seen in Fig. 4-7C. These results indicate tha the deletion of the N-linked carbohydrate moieties at position N379 of GC-C resulted i a marked loss in cyclase catalytic capability in the context of ligand-binding activity an that the N-linked glycosylation at N379 plays a role in maintaining the functiona structure in both the binding with STp and the cyclase catalysis of GC-C.

4.3 DISCUSSION

We were successful in generating a large amount of the extracellular domain (ECD) of GC-C to molecular homogeneity using an insect cell and baculovirus system and demonstrated that ECD exhibits a ligand-binding ability similar that of GC-C, as described in chapter 1. The truncation of the transmembrane and intracellular portions of GC-C made the isolation and purification of ECD as a soluble protein simple and straightforward, providing sufficient material for further analysis of the biochemical behavior of GC-C. As a result, we were able to study the influence of the mutation of the Asn residue to an Ala residue at the N-linked glycosylation sites in the consensus sequence (Asn-Xaa-Thr/Ser) on ECD on its biochemical properties.

The cDNA sequences coding for GC-C determined thus far pointed to a high content of carbohydrate chains at the putative N-linked glycosylation sites (Asn-Xaa-Thr/Ser) on ECD of GC-C, as shown in Fig. 4-1. An abundance of carbohydrate chains may be present to protect GC-C from exposure to various proteolytic enzymes on the epithelial cell membranes of the intestine where GC-C is specifically expressed and localized (Forte & Currie, 1995). Previous studies have demonstrated that N-linked carbohydrate chains play an essential role in various protein functions such as folding, stability, targeting and molecular recognition (Kobata, 1992; Lis & Sharon, 1993). For example, natriuretic peptide receptor-B (GC-B), one of the particulate guanylyl cyclases, shows a decreased ligand binding ability and cyclase catalytic activity as the result of the removal of an N-linked carbohydrate moiety ; the deletion of the N-linked carbohydrate moiety at position 24 causes a 90 % loss in ligand-binding and cGMP production, although the mutant protein lacking the carbohydrate chain at position 24 exerted an EC_{50} value for its ligand which was not significantly different from that of GC-B (Fenrick *et al.*, 1997). The authors in their report suggested that the N-linked carbohydrate moiety plays a role in stabilizing the functional structure of GC-B in recognition of its ligand.

The purified ECD6H, when treated with PNGase F, showed a molecular weight of 45-kDa on SDS-PAGE, which was close to that calculated from the amino acid sequence (46,981), and lost the ligand-binding capability, as judged from the results

obtained by the photoaffinity-labeling experiments, as shown in Fig. 4-2. This provides a clear demonstration that the truncation of the N-linked carbohydrate chains of ECD strongly affects on its ligand-binding ability and raises an important question, namely, which of the eight putative N-linked carbohydrate chains on ECD are directly involved in the interaction with its ligand or in stabilizing the functional structure for recognizing its ligand ? The influence of the mutation of an Asn to an Ala residue at each of the eight N-glycosylation sites in ECD on its ligand-binding activity were classified into three groups of the mutant proteins ; In the case of the first group (group 1), the mutation had no effect, or only slightly decreased the ligand-binding ability of ECD (N9, N20, N56, N284, and N334). For the second (group 2), the mutation strongly affected ligand-binding (about an 80 % decrease, N172 and N261), while for the case of the third (group 3) the mutation resulted in the complete loss in ligand-binding (more than a 90 % decrease, N379). The majority of the N-linked glycosylation sites of GC-C are conserved among the currently available mammalian sequences of five species, porcine, bovine, human, rat, and guinea pig (Fig. 4-1). The exception for porcine GC-C is the N-linked glycosylation site at N20, which is seen in porcine and bovine GC-C's but not in human, rat, and guinea pig GC-C. Therefore, it may be reasonable that the deletion of the N-linked carbohydrate chain at N20 has no influence on ligand-binding ability. However, the loss of or the survival of the binding activity by deletion of the N-linked carbohydrate moiety may be difficult to explain, based only on the sequence homology.

The estimation of the ligand binding activity of the mutant proteins of ECD indicated that the defect in the N-linked carbohydrate chain affected the maximum ligand-binding capacity (B_{max}), not the K_D value, suggesting that the carbohydrate chain is not directly involved in ligand recognition and that the mutation causes the decrease of the functional protein, which is able to interact with the ligand, in the total protein. This is supported by the observation in Fig. 4-5 that the ligand-binding capacities of the mutant proteins were different from one another, even for the same amount of the mutant proteins. The decrease in maximum ligand-binding capacity in the mutant proteins of ECD suggests the possibility that the mutation altered, more or less, the native structure which is concerned with binding to the ligand.

We tested the stability of ECD and its mutant proteins, N9A, N172A, and N379A,

as representatives of each groups 1, 2, and 3 respectively, in aqueous urea. The result clearly indicates that the stability of these mutant proteins to the denaturant is correlated to their ligand-binding activity. The ΔG values of denaturation in the absence of urea were 4.3 kcal/mol (ECD6H), 3.6 kcal/mol (N9A), 2.9 kcal/mol (N172A), and 1.9 kcal/mol (N379A), calculated according to the equation (Schellman, 1978) ($\Delta G = -RT\ln[D]/[N] = -RT\ln\{(B_0-B) / B\}$) and using the result obtained in Fig. 4-6B, where [D] and [N] represent concentration of the denatured and the native proteins, respectively, and B and B_0 represent the binding quantity of ^{125}I-STp(4-17) in the presence (various concentrations) and absence of urea, respectively. Therefore, the degrees of the instability ($\Delta\Delta G$) of the mutant proteins (N9A, N172A, and N379A), containing a deleted carbohydrate chain at N9, N172, and N379, are calculated to be 0.7, 1.4, and 2.4 kcal/mol, respectively. Consequently, the urea-induced inactivation of the mutant proteins reveals that the carbohydrate moiety in group 1 does not contribute to the stability of the structure of ECD, although the slight decrease in stability may affect the amount of the expression of the mutant proteins which are expressed. On the contrary, deletion of a carbohydrate chain at N172 and N379 in groups 2 and 3, respectively, resulted in a significant decrease in the stability of N172A and N379A. This is consistent with the result observed in the treatment of ECD with PNGase F.

The results obtained in the analysis of the biochemical properties of ECD were further supported by characterization of the entire GC-C using site-directed mutagenesis. That is, the three mutant proteins of GC-C (GC-C(N9A), GC-C(N172A), and GC-C(N379A)), which correspond to the representatives in group 1, group 2, and group 3 in ECD and which are deprived of carbohydrate moieties at N9, N172, and N379, respectively, were examined in the ligand-binding and ligand-stimulated guanylyl cyclase catalytic activity (Fig. 4-7). Among them, two mutant proteins (GC-C(N172A) and GC-C(N379A)) remarkably diminished the activities of GC-C, while the properties of GC-C(N9A) were the same as GC-C. Moreover, the mutant proteins (GC-C(S11A), GC-C(T174A), and GC-C(T381A)) showed the same properties as those of the corresponding mutant proteins (GC-C(N9A), GC-C(N172A), and GC-C(N379A)), respectively (Fig. 4-7).

This study permitted us to define the influence of the mutation of ECD and GC-C,

which contained a deleted carbohydrate moiety at each of the putative N-linked glycosylation sites, on biochemical properties of GC-C. It is likely that a carbohydrate moiety at N379 plays a role in the stabilizing the functional structure of ECD, which is necessary for an interaction between ECD and its ligand, although the carbohydrate chain may be not directly involved in this interaction. This result is consistent with the data that the N-glycosylation site, N379, is completely conserved in the primary structure of GC-C's determined thus far, not only for mammalian species but for an amphibian and another vertebrate species as well (MacFarland, 1995; Mantoku & Suzuki, 1997). N379 is located near the transmembrane region, which takes part in the transmission of an external signal from the extracellular portion to the intracellular portion. The author identified a peptide fragment, which encompasses a region near N379, in the enzymatic digest of ECD photolabeled with a STa analog, as described in chapter 3. This experiment also supports the hypothesis that a carbohydrate moiety at N379 plays an important role in interactions between ECD and its ligand.

In addition, the present result demonstrates that a single defect of a carbohydrate chain in the eight N-linked glycosylation sites on ECD causes a variety of distinct influence with respect to binding to its ligand. This observation raises the question of whether each of the N-linked carbohydrate moieties is required to play different roles for the interaction of ECD with the ligand, the stability of the functional structure of ECD, the terminal glycosylation, and the expression of a maturely functional receptor at the cell surface. This may be possibly explained by the observation that the mutant protein of ECD, which contained five simultaneously deleted N-linked carbohydrate moieties at N9, N20, N56, N284 and N334 (group 1), could not be secreted into a culture medium (data not shown). Further experiments are clearly called for in explaining the role of carbohydrate moieties at N-linked glycosylation sites. In any case, the present results provide new insights into how GC-C recognizes a ligand and transmit its signal from the outside to the inside cells.

4.4 MATERIALS AND METHODS

4.4.1 Materials

Chemicals were purchased from Nacalai tesque inc. (Kyoto) or Katayama chemical industries, Inc. (Osaka). Restriction enzymes were obtained from TOYOBO (Tokyo). Dulbecco's modified eagle medium, Grace's insect medium and fetal bovine serum were from Sigma, Gibco/BRL (MD) and Dainippon Pharmaceutical Co. (Osaka), respectively. A TaKaRa ligation kit (Takarashuzo, Tokyo), and a Flexi Prep Kit (Pharmacia, Uppsala) were used for the construction and preparation of plasmids. Ni-NTA agarose and PNGase F were purchased from QIAGEN (Hilden, Germany) and Boehringer Mannheim GmbH (Mannheim, Germany), respectively. STp(4-17), which is a full agonistic STa analog, and BB-STp(4-17) were synthesized as described previously (Aimoto *et al.*, 1983; Yoshimura *et al.*, 1984; Yamasaki *et al.*, 1990; Gariépy & Schoolnik, 1986). $Na^{125}I$ (carrier free) was purchased from DuPont NEN (MA) and was used for iodination of STp(4-17) and BB-STp(4-17) as described in section 2.3.5. An anti-GC-C antibody was raised against a synthetic peptide corresponding to C-terminal region (amino acid residues 1036 to 1050, EYLQLNTTDNESTHF) of porcine GC-C, according to the procedure described by Vaandrager *et al.* (1993).

4.4.2 Constructions of transfer vectors carrying cDNA of GC-C, ECD and their mutant proteins

The construction of plasmids and the expression of the recombinant ECD (amino acid residues 1 to 407 in Fig. 4-1) of porcine GC-C in Sf21 cells were described in section 1.4.2. A site-directed mutagenesis was performed by PCR using pVL-egtECD as a template. The first PCR fragment was prepared by using primer 1 (pVL1392 forward primer, 5'-AAA TGA TAA CCA TCT CGC-3') and primer 2 (antisense primers for the mutation), and the second PCR fragment was prepared by using primer 3 (pVL1392 reverse primer, 5'-GTC CAA GTT TCC CTG-3') and primer 4 (sense primers, summarized in Table 4-2). The third PCR fragment was constructed with primers 1 and 3 using the first and second PCR fragments as templates. The third PCR fragment was digested with *Pst*I and *Bam*HI and inserted into the *Pst*I and *Bam*HI sites of pVL1392, resulting in the construction of the transfer vector for the expression of the mutant proteins of ECD. For detailed analysis, the mutant proteins (N9A, N172A, and N379A) attached by the His_6 tag at each C-terminus of the mutant proteins were prepared using

Table 4-2 Primers used for the mutation of ECD and GC-C

Mutant protein	Oligonucleotide
N9A	CAGAATTGCCAC**GC**TGGCAGCT
N20A	GCTGATGATGG**CC**AACTCAGC
N56A	CAGTGACTGTGG**CT**GCCACCT
N172A	CTATGTTTTCAAG**GC**TAGTACAGAG
N261A	CTTCATGGAC**GC**TGTCACAGC
N284A	CTGTCTCAG**CT**AGCTAGCTCCTTC
N334A	CTTTCAGG**GC**CATCACTTTTGAAG
N379A	CCGCAAAG**CC**TATACAAACC
S11A	TGCCACAATGGC**GC**CTACGAGATAAGC
T174A	TTCAAGAATAGT**GC**CGAGTCTGAGGAC
T381A	CGCAAAAACTAT**GC**CAACCCGGTGGAT

Asterisks (*) idicate position of the mutated nucleotides.

pVL-egtECD6H as a template by the same procedure as described above.

The construction of plasmids and the expression of the recombinant GC-C and its mutant proteins in 293T embryonic kidney cells were carried out according to methods reported previously (Wada *et al.*, 1994). Briefly, a 1.0 kb cDNA fragment between *Xba*I and *Hind*III sites (bases 90-1742) of porcine GC-C, which contain the mutation, was prepared by PCR as described above. The fragment was inserted into the pCG vector and, then, ligated with a 1.7 kb cDNA fragment (bases 1743-3371) by *Hind*III sites at both ends. The DNA sequences of the vectors constructed in this study were confirmed by digestion with restriction enzymes and an Applied Biosystems 373A DNA Sequencing System using an ABI PRISM Dye terminator cycle sequencing kit (Perkin Elmer).

4.4.3 Expression of recombinant GC-C and its mutant proteins in Sf21 insect cells or 293T mammalian cells

The recombinant baculovirus was prepared by the homologous recombination method according to the manufacture's specification (Baculo Gold, Phar-Mingen). Sf21

insect cells were cultured in Grace's medium with 10% fetal bovine serum and gentamycin (30 μg/ml) at 27 °C. Expression of the recombinant protein was performed by infection of a recombinant baculovirus, of which the titer was 5-10 fold the multiplicity of infection, to the cells (5×10^7, 80% confluent state) in a 175 cm^2 flask for 1 h. The infected cells were scraped into a fresh SF-900II medium (1×10^6 cells/ml) and again cultured in a spinner flask at 27 °C for 2 d. The 293T human embryonic kidney cells were grown in DMEM medium (Sigma) supplemented with 10 % fetal bovine serum. The recombinant GC-C and its mutant proteins were transiently expressed in the cells using a Superfect transfection reagent according to the manufacturer's specification (QIAGEN).

4.4.4 Purification of ECD6H and its mutant proteins

Purification of the His_6 tagged ECD (named ECD6H) and its mutant proteins were proceeded as described in section 1.4.5. The supernatant from the Sf21 cells culture (400 ml) was applied to Con A-immobilized agarose (5 ml) and packed into a column (3.0 × 12 cm). The column was washed with buffer A (20 mM HEPES (pH 7.4), 100 mM NaCl, and 10 % glycerol). The protein which was adsorbed to the resin was eluted with 5 bed volumes of buffer A containing 500 mM α-methyl-D-mannoside. The eluate containing ECD6H or its mutant proteins was analyzed by SDS-PAGE and the ligand-binding assay and then incubated with Ni-NTA resin (2 ml) at room temperature for 1 h. The resin was packed into a column (1.0 × 10 cm) and washed with buffer A containing 20 mM imidazole. ECD6H or its mutant proteins was eluted from the column with buffer A containing 100 mM imidazole and 0.1 % sucrose monolaurate (Dojin Chemical Laboratory, Kumamoto). The purity of the protein was confirmed by SDS-PAGE and western blot analysis. The fraction which contained ECD6H or its mutant proteins were pooled and concentrated by Centricon-10 (Amicon).

4.4.5 Deglycosylation of ECD6H

The purified ECD6H (5 μg) was treated with PNGase F (0.4 U) at 37 °C for 16 h in buffer A. The digest was run on SDS-PAGE and then western-blotted on a nitrocellulose membrane. The deglycosylation of ECD6H was confirmed using

succinylated-Con A conjugated with HRP (Vector Lab. Inc.) and an HRP Conjugate Substrate Kit (Bio-Rad). Detection of His_6-tagged proteins was done using QIAexpress Ni-NTA Conjugates (QIAGEN) and a BCIP/NBT Phosphatase Substrate System according to the manufacture's specifications (Kirkegaard & Perry Lab.).

4.4.6 Photoaffinity-labeling of recombinant GC-C, ECD, and their mutant proteins

ECD6H and its mutant proteins purified by Con A affinity chromatography or GC-C and its mutant proteins separated on the cell membranes (from 5×10^5 cells) were incubated with ^{125}I-BB-STp(4-17) (7.0×10^5 cpm) in PBS(-) (60 μl) in the presence or absence of 1 μM unlabeled STp(4-17) at 37 °C for 1 h in the dark. The mixtures was exposed to UV light (254 nm, Model UVG-54, UVP Inc., CA) for 30 min on ice, boiled for 3 min in the SDS-PAGE sample buffer (1.8 % SDS, 30 mM Tris-HCl (pH6.8), 4 % glycerol, 5 % DTT, and 0.05 % bromophenol blue), and then subjected to SDS-PAGE. After drying the gel, the photoaffinity-labeled protein was analyzed by autoradiography on a Fujix Bio-image analyzer BAS 2000 (Fuji film, Tokyo).

4.4.7 STa-binding assay of ECD and its mutant proteins

The culture medium (10 μl) containing ECD or its mutant proteins was diluted to PBS(-) (60 μl) in the presence of ^{125}I-STp(4-17) (1×10^{-10} - 2×10^{-8} M) at 37 °C for 1 h. The ligand bound to the proteins was collected on a TLK-3000 ultrafree filter (Millipore) by centrifugation (1,000 × g, 10 min) at 4 °C and washed twice with cold PBS(-) (150 μl). The non-specific binding of ^{125}I-STp(4-17) was determined by addition of 10 μM STp(4-17). The radioactivity of the filter was measured with an ARC-361 γ-well counter (Aloka, Tokyo; count efficiency of 55 % using ^{131}I as a standard). All experiments were performed in triplicate at each peptide concentration.

4.4.8 Urea-induced inactivation of ECD6H and its mutant proteins

The purified ECD6H or its mutant proteins was incubated at 37 °C in aqueous urea (100 μl) ranging from 0 to 8 M in buffer A for 30 min. The residual activity of ECD6H or its mutant proteins was measured by the ligand binding assay, as described

above.

4.4.9 cGMP assay

The 293T cells expressing the recombinant GC-C or its mutant proteins was subjected to the cGMP assay as described previously (Wada *et al.*, 1994). The cGMP concentration was estimated by means of a radioimmunoassay kit (YAMASA).

Summary

1) The present study established the large-scale expression and purification system of the extracellular domain of porcine guanylyl cyclase C (GC-C) by a baculovirus and Sf21 insect cell system. The extracellular domain, which was generated as a secretory protein from the insect cell, could be of use for studies on the interaction between GC-C and its ligand and the activation mechanism of GC-C.

2) The extracellular domain exhibited multiple ligand-binding affinities and the formation of an oligomer only in the presence of a ligand. These features imply that the oligomerization of the extracellular domain is directly coupled to the activation of the intracellular domain.

3) STp(4-17) containing *p*-azido-L-phenylalanine at position 11 in the central portion of the STa toxic domain showed high efficiency in the photoaffinity-labeling reaction, in which the STa analog covalently cross-linked with GC-C by radiation with UV light. These data clearly demonstrate that the central region (Asn-11, Pro-12, and Ala-13) of the STa molecule directly interacts with GC-C.

4) The region to bind to a ligand in GC-C was determined by a photoaffinity-labeling STa analog, biotinyl($NH(CH_2)_4CO)_2$[Gly^4,Pap^{11}]STp(4-17). The STa analog was linked to the region (residue-387 to residue-393) located in the near-transmembrane region of the extracellular domain. Taken together with the site-directed mutational analysis of this region, the present result

provides the possibility that the hydrophobic side chains in Thr-389, Phe-390 and Trp-392 of GC-C directly interact with the hydrophobic side chain of the receptor-binding region (Pro-12 and Ala-13) of STa.

5) A single defect of a carbohydrate chain at Asn-379 in eight N-glycosylation sites on the extracellular domain causes considerable influence with respect to binding of GC-C to its ligand. The carbohydrate moiety at Asn-379 plays a role in the stabilizing the functional structure of the extracellular domain, which is necessary for an interaction between the extracellular domain and its ligand.

Publications

1 Hidaka, Y., Wada, A., Idomoto, M., **Hasegawa, M.,** Hirayama, T., Karasawa, T., Takeda, Y., & Shimonishi, Y. **(1993)** Syntheses and biological properties of guanylin and its analogs. in *Peptide Chemistry 1992* : Proceedings of the 2nd Japan Symposium on Peptide Chemistry (Yanaihara, N., Ed.) pp. 347-349, ESCOM, Leiden.

2 **Hasegawa, M.,** Hidaka, Y., Matsumoto, K., Sato, T., & Shimonishi, Y. **(1995)** Identification of the binding region in *E. coli* heat-stable enterotoxin to its receptor with photoaffinity-labeling method. in *Peptide Chemistry 1994* : Proceedings of the 32th Japanese Peptide Symposium (Ohno, M., Ed.) pp. 337-340, Protein Research Foundation, Osaka.

3 Wada, A., Hirayama, T., Kitaura, H., Fujisawa, J., **Hasegawa, M.,** Hidaka, Y., & Shimonishi, Y. **(1996)** Identification of ligand recognition sites in heat-stable enterotoxin receptor, membrane-associated guanylyl cyclase C by site-directed mutational analysis. *Infection and Immunity* **64**, 5144-5150.

4 Wada, A., **Hasegawa, M.,** Matsumoto, K., Niidome, T., Kawano, Y., Hidaka, Y. Padilla, P.I., Kurazono, H., Shimonishi, Y., & Hirayama, T. **(1996)** The significance of Ser^{1029} of the heat-stable enterotoxin receptor (STaR): relation of STa-mediated guanylyl cyclase activation and signaling by phorbol myristate acetate. *FEBS Letters* **384**, 75-77.

5 **Hasegawa, M.,** Fujii, J., Kawano, Y., Matsumoto, K., Wada, A., Hirayama, T., Taniguchi, N., & Shimonishi, Y. **(1996)** High-level expression of heat-stable enterotoxin (ST) receptor with exchange of the signal peptide in baculovirus/insect cells system. in *Peptide Chemistry 1995* : Proceedings of the 33th Japanese Peptide Symposium (Nishi, N., Ed.) pp. 325-328, Protein Research Foundation, Osaka.

6 **Hasegawa, M.,** Kawano, Y., Matsumoto, K., Hidaka, Y., Sato, T., & Shimonishi, Y. **(1997)** Identification of a binding region on *Escherichia coli* heat-stable enterotoxin to intestinal guanylyl cyclase C. *Letters in Peptide Science* **4**, 1-11.

7 **Hasegawa, M.,** Kawano, Y., Matsumoto, K., Hidaka, Y., Fujii, J., Taniguchi, N., & Shimonishi, Y. **(1997)** Ligand-induced aggregation of extracellular domain of a heat-stable enterotoxin receptor (guanylyl cyclase C). in *Peptide Chemistry* 1996 : Proceedings of the 34th Japanese Peptide Symposium (Kitada, C. Ed.) pp. 169-172, Protein Research Foundation, Osaka.

8 **Hasegawa, M.,** Hidaka, Y., Matsumoto, Y., Wada, A., Hirayama, T., & Shimonishi, Y. **(1999)** Interaction between heat-stable enterotoxin and its receptor (guanylyl cyclase C): influence of mutation at N-linked glycosylation site on its ligand binding. in *Peptide Science — Present and Future* : Proceedings of the 1st International Peptide Symposium (Shimonishi, Y. Ed.), Kluwer Academic Publishers, Dordrecht, *in press.*

9 **Hasegawa, M.,** Kawano, Y., Matsumoto, Y., Hidaka, Y., Fujii, J., Taniguchi, N., Wada, A., Hirayama, T., & Shimonishi, Y. **(1999)** Expression and characterization of the extracellular domain of guanylyl cyclase C from a baculovirus and Sf21 insect cells. *Protein Expression and Purification* **15**, *in press.*

10 **Hasegawa, M.,** Matsumoto, Y., Sanni, T., Hidaka, Y., & Shimonishi, Y. **(1999)** Interaction between heat-stable enterotoxin and extracellular domain of guanylyl cyclase C. in *Peptides* : Proceedings of the 25th European Peptide Symposium (Bajusz, S. Ed.), Kluwer Academic Publishers, Dordrecht, *in press.*

11 **Hasegawa, M.,** Hidaka, Y., Wada, A., Hirayama, T., & Shimonishi, Y. **(1999)** The relevance of N-glycosylation to the binding of ligands to guanylyl cyclase C. *Eur. J. Biochem., submitted.*

12 **Hasegawa, M.,** Hidaka, Y., Matsumoto, Y., Sanni, T., & Shimonishi, Y. **(1999)** Identification of photoaffinity labeling of the specific site on the extracellular domain of guanylyl cyclase C involved in ligand binding. *in preparation.*

REFERENCES

Aimoto, S., Takao, T., Shimonishi, Y., Hara, S., Takeda, T., Takeda, Y., & Miwatani, T. (1982) Amino-acid sequence of a heat-stable enterotoxin produced by human enterotoxigenic *Escherichia. coli. Eur. J. Biochem.* **129**, 25-263.

Aimoto, S., Watanabe, H., Ikemura, H., Shimonishi, Y., Takeda, T., Takeda, Y., & Miwatani, T. (1983) Chemical synthesis of a highly potent analog of a heat-stable enterotoxin produced by a human strain of enterotoxigenic *Escherichia coli. Biochem. Biophys. Res. Commun.* **112**, 320-326.

Arita, M., Honda, T., Miwatani, T., Takeda, T., Takao, T., & Shimonishi, Y. (1991) Purification and characterization of a heat-stable enterotoxin of *Vibrio mimicus. FEMS Microbiol. Lett.* **79**, 105-110.

Ashman, D. F., Lipton, R., Melicow, M. M., & Price, T. D. (1963) Isolation of adenosine 3', 5'-monophosphate and guanosine 3',5'-monophosphate from rat urine. *Biochem. Biophys. Res. Commun.* **11**, 330-334.

Basu, A., Raghunath, M., Bishayee, S., & Das, M. (1989) Inhibition of tyrosine kinase activity of the epidermal growth factor (EGF) receptor by a truncated receptor form that binds to EGF. *Mol. Cell Biol.* **9**, 671-677.

Bayley, H., & Knowles, J. R. (Ed.) (1977) *Methods in Enzymol.* **46**.

Carpick, B. W., & Gariépy, J. (1993) The *Escherichia coli* heat-stable enterotoxin is a long-lived superagonist of guanylin. *Infect. Immun.* **61**, 4710-4715.

Chao, A. C., de Sauvage, F. J., Dong, Y. J., Wagner, J. A., Goeddel, D. V., & Gardner, P. (1994) Activation of intestinal CFTR CI- channel by heat-stable enterotoxin and guanylin via cAMP-dependent protein kinase. *EMBO. J.* **13**, 1065-1072.

Chinkers, M., Singh, S., & Garbers, D. L. (1991) Adenine nucleotides are required for activation of rat atrial natriuretic peptide receptor/guanylyl cyclase expressed in a baculovirus system. *J. Biol. Chem.* **266**, 4088-4093.

Chou, P. Y. & Fasman, G. D. (1974) Conformatinal Parameters for amino acids in helical, β-sheet and ramdom coil regions calculated from proteins. Prediction of protein conformation. *Biochemistry* **13**, 211-245.

Cohen, M. B., Jensen, N. J., Hawkins, J. A., Mann, E. A., Thompson, M. R., Lentze, M. J., & Giannella, R. A. (1993) Receptors for *Escherichia coli* heat-stable enterotoxin in human intestine and in a human intestinal cell line (Caco-2). *J. Cell Physiol.* **156**, 138-144.

Currie, M. G., Fok, K. F., Kato, J., Moore, R. J., Hamra, F. K., Duffin, K. L., & Smith,

C. E. (1992) Guanylin: An endogenous activator of intestinal guanylate cyclase. *Proc. Natl. Acad. Sci. USA* **89**, 947-951.

de Sauvage, F. J., Camerato, T. R., & Goeddel, D. V. (1991) Primary structure and functional expression of the human receptor for *Escherichia coli* heat-stable enterotoxin. *J. Biol. Chem.* **266**, 17912-17918.

de Sauvage, F.J., Horuk, R., Bennet, G., Quan, C., Burnier, J. P., & Goeddel, D.V. (1992) Characterization of the recombinant human receptor for *Escherichia coli* heat-stable enterotoxin. *J. Biol. Chem.*, **267** (1992) 6479-6482.

de Sauvage, F. J., Keshav, S., Kuang, W. J., Gillett, N., Henzel, W., & Goeddel, D. V. (1992) Precursor structure, expression, and tissue distribution of human guanylin. *Proc. Natl. Acad. Sci. USA* **89**, 9089-9093.

Deshmane, S. P., Carrithers, S. L., Parkinson, S. J., Crupper, S. S., Robertson, D. C., & Waldman, S. A. (1995) Rat guanylyl cyclase C expressed in COS-7 cells exhibits multiple affinities for *Escherichia coli* heat-stable enterotoxin. *Biochemistry* **34**, 9095-9102.

de Vos, A. M., Ultsch, M., & Kossiakoff, A. A. (1992) Human growth hormone and extracellular domain of its receptor : crystal structure of the complex. *Science* **255**, 306-312.

Duda, T., Goraczniak, R. M., & Sharma, R. K. (1991) Site-directed mutational analysis of a membrane guanylate cyclase cDNA reveals the atrial natriuretic factor signaling site. *Proc. Natl. Acad. Sci. USA* **88**, 7882-7886.

Eberle, A.N., and de Graan, P.N.E. (1985) General principles for photoaffinity labeling of peptide hormone receptors. in *Methods Enzymol.* **109** (Birnbaumer, L. & O'Malley, Ed.) 129-156.

Fenrick, R., Bouchard, N., McNicoll, N., & de Lean, A. (1997) Glycosylation of asparagine 24 of the natriuretic peptide receptor-B is crucial for the formation of a competent ligand binding domain. *Mol. Cell. Biochem.* **173**, 25-32.

Forte, L. R., & Currie, M. G. (1995) Guanylin: a peptide regulator of epithelial transport. *FASEB J.* **9**, 643-650.

Fulle, H. -J., Vassar, R, Foster, D. C., Yang, R. -B., Axel, R., & Garbers, D. L. (1995) A receptor guanylyl cyclase expressed specifically in olfactory sensor neurons. *Proc. Natl. Acad. Sci. USA* **92**, 3571-3575.

Garbers, D. L. (1992) Guanylyl cyclase receptors and their endocrine, paracrine, and autocrine ligands. *Cell* **71**, 1-4.

Garbers, D. L., & Lowe, D. G. (1994) Guanylyl cyclase receptors. *J. Biol. Chem.* **269**, 30741-30744.

Gariépy, J., & Schoolnik, G. K. (1986) Design of a photoreactive analogue of the *Escherichia coli* heat-stable enterotoxin STIb: Use in identifying its receptor on rat brush border membranes. *Proc. Natl. Acad. Sci. USA* **83**, 483-487.

Giannella, R. A. (1981) Pathogenesis of acute bacterial diarrheal disorders. *Ann. Rev. Med.* **32**, 341-357.

Goraczniak, R. M., Duda, T., & Sharma, R. K. (1997) direct submission to EMBL/GENBANK/DDBJ data banks, accession no. AF081464.

Hamra, F. K., Forte, L. R., Eber, S. L., Pidhorodeckyj, N. V., Krause, W. J., Freeman, R. H., Chin, D. T., Tompkins, J. A., Fok, K. F., & Smith, C. E. (1993) Uroguanylin: Structure and activity of a second endogenous peptide that stimulates intestinal guanylate cyclase. *Proc. Natl. Acad. Sci. USA* **90**, 10464-10468.

Hidaka, Y., Kubota, H., Yoshimura, S., Ito, H., Takeda, Y., & Shimonishi, Y. (1988) Disulfide linkages in heat-stable enterotoxin (STp) produced by a porcine strain of enterotoxigenic *Escherichia coli*. *Bull. Chem. Soc. Jpn.*, **61** (1988) 1265-1271.

Hidaka, Y., Wada, A., Idomoto, M., Hasegawa, M., Hirayama, T., Karasawa, T., Takeda, Y., & Shimonishi, Y. (1993) Syntheses and biological properties of guanylin and its analogs. in *Peptide Chemistry 1992*, Proceedings of the 2nd Japanese Symposium on Peptide Chemistry (Yanaihara. N., Ed), pp. 347-349, ESCOM, Leiden.

Hill, O., Zucht, H. D., Luttermann, D., Maegert, H. J., Forssmann, W.-G. (1997) direct submission to EMBL/GENBANK/DDBJ data banks, accession no. Z73607.

Hirayama, T., Wada, A., Iwata, N., Takasaki, S., Shimonishi, Y., & Takeda, Y. (1992) Glycoprotein receptor for a heat-stable enterotoxin (STh) produced by enterotoxigenic *Escherichia coli*. *Infect. Immun.* **60**, 4213-4220.

Hugues, M., Crane M. R., Thomas, B. R., Robertson, D., Gazzano, H., O'Hanley, P., & Waldman, S. A. (1992) Affinity purification of functional receptor for *Escherichia coli* heat-stable enterotoxin from rat intestine. *Biochemistry* **31**, 12-16.

Hunter, W.M., & Greenwood F.C. (1962) Preparation of iodine-131 labelled human growth hormone of high specific activity. *Nature* **194**, 495-496.

Hurwitz, D. R., Emanuel, S. L., Nathan, M. H., Sarver, N., Ullrich, A., Felder, S., Lax, I., & Schlessinger, J. (1991) EGF induces increased ligand binding affinity and dimerization of soluble epidermal growth factor (EGF) receptor extracellular domain. *J. Biol. Chem.* **266,** 22035-22043.

Jarvis, D. L., Summers, M. D., Garcia, A. Jr., & Bohlmeyer, D. A. (1993) Influence of different signal peptides and prosequences on expression and secretion of human tissue plasminogen activator in the baculovirus system. *J. Biol. Chem.* **268**, 16754-16762.

Katwa, L. C., Parker, C. D., Dybing, J. D., & White, A. A. (1991) Solubilization and reprecipitation from intestinal brush border membranes of a complex containing guanylate cyclase activatable by the heat-stable enterotoxin. *Arch. Biochem. Biophys.* **290**, 397-406.

Klotz, I. M. (1985) Ligand-receptor interactions: facts and fantasies. *Q. Rev. Biophys.*, **18**, 227-259.

Kobata, A. (1992) Structures and functions of the sugar chains of glycoproteins. *Eur. J. Biochem.* **209**, 483-501.

Kozak, M. (1986) Point mutations define a sequence flanking the AUG initiator codon that modulates translation by eukaryotic ribosomes. *Cell* **44**, 283-292.

Kruhoeffer, M., Cetin, Y., Kaempf, U., & Forssmann, W.-G. (1996) direct submission to EMBL/GENBANK/DDBJ data banks, accession no. P70106.

Kuno, T., Kamisaki, Y., Waldman, S.A., Gariépy, J., Schoolnik, G., & Murad, F. (1986) Characterization of the receptor for heat-stable enterotoxin from Escherichia coli in rat intestine. *J. Biol. Chem.*, **261** (1986) 1470-1476.

Lauffenburger, D. A., & Linderman, J. J. (1993) Receptors: models for binding, trafficking, and signaling. Oxford University Press NY.

Lax, I., Mitra, A, K., Ravera, C., Hurwitz, D. R., Rubenstein, M., Ullrich, A., Stroud, R. M., & Schlessinger, J. (1991) Epidermal growth factor (EGF) induces oligomerization of soluble extracellular ligand-binding domain of EGF receptor. *J. Biol. Chem.* **266**,13828-13833.

Lis, H., & Sharon, N. (1993) Protein glycosylation: structural and function aspects. *Eur. J. Biochem.* **218**, 1-27.

Lockow, V. A., & Summers, M. D. (1988) Trends in the development of baculovirus expression vectors. *Bio/Technology* **6**, 47-55.

Lockow, V. A., & Summers, M. D. (1989) High-level expression of nonfused foreign genes with *Autographa californica* Nuclear Polyhedrosis Virus Expression vectors. *Virology* **170**, 31-39.

MacFarland, R. T. (1995) direct submission to EMBL/GENBANK/DDBJ data banks, accession D49837.

Mantoku, T., & Suzuki, N. (1997) direct submission to EMBL/GENBANK/DDBJ data banks, accession no. AB007192.

Marshall R. D. (1972) Glycoproteins. *Ann. Rev. Biochem.* **41**, 673-702.

Marx, U. C., Klodt, J., Meyer, M., Gerlach, H., Rosch, P., Forssmann, W,-G., & Adermann, K. (1998) One peptide, two topologies: structure and interconversion dynamics of human uroguanylin isomers. *J. Peptide Res.* **52**, 229-240.

McNicoll, N., Escher, E., Wilkes, B. C., Schiller, P. W., Ong, H., & de Léan, A. (1992) Highly efficient photoaffinity labeling of hormone binding domain of atrial natriuretic factor receptor. *Biochemistry* **31**, 4487-4493.

McNicoll, N., Gangon, J., Rondeau, J. -J., Ong, H., & de Léan, A. (1996) Localization by photoaffinity labeling of natriuretic peptide receptor-A binding domain. *Biochemistry* **35**, 12950-12956.

Miyazato, M., Nakazato, M., Matsukura, S., Kangawa K., Matsuo, H. (1996) direct submission to EMBL/GENBANK/DDBJ data banks, accession no. U41322.

Munson, P. J., & Rodbard, D. (1980) LIGAND: a versatile computerized approach for characterization of ligand-binding systems. *Anal. Biochem.* **107**, 220-239.

Murphy, C. I., McIntire, J. R., Davis, D. R., Hodgdon, H., Seals, J. R., & Young, E. (1993) Enhanced expression, secretion, and large-scale purification of recombinant HIV-1 gp120 in insect cells using the baculovirus egt and p67 signal peptides. *Protein Expression Purif.* **4**, 349-357.

Nandi, A., Mathew, R., & Visweswariah, S. (1996) Expression of the extracellular domain of the human heat-stable enterotoxin receptor in *Escherichia coli* and generation of neutralizing antibodies. *Protein Expression and Purif.* **8**, 151-159.

Okumura, T., Sato, T., Ozaki, H., Wada, A., Hidaka, Y., and Shimonishi, Y. (1994) in *Peptide Chemistry 1993* : Proceedings of 31th Japanese Peptide Symposium (Okada, Y., Ed.) pp. 217-221, Protein Research Foundation, Osaka.

Ozaki, H., Sato, T., Kubota, H., Hata, Y., Katsube, Y., & Shimonishi, Y. (1991) Molecular structure of the toxic domain of heat-stable enterotoxin produced by enterotoxigenic *Escherichia coli*. *J. Biol. Chem.*, **266**, 5934-5941.

Pandey, K. N., Inagami, T., & Misono, K. S. (1986) Atrial natriuretic factor receptor on cultured leydig tumor cells : ligand binding and photoaffinity labeling. *Biochemistry* **25**, 8467-8472.

Pfeifer, A., Aszódi, A., Seider, U., Ruth, P., Hofmann, F., & Fässler, R. (1996) Intestinal secretory defects and dwarfism in mice lacking cGMP-dependent protein kinase II. *Science* **274**, 2082-2086.

Runder, X. L., Mandal, K. K., de Sauvage, F. J., Kindman, L. A., & Almenoff, J. S. (1995) Regulation of cell signaling by the cytoplasmic domains of the heat-stable enterotoxin receptor: Identification of autoinhibitory and activating motifs. *Proc. Natl.*

Acad. Sci. USA **92**, 5169-5173.

Sato, T., Ozaki, H., Hara, Y., Kitagawa, Y., Katsube, Y., & Shimonishi, Y. (1994) Structural Characteristics for biological activity of heat-stable enterotoxin produced by enterotoxigenic *Escherichia coli* : X-ray crystallography of weak-toxic and non-toxic analog. *Biochemistry* **33**, 8641-8651.

Scatchard, G. (1949) The attractions of proteins for small molecules and ions. *Ann. NY Acad. Sci.* **51**, 660-672.

Schellman, J. A. (1978) Solvent Denaturation. *Biopolymers* **17**, 1305-1322.

Schulz, S., Green, C. K., Yuen, P. S. T., & Garbers, D. L. (1990) Guanylyl cyclase is a heat-stable enterotoxin receptor. *Cell* **63**, 941-948.

Schulz, S., Wedel, B. J., Matthews, A., & Garbers, D. L. (1998) The cloning and expression of a new guanylyl cyclase orphan receptor. *J. Biol. Chem.* **273**, 1032-1037.

Schwyzer, R., & Caviezel, M.(1971) *p*-azido-L-phenylalanine : a photoaffinity 'probe' related to tyrosine. *Helv. Chim. Acta* **54**, 1395-1400.

Singh, S., Singh, G., Heim, J.-M., & Gerzer, R. (1991) Isolation and expression of a guanylate cyclase-coupled heat-stable enterotoxin receptor cDNA from a human colonic cell line. *Biochem. Biophys. Res. Commun.* **179**, 1455-1463.

Smith, G. E., Summers, M. D., & Fraser, M. J. (1983) Production of human beta interferon in insect cells infected with a baculovirus expression vector. *Mol. Cel. Biol.* **3**, 2156-2163.

Smith, H. W., & Gyles C. L. (1970) The relationship between two apparently different enterotoxins produced by enteropathogenic strains of *Escherichia coli* of porcine origin. *J. Med. Microbiol.* **3**, 387-401.

Sutherland, E. W, & Rall, T. W. (1960) The relation of adenosine-3',5'-phosphate and phosphorylase to the actions of catecholamines and other hormones. *Pharmacol Rev.* **12**, 265-299.

Takao, T., Hitouji, T., Aimoto, S., Shimonishi, Y., Hara, S., Takeda, T., Takeda, Y., & Miwatani T. (1983) Amino acid sequence of a heat-stable enterotoxin isolated from enterotoxigenic *Escherichia coli* strain 18D. *FEBS Lett.* **152**, 1-5.

Takao, T., Shimonishi, Y., Kobayashi, M., Nishimura, O., Arita, M., Takeda, T., Honda, T., & Miwatani, T. (1985) Amino acid sequence of heat-stable enterotoxin produced by *Vibrio cholerae* non-O1. *FEBS Lett.* **193**, 250-254.

Takeda T, Nair, G. B., Suzuki, K., Zhe, H. X., Yokoo, Y., de Mol, P., Hemelhof, W., Butzler, J.-P., Takeda, Y., & Shimonishi, Y. (1993) Epitope mapping and

characterization of antigenic determinants of heat-stable enterotoxin (STh) of *Escherichia coli* by using monoclonal antibody. *Infect. Immun.* **61**, 289-294.

Tessier, D. C., Thomas, D. Y., Khouri, H. E., Laliberte, F., & Vernet, T. (1991) Enhanced secretion from insect cells of a foreign protein fused to the honeybee melittin signal peptide. *Gene (Amst.)* **98**, 177-183.

Vaandrager, A. B., Schulz, S., de Jonge, H. R., & Garbers, D. L. (1993) Guanylyl cyclase C is an N-linked glycoprotein receptor that accounts for multiple heat-stable enterotoxin-binding proteins in the intestine. *J. Biol. Chem.* **268**, 2174-2179.

Vaandrager, A. B., van der Wiel, E., Hom, M. L., Luthjens, L. H., & de Jonge, H. R. (1994) Heat-stable enterotoxin receptor/guanylyl cyclase C is an oligomer consisting of functionally distinct subunits, which are non-covalently linked in the intestine, *J. Biol. Chem.* **269**, 16409-16415

Wada, A., Hirayama, T., Kitao, S., Fujisawa, J., Hidaka, Y., & Shimonishi, Y. (1994) Pig intestinal membrane-bound receptor (guanylyl cyclase) for heat-stable enterotoxin: cDNA cloning, functional expression, and characterization. *Microbiol. Immunol.* **38**, 535-541.

Wada, A., Hirayama, T., Kitaura, H., Fujisawa, J., Hasegawa, M., Hidaka, Y., & Shimonishi, Y. (1996a) Identification of ligand recognition sites in heat-stable enterotoxin receptor, membrane-associated guanylyl cyclase C by site-directed mutational analysis. *Infect. Immun.* **64**, 5144-5150.

Wada, A., Hasegawa M., Matsumoto, K., Niidome, T., Kawano, Y., Hidaka, Y., Padilla, P. I., Kurazono, H., Shimonishi, Y., & Hirayama, T. (1996) The significance of Ser1029 of the heat-stable enterotoxin receptor (STaR): relation of STa-mediated guanylyl cyclase activation and signaling by phorbol myristate acetate. *FEBS Lett.* **384**, 75-77.

Wedel, B. J., & Garbers, D. L. (1997) New insights on the function of the guanylyl cyclase receptors. *FEBS Lett.* **410**, 29-33.

Wiegand, R. C., Kato, J., Huang, M. D., Fok, K. F., Kachur, J. F., Currie, M. G. (1992) Human guanylin: cDNA isolation, structure, and activity. *FEBS Lett.* **311**, 150-154.

Wilson, E. M., & Chinkers, M. (1995) Identification of sequences mediating guanylyl cyclase dimerization. *Biochemistry* **34,** 4696-4701.

Yamasaki, S., Sato, T., Hidaka, Y., Ozaki, H., Ito, H., Hirayama, T., Takeda, Y., Sugimura, T., Tai, A., & Shimonishi, Y. (1990) Structure-activity relationship of Escherichia coli heat-stable enterotoxin: Role of Ala residue at position 14 in toxin-receptor interaction. *Bull. Chem. Soc. Jpn.* **63**, 2063-2070.

Yang, R. -B., Foster, D. C., Garbers, D. L., & Fulle, H. -J. (1995) Two membrane forms of guanylyl cyclase found in the eye. *Proc. Natl. Acad. Sci. USA* **92**, 602-606.

Yoshimura, S., Takao, T., Ikemura, H., Aimoto, S., Shimonishi, Y., Hara. S., Takeda, T., Takeda, Y., & Miwatani, T. (1984) Chemical synthesis of fully active fragments of heat-stable enterotoxin of enterotoxigenic *Escherichia coli* strain 18D. *Bull. Chem. Soc. Jpn.* **57**, 1381-1387.